The Shuddering Mandarin Orange and the Rocking Plank: dynamics of unusual oscillations

John Coffey, Cheshire, UK.

2021

Summary: The article gives experimental measurements and theoretical models of the oscillation under gravity of various cylindrical (constant cross-section) objects. Once tilted and released, all objects rocking to and fro will slow down then stop. However the oscillations appear to speed up to some extent. All objects, including ones with a circular section, have longer period when the initial displacement is large, but those with circular or elliptical section do not speed up so much that they appear to shudder. Instead they undergo decaying simple harmonic motion (SHM) at almost constant frequency. In contrast, cylinders with a sufficiently flattened base have oscillations which get progressively faster (shorter periods) as they die away. Friction with the ground is necessary for the object to rock without slipping and sliding, and the inevitable loss of energy causes the amplitude of oscillations to decrease and the motion eventually halt. It is a paradox that the frequency increases as the maximum velocity is decreasing. Theory shows that SHM is the limiting behaviour of those cylinders which have a non-zero second derivative (*i.e.* a quadratic term) in the Taylor series of their profile about the central equilibrium position. Where the base is so flat that there is no quadratic component, the frequency continues to rise as the amplitude decays. In shuddering the amplitude decays more rapidly than the maximum velocity, and the ratio 'velocity / amplitude' is proportional to frequency.

1 The phenomenon

This article started when I was amused by the behaviour of a mandarin orange when it is tilted and let go. Place a mandarin on the table with the stalk point uppermost, tip it through 30 degrees or more and let go. Almost all mandarins will wobble from side to side, then right themselves with a final rapid shudder – a speeded up oscillation just before they settle. Some mandarins have a most remarkable shudder. Why do they get faster just before coming to a stop?

I asked a non-technical friend. She replied that 'it speeds up because it goes a smaller distance'. After much thinking about this, I think she is basically correct, though this pithy assessment needs unpacking and quantifying. My initial suspicion was that this shudder or quiver is due to the squat shape with a dimple on the underside. Unlike oranges and some other citrus fruits, mandarins have a flattened area at the base and inside this is a slight concave depression. I first gained support for this conjecture from observing how a wooden cylinder with a flattened area settles when tipped to the side; its rate of oscillation also increases to a shudder. I later found that a plank of wood, standing on its narrow edge, will also rock from side to side and speed up before halting. Those readers familiar with simple harmonic motion, as seen in pendulums and weights on springs, will

know that even when damping is present, the period of oscillation does not vary perceptibly as the object comes to a halt. In fact damping prolongs the period a little, so the speeding up we observe with the mandarin and plank must involve non-linear effects.

This article describes my rambling investigation into these unusual dynamics. This has involved some casual observations of several flat-bottomed cylindrical objects which lay to hand, followed by more careful measurements on a short plank of wood and on two specially made wooden blocks with mathematically defined cross-sectional profiles. The objects span the range of profiles from a rectangular plank to a circular tube. The article deals with these roughly in order of increasing complexity or widening generality:

1. §2 describes some preliminary observations and measurements to demonstrate that speeding up does in fact occur, and to present examples of objects which show this behaviour.

2. I found that a wooden plank standing on its narrow face is perhaps the simplest and most instructive example, so §3 presents experimental results and gives a theoretical analysis which fits fairly well with the observed rocking behaviour. This is the 'bottom line' of this article so the reader may feel they need read no further.

3. The substantial remainder of the article describes measurements on specially constructed objects and attempts to model them with theory. §4 describes an oscillating system which does not speed up; it is a cylindrical pipe with an iron weight placed eccentrically inside it. The dynamics are solved using Lagrange's equation of motion and are in close agreement with experimental measurements.

4. §5 describes measurements on the first of two specially made cylindrical wooden blocks. The cross-section of this one was profiled to the involute of a circle which gives it the property that the torque causing angular acceleration is constant as it rocks and rolls under gravity.

5. §6 describes the rocking and rolling of an elliptical cylinder and shows by numerical example that it does *not* speed up when the amplitude is small.

6. §7 presents experimental results for the second wooden block whose base was profiled to the curve $y = 1 \cdot 2\, x^4$. This was chosen as a curve with a fairly simple mathematical formula and a flat-bottomed shape, aiming to focus on the rapid closing oscillations before the body come to rest. §8 gives the theory of constant cross-section objects whose profile at the base fits $y = f(x)$, particularly $y = Ax^4 + Bx^2$, and presents calculations for several cases.

7. §9 is a brief conclusion which explains in simple, non-mathematical terms what is happening with these rocking, rolling objects. The crucial result is Eq 50: when attenuation is small, the period of a cylinder with base profile $y = x^n$ decreases as $x_0^{\frac{n}{2}-1}$ as $x_0 \to 0$, x_0 being the initial displacement. The determining factor is the shape of the base at the resting position; in particular the relative amount of second derivative in the series expansion of the profile about this point. Curves in which the dominant term is x^4 or higher are flatter and do oscillate faster, those with a dominant x^2 term do not. Curves $y = x^n$, n even, span the cross-sectional shapes from mandarin orange to wooden plank.

8. There are three appendices. Appendix 1 (§10) gives examples of simple oscillating systems which can be solved using conservation of energy. Appendix 2 (§11) is about the geometry of curves used as profiles for the cylindrical objects in the body of the article. This includes calculation of their curvature and evolutes. Appendix 3 (§12) describes theory and experiments to determine the moment of inertia of the cylinder studied in §5.

2 Preliminary observations

Since this article presents several sets of measurements of oscillations, I will first explain how they have been made. The object was placed on a horizontal table, held by hand at maximum tilt to one side and released. A video recording was made of it rocking using a digital camera capturing at 50 frames per second. Time was therefore measured by frame number in steps of $\frac{1}{50}$ second. The camera looked either at the side face or the top. The block was marked on its side with the vertical symmetry axis, and its top marked with a central fiducial line. The mp4 file was examined frame by frame on the computer in a video editor (Blender 2.90). An on-screen protractor was used to measure angles and a cursor to measure co-ordinates of position in pixels. The position of the axis and/or fiducial mark was recorded frame by frame. Special attention was given to the positions and times of the peaks and troughs in the oscillation waveform, corresponding to the maximum tilts of the object to left and to right. The values were stored and processed in the Excel spreadsheet, and first and second derivatives calculated from the first and second divided differences. The pixel measurements were converted to real world units by reference to calibration marks.

The oscillations of a mandarin at too rapid to measure with the equipment I have at home, so I examined a much larger model – a near-cylinder made from a roll of roofing lead strip 2 mm thick. Figure 1 is an end-on photograph of this; note the slightly flattened arc where it sits on the wooden board. It weighs about $6 \cdot 9$ kg, its section is 91 mm high, 103 mm wide, and the roll is 150 mm wide. A clamp at each end gripped the sheets together to limit their slight tendency to spring open. The measured positions as plotted in the two graphs in Figure 2. The upper shows the decaying amplitude, and the lower plots the number of frames between successive half cycles against the cycle index. The fitted curve shows an exponential change in period from about 13 frames per half cycle (equivalent to $1 \cdot 92$ Hz) to 6.5 frames, or $0 \cdot 96$ Hz. This crude demonstration is evidence of substantial speeding up.

I flattened the base of the lead roll further (Figure 3) and repeated the measurements. The results are in the right panel of Figure 3, where the horizontal axis is proportional to time, not cycle number as used in Figure 2. The units are video frame number at the rate of 50 per second.

Figure 1: A roll of roofing lead used to demonstrate oscillations of a flattened cylinder.

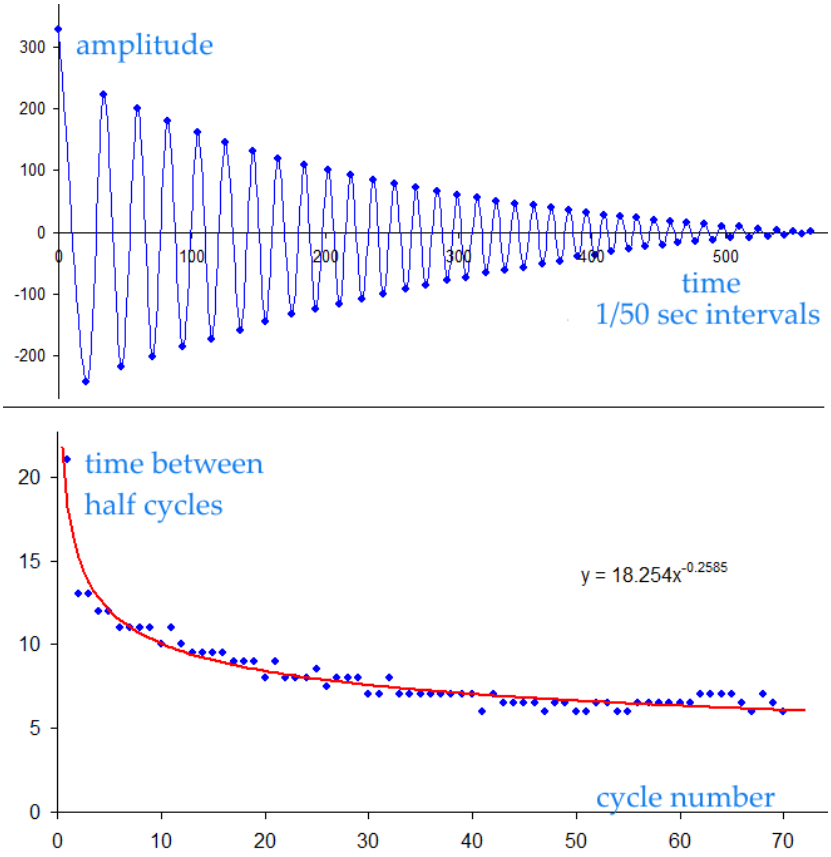

Figure 2: Upper panel: decay of oscillations when the lead roll in Figure 1 was tipped to the side and released. Lower panel: time interval between half cycles, at frame rate of 50 per second.

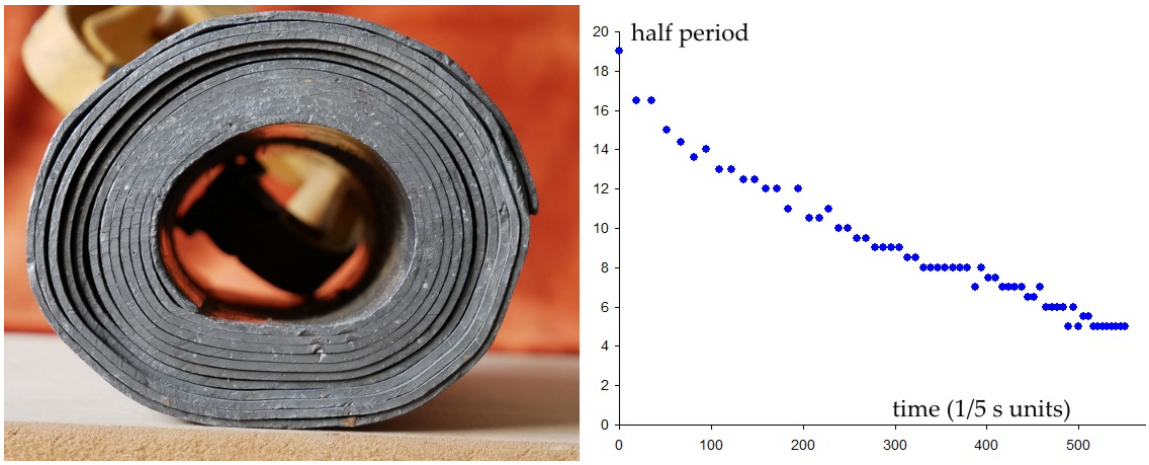

Figure 3: Repeat measurement of oscillations with the lead roll flatter at its base.

This graph shows an almost 4-fold increase in frequency over about 30 cycles. After the first few wide-amplitude cycles the half-period (time between left and half cycles) falls almost linearly with time.

I flattened the lead roll even more. Then it did not oscillate; instead its base just landed with a noisy smack on the table. This is no longer a rigid body situation in which energy is conserved;

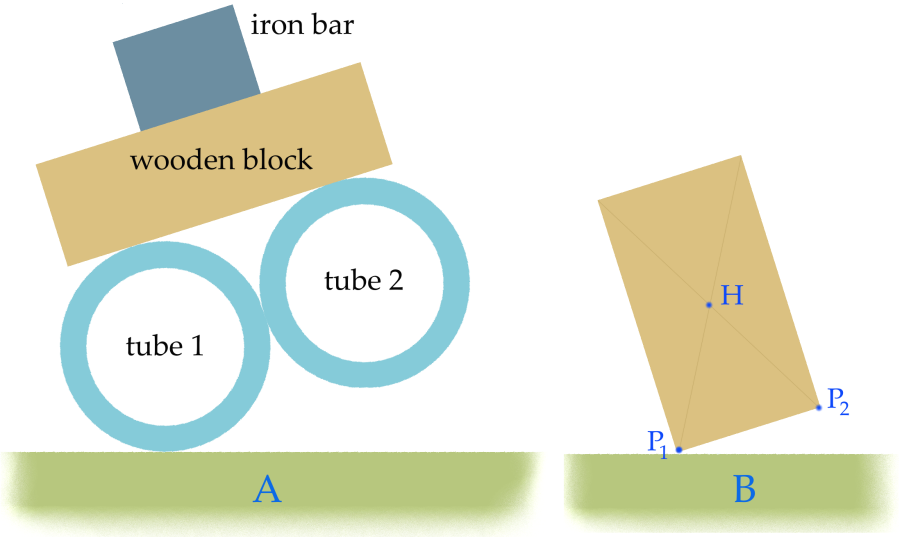

Figure 4: Oscillating object made from two tubes and a weight.

now the energy is dissipated in the slap sound, in the elastic waves which travel through the metal and the table, and probably in heat and plastic deformation of the soft metal too.

I have also assembled several objects made from two equal cylinders in contact, as in Figure 4A. The tubes were i) two length of plumber's plastic waste pipe, ii) two lengths of wooden stair hand-rail, and iii) two beer bottles. I simply bound them together with sticky parcel tape, and fixed the wooden block and iron weight with tape. Two such cylinders without the block and iron weight will not oscillate, but if the weight is sufficiently high, they will rock from one to the other and settle with a shudder like the mandarin. Simplifying the system even further, a rectangular wooden block will oscillate and shudder if the aspect ratio is suitable. I tested several blocks of wood to hand as in Figure 4b and found that if the aspect ratio is greater than about $14/9$ $(1 \cdot 55)$ it will rock rather than just fall, and in one case I have observed also that its oscillations speed up. These rough and ready experiments suggest that the conditions for oscillations which speed up as they die away are:

1. two symmetrically placed curved sections separated by an almost flat (or absent) central base. The curved sections can be reduced to mere lines of contact P_1, P_2 though perhaps not always with increasingly rapid oscillation.

2. a sufficiently high centre of gravity, H, which is equivalent to the combined object having a sufficiently high moment of inertia about the instantaneous point of contact with the ground plane,

3. a sufficiently large initial displacement to provide the initial potential energy,

4. enough friction with the ground to prevent slipping.

Can we say in broad terms what is happening physically? Take the simplest case as in Figure 4b. The initial tilt to the left gives the object potential energy, and creates a moment about contact points P_1 so that when the block is released, it falls by turning about P_1, accelerating as it falls. Its motion is suddenly arrested by contact with the ground when some energy will be lost in the impact. However the angular momentum it has acquired keeps the block turning clockwise, and it continues to roll but now about contact point P_2. Such turning raises the centre of gravity until the object

comes to a momentary halt and it starts to fall anticlockwise in the second half of its cycle. This would seem to be a rigid body phenomenon, though perhaps aided by the elasticity of the object and ground during the 'bounce' from one highly curved section to the opposite one. But this does not explain why it speeds up.

I have done yet other kitchen table experiments with a cylindrical tube with an eccentric metal weight inside, and these show that with objects which have a truly circular cross-section, the oscillations decay to zero without any such rapid shuddering. Figure 6 in §3 is a photograph of this equipment and it is described in detail in §4. The steel bar is placed inside the rigid plastic tube parallel to its axis, and the tube lies across a firm horizontal board, on which it will rock from side to side when rolled a little. Also shown on the right is the wooden cylinder (an off-cut from a stairway bannister) with its flattened underside. To gain some experience with the mathematics of this phenomenon I first try to solve this simpler case of the perfectly circular cylinder with the eccentric metal weight inside. Though this does not shudder as it settles, it is amenable to theory.

Before we leave these general observations, it is fair to ask whether oscillations of wide amplitude will be slower than small amplitude ones simply because wide swings, having a larger distance to travel, should take longer? There is some truth in this. Take the case of a simple pendulum which satisfies the differential equation[1] $h\ddot{\theta} + \mu\dot{\theta} + g\sin\theta = 0$. Here θ is the angle from the vertical, h the length of the rod, g the acceleration due to gravity and μ is a damping factor which causes the oscillations to die away. Solving this numerically for a starting angle of $1\cdot2$ radians, 69 degrees, the first few cycles are about 5% longer that those around the 30th. This is not large enough to explain the four-fold decrease in period in Figure 3.

3 The rocking plank

A plank with rectangular section is at one extreme of those objects which will rock, in that it has two sharp edges around which it swings, as in Figure 4b. This section reports some experimental observations and attempts a theory. §2 reports that I tested 8 rectangular wooden blocks and found that, if stood upon their narrow face, they would oscillate provided the aspect ratio was greater than about $1\cdot55$. Blocks which were more square than this just fell onto their larger face. For the block to roll the momentum of its centre of mass must be mostly in the horizontal direction.

3.1 Observations on a short wooden plank

The short length of oak plank I selected for study is 407 mm long, 101 mm deep and 27.3 mm wide. It weights 668 grams so has specific gravity $0\cdot60$. I stood it on a horizontal glass plate and recorded video footage at 50 frames per second of it rocking, with views from the top and side. Call the narrow width on which it stands a and the height b. The theoretical maximum angle of tilt, θ_m is such that the centre of mass at H is vertically above the point of contact P_1. This is $\theta_m = \tan^{-1}(a/b)$ which is $15\cdot2$ degrees for this plank. The maximum starting angle I recorded was $14\cdot7°$, very close to the limit. By examining the video frame by frame and using on-screen cursor measuring software, the position of a fiducial line on the top face of the plank was noted over about 160 frames. The values have been converted to degrees and are plotted in the upper panel of Figure 5. They show the slow start to oscillations from the near maximum tilt to the left, followed by a non-sinusoidal cycle and then another half dozen more sinusoidal cycles over which the amplitude rapidly dies to zero. The first divided difference of these frame-by-frame values approximates the angular velocity in

[1] The double dot is Newton's notation for differentiation twice with respect to time.

degrees per second, and the second difference approximates the angular acceleration. These graphs are remarkable because, over the middle few cycles at least, they show that the velocity changes in an apparently linear zigzag manner as the acceleration switches every half cycles from being a positive near-constant to its negative. The angular displacement, therefore, has wave shape made piecewise from upwards and downwards curves which are almost parabolas. We will see this characteristic motion with the specially shaped curved block in §5, and I suspect that mandarins show similar behaviour.

These oscillations die away after about 3 seconds. Over that time each half cycle is shorter than the previous, as the left panel in Figure 6 shows. This plots the duration in seconds of successive half-cycles (movement left to right) against an integer count of peaks and troughs in the waveform. The fitted trend curve falls roughly at $1/t$. The right panel plots the peak or trough amplitude

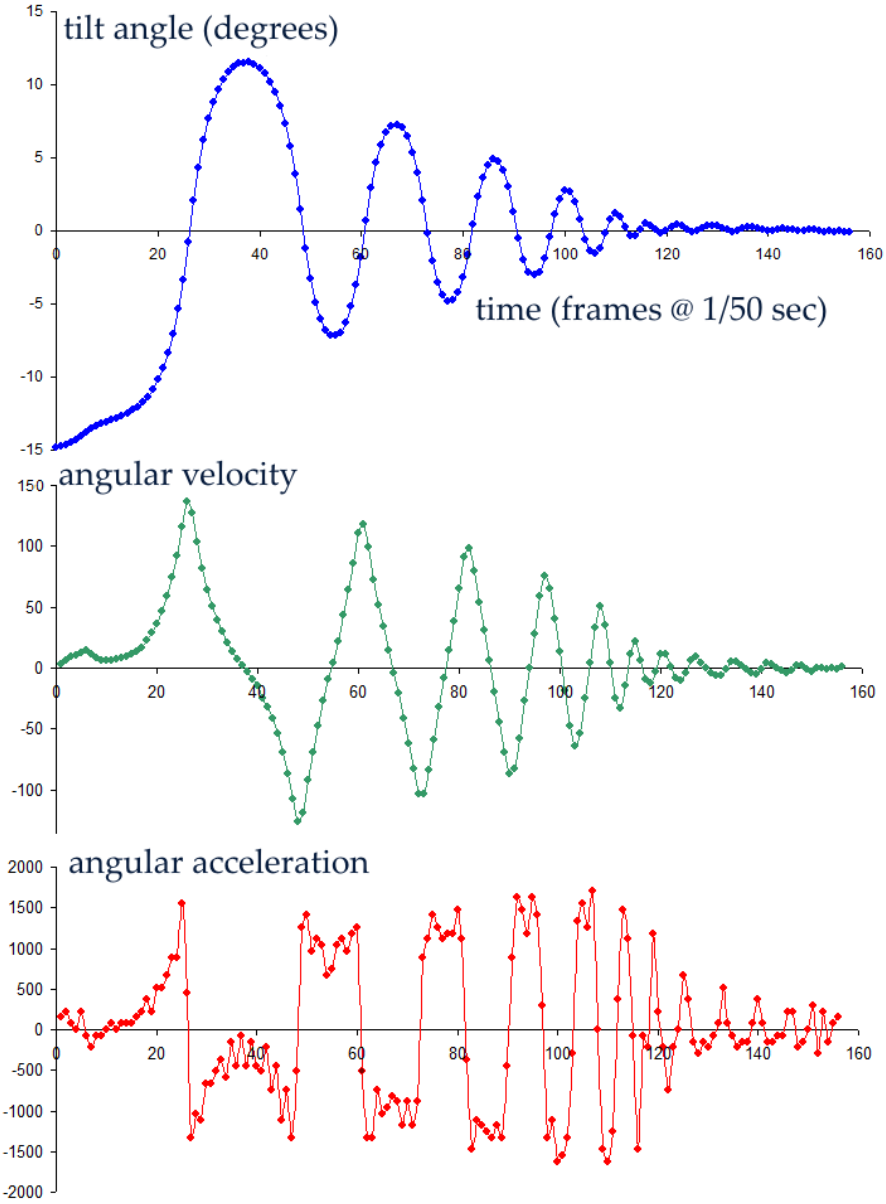

Figure 5: Oscillations on a short wooden plank about its narrow face.

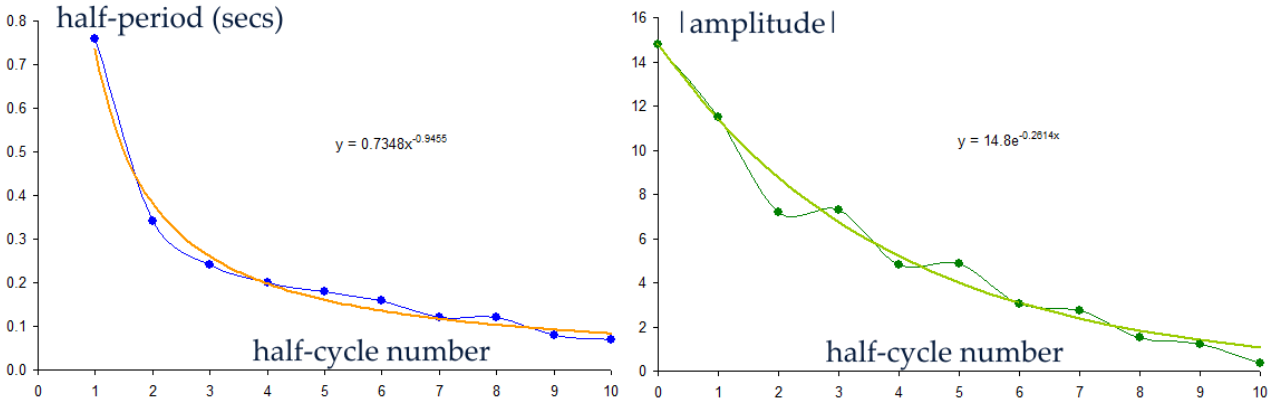

Figure 6: The peaks and troughs of the oscillating plank's waveform. Left: half-period duration in $\frac{1}{50}$ units versus half-cycle index. Right: peak and trough amplitudes versus half-cycle index.

against the integer half-cycle index. The light green curve is a geometric series with ratio $0\cdot77$ per half-cycle.

To see what changes come with a slight curvature of the base contact surface, I used abrasive paper to round the narrow face slightly, taking off the sharp corners. I emphasise that this was a gentle rounding with hardly any wood removed. The effect on the motion, however, was remarkable – the plank oscillated for a much longer time and in a smoother manner. Figure 7 shows the first few cycles. The by-hand rounding has clearly not been symmetric since the excursions to the right (positive θ) are not a mirror of those to the left. However the plots of velocity at the fiducial point on the top face, converted to degrees, and the acceleration look very similar to those in Figure 5. Almost 60 half-cycles could now be discerned, lasting about $7\cdot5$ secs. The decay in amplitude per full cycle was $0\cdot80$ for swings to the left and $0\cdot85$ for swings to the right, meaning that about 90% of the energy is transferred each time the plank is instantaneously upright. This compares with 77% when the corners are sharp right angles. The half periods over the whole motion again became shorter, their duration being closely represented by $T_{1/2}\approx -4\cdot65\ln N+21\cdot2$ where N is the index of the half cycle and the units are frames ($\frac{1}{50}$ sec). Thus the 26th half-cycle lasts $6/50=0\cdot12$ secs. The rounding clearly softens the impact when the plank swaps from one pivot to the other. Less energy is dissipated and so the plank can swing to a larger angle on the other side. However, rounding does not alter the fact that the plank is repeatedly falling and bouncing back on the other side of the equilibrium position, as the similar velocity and acceleration graphs in Figure 5 and 7 bear witness. The rounding was not enough to change the positions P_1, P_2 of the corner pivots except for tilts only slightly off upright.

3.2 A theory of the plank's oscillation

This subsection will develop a simple model for the oscillation of a rectangular plank with sharp corners, assuming that it is essentially a fall from a tilted position to its equilibrium position, and the time reversed version of this motion. Four stages of the motion are depicted in Figure 8. In the third picture the plank is instantaneously standing on its narrow face, width a. The centre of mass is at H which is at height $h(0)=b/2$ from the base and diagonal distance $c=\sqrt{a^2+b^2}/2$ from each corner. To reference the tilt angle θ we will use the long edge, so at the resting position $\theta=0$. The maximum possible tilt, θ_m, is shown in the first panel: $\tan\theta_m=a/b$. θ_m measures the aspect ratio of the plank's cross-section. The second and last pictures show the plank at a general angle θ to the left and to the right. The centre of mass rises from $h(0)$ to $h(\theta)=c\cos(\theta_m-\theta)$. The sign convention

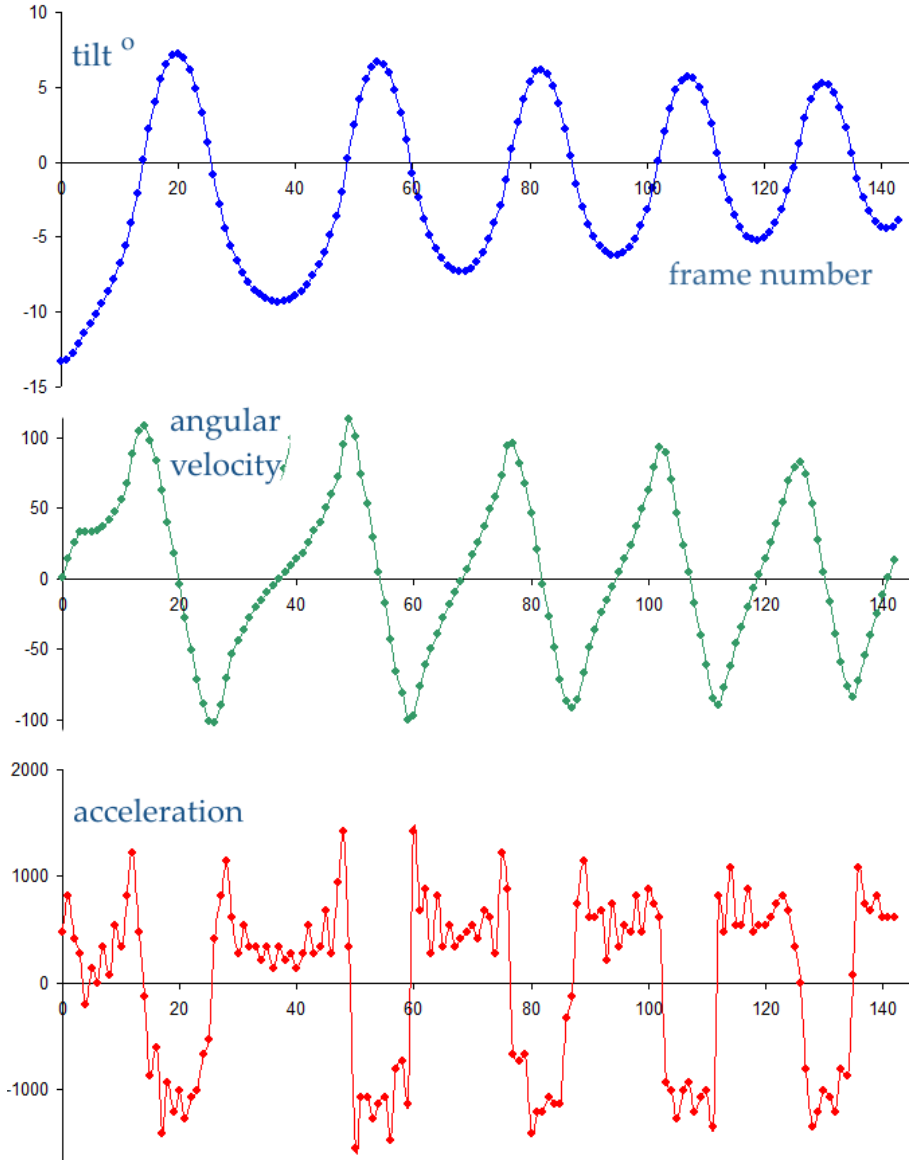

Figure 7: The first few cycles of the plank with slightly rounded base. Displacement in degrees (top panel) and its first and second divided differences. Frames are at 50 per second.

is that $\theta_m - \theta$ is always positive and that clockwise rotations, moments, velocities and accelerations are positive. We can take the zero of potential energy to be at $\theta = 0$, so the potential energy is $mg[c\cos(\theta_m - \theta) - b/2]$.

When the plank is released, it will fall. This simple, obvious fact seems to be crucial to understanding the dynamics not just of the plank but of the mandarin and other rocking objects such as the two-pipe constructions in Figure 4a and the $y = Ax^4$ object of §6. Although the fall is moderated by the profile of the base, it is nevertheless essentially a fall under gravity, hinged about the instantaneous point of contact.

When the plank is tilted at general angle $\theta(t)$, there is a moment about P_1 due to the centre of mass being offset by distance $c\sin(\theta_m - \theta)$ from the vertical through P_1. This moment causes

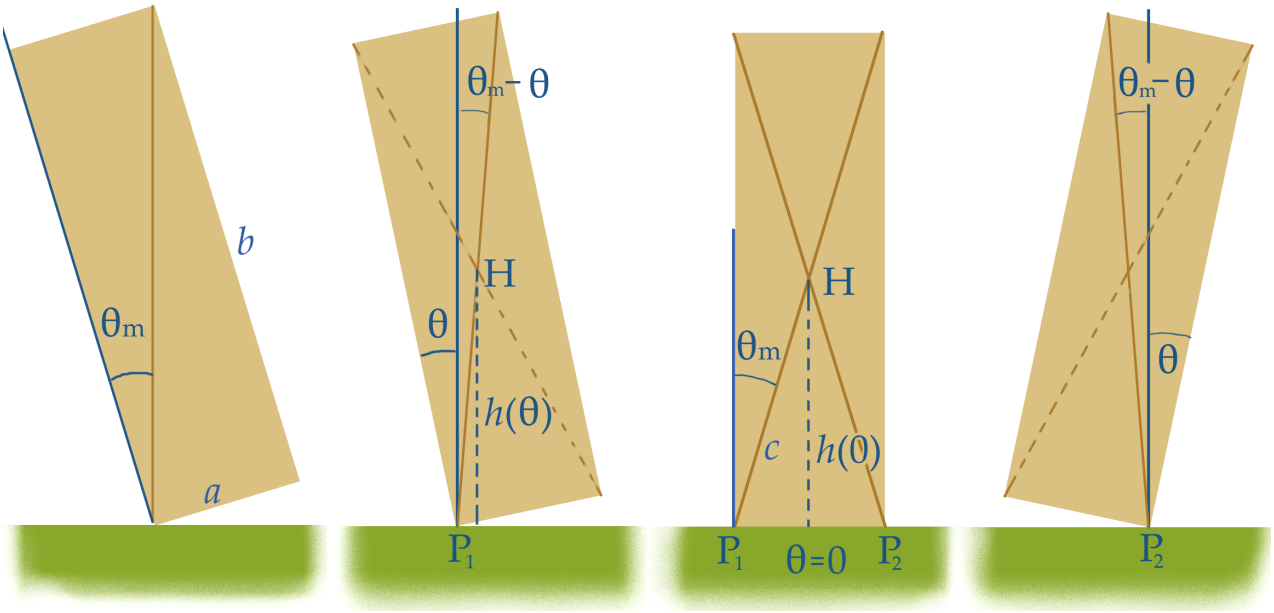

Figure 8: Four instances in the geometry of the rocking plank.

angular acceleration with the equation of motion[2]

$$I_P\,\ddot{\theta}(t) \;=\; -mgc\,\sin(\theta_m - \theta(t))\,. \tag{1a}$$

where I_P is the moment of inertia about the corner. The minus sign is because the moment is clockwise when θ and θ_m are both anticlockwise, and *vice versa*. Forces of constraint at P (normal reaction and friction) are present, but do not feature in the equation of motion. The starting position is $\theta_0 < \theta_m$ where $\dot{\theta}(0) = 0$ since it is released from rest. This equation does not admit a simple solution, but if angles are small so that $\sin(\theta_m - \theta) \approx \theta_m - \theta$, the general solution is

$$\theta_m - \theta \;=\; C_1\,e^{\alpha t} + C_2\,e^{-\alpha t}, \qquad \dot{\theta} \;=\; -\alpha C_1\,e^{\alpha t} + \alpha C_2\,e^{-\alpha t}, \qquad \alpha^2 \;=\; \frac{mgc}{I_P}\,, \tag{1b}$$

C_1, C_2 are constants to be determined by the initial conditions in each quarter cycle. For a plank turning about its corner $I_P = \frac{1}{3}m(a^2 + b^2) = 4mc^2/3$ which is $0\cdot002415$ kg m^2 for the one described in §3.1. For a general rectangular plank $\alpha^2 = 3g/4c$, which is $141\cdot3$ sec^{-2} for this one. At maximum possible tilt the centre of mass has risen only $c - b/2 = 1\cdot8$ mm.

Suppose the plank is tilted to the left then released. When it is upright, the energy still in the motion causes it to transfer to pivot P_2 and continue turning to the right until all its energy is again potential. Only the fraction k of the velocity is transferred at each instantaneous upright position so the amplitudes decease. The oscillation over each cycle is made piecewise of four quarter cycles: left to centre, centre to right, right to centre, centre to left. The values of the variables are shown in the scheme in Figure 9 below. Time moves down the page from $t = t_0 = 0$ in the top left cell. At the end of the first quarter cycle the time is t_1, $\theta = \theta_1 = 0$ and the velocity is some value $\dot{\theta}_1$ to be calculated from Eq 1b. The velocity is then reduced to a fraction $k \approx 0\cdot9$ as the pivot shifts from P_1 to P_2. At the end of the next quarter cycle the time is t_2, the plank has swung to the right at maximum excursion θ_2, and the velocity is instantaneously zero. We now have to calculate all the unknown quantities in this diagram.

[2] The equation can be written alternatively as $I_p\ddot{\theta} + mg(\frac{a}{2}\cos\theta - \frac{b}{2}\sin\theta) = 0$. Here $\frac{a}{2}\cos\theta - \frac{b}{2}\sin\theta$ is the arm of the moment of H about P_1. This form is transformed to Eq 1a using $a = 2c\sin\theta_m$, $b = 2c\cos\theta_m$.

First quarter-cycle Here $C_2 = -C_1 + (\theta_m - \theta)$ and the condition that the plank falls from rest imposes $2C_1 = \theta_m - \theta_0$ so

$$\theta = \theta_m - (\theta_m - \theta_0)\cosh(\alpha t)\,, \qquad \dot{\theta} = -\alpha(\theta_m - \theta)\sinh(\alpha t)\,. \tag{2}$$

The time, t_1, taken to fall from θ_0 to the upright position is

$$t_1 = \frac{1}{\alpha}\cosh^{-1}\left(\frac{\theta_m}{\theta_m - \theta_0}\right)\,. \tag{3}$$

If $\theta_0 = \theta_m$, the arccosh factor would be infinite, meaning the plank would not move because it would be balanced precisely and precariously on its corner. To obtain a sensible answer we must assume a small non-zero starting angle. The experiments suggest this could be as small as $0\cdot5°$, so take $\theta_0 = 14\cdot7°$. For the plank in question the time to fall to the upright position is $t_1 = 0\cdot346$ secs or about 17 frames of the video. This is smaller than I observed – the plank is upright at frame 26. However, one should not read too much into this discrepancy in timing because I cannot be sure of the starting tilt nor could I have withdrawn my supporting hand instantaneously. From Eq 2 the angular velocity at the end of this quarter cycle is

$$\dot{\theta}(t_1) = -\alpha(\theta_m - \theta_0)\sinh\alpha t_1 = -\alpha\sqrt{2\theta_m\theta_0 - \theta_0^2} = \alpha\xi\,. \tag{4}$$

The expression $\sqrt{(}2\theta_m\theta_0 - \theta_0^2) = \sqrt{(}\theta_m^2 - (\theta_m - \theta_0)^2)$ will occur again in this calculation so I will write ξ for this. In our case $\dot{\theta}(t_1)$ is $-3\cdot15$ radians/sec, the minus sign meaning that it is in the opposite sense to that in which θ increases.

Second and third quarter-cycles The second starts at time t_1. Write $\tau = t - t_1$ so $\tau = 0$ when $\theta = 0$ and $\dot{\theta} = v_1 = -k\dot{\theta}_1$ which is $+2\cdot84$ if $k = 0\cdot9$. The initial conditions require that $C_1 = (\alpha\theta_m - v_1)/(2\alpha)$, $C_2 = (\alpha\theta_m + v_1)/(2\alpha)$. The opposite peak is reached at time t_2 when $\dot{\theta} = 0$, which is when

$$\tau = \frac{1}{2\alpha}\ln\left(\frac{\alpha\theta_m + v_1}{\alpha\theta_m - v_1}\right) = \frac{1}{2\alpha}\ln\left(\frac{\theta_m + k\xi}{\theta_m - k\xi}\right)\,. \tag{5}$$

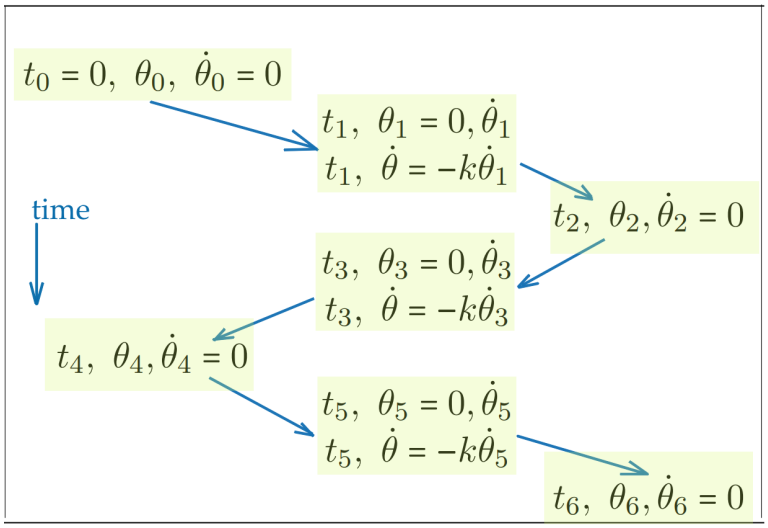

Figure 9: Schematic of successive quarter cycles in the oscillation of a plank. Time advances down the page as the position of the centre of mass swings from left to centre then right, then back again. $1\frac{1}{2}$ cycles are listed here.

This evaluates to $\tau = 0 \cdot 124$ secs, making t_2 $0 \cdot 470$ secs. We can see the similarity to t_1 better if the arccosh in Eq 3 is written in terms of logarithms:

$$t_1 = \frac{1}{\alpha} \ln\left(\frac{\theta_m + \xi}{\theta_m - \theta_0}\right) = \frac{1}{2\alpha} \ln\left(\frac{\theta_m + \xi}{\theta_m - \xi}\right).$$

The second relation follows from the fact that if $k = 1$, the second quarter cycle is simply the first in time reversal (plus a right to left flip). Since the third quarter cycle is the time reversal of the second, τ is also $t_3 - t_2$. We therefore have

$$t_1 = \frac{1}{2\alpha} \ln\frac{(\theta_m + \xi)}{(\theta_m - \xi)}, \quad t_2 = \frac{1}{2\alpha} \ln\frac{(\theta_m + \xi)(\theta_m + k\xi)}{(\theta_m - \xi)(\theta_m - k\xi)}, \quad t_3 = \frac{1}{2\alpha} \ln\frac{(\theta_m + \xi)(\theta_m + k\xi)^2}{(\theta_m - \xi)(\theta_m - k\xi)^2}.$$

The maximum tilt at the end of $\frac{1}{4}$-cycle number 2 is

$$\theta_2 = \theta_m - \sqrt{\theta_m^2 - \left(\frac{v_1}{a}\right)^2} = \theta_m - \sqrt{\theta_m^2 - k^2\xi^2}. \tag{6}$$

Subsequent quarter-cycles Let q be an integer to index the quarter cycles, and p index the half cycles. The pattern in the values of t_q and θ_q is beginning to show. Each time the plank flips through the upright position a factor of k is applied. Each swing of the plank from centre to left or right and back to the centre is made of two mirror image quarter-cycles. Therefore

$$t_q = \frac{1}{2\alpha} \ln\frac{(\theta_m + \xi)(\theta_m + k\xi)^2 \ldots\ldots (\theta_m + k^p\xi)^r}{(\theta_m - \xi)(\theta_m - k\xi)^2 \ldots\ldots (\theta_m - k^p\xi)^r}. \tag{7}$$

where $r = 1$ if q is even, 2 if odd, and p is the integer part of $q/2$. The ratio of the half-periods of two contiguous half-cycles (centre-right-centre then centre-left-centre) is the ratio of two logarithms:

$$\frac{\ln\left(\dfrac{\theta_m - k^{p+1}\xi}{\theta_m - k^{p+1}\xi}\right)}{\ln\left(\dfrac{\theta_m - k^p\xi}{\theta_m - k^p\xi}\right)}. \tag{8}$$

However, the limit of this ratio as $p \to \infty$ is k. This rather remarkably simple outcome means that after a few oscillations the half-periods becomes shorter and shorter, almost in geometric series.

The maximum tilt in each half cycle is

$$\theta_p = \theta_m - \sqrt{\theta_m^2 - k^{p/2}\xi^2}. \tag{9}$$

The amplitude ratio of sequential half-cycles in the limit $p \to \infty$ is also k. Consequently, θ_p and τ_p both tend to geometric series with the same common ratios, and hence θ_p and τ_p become proportional. As my non-technical friend suggested, the oscillations speed up because the plank moves a smaller distance; *amplitude and half-period are proportional and decrease almost in geometric series* – a common ratio to the power of the index number of the half-period. This explains the shudder and is perhaps the central result of this article.

Figure 11 plots calculated values of θ, $\dot{\theta}$ and $\ddot{\theta}$ over five cycles to compare with the measurements for the sharp-cornered plank, Figure 5, and the one with a slightly rounded base, Figure 7. The shortening half periods are clear, as are the kinks in the otherwise straight zig-zag lines in the

velocity graphs due to the cosh factor in Eq 2, and the alternating arches in the piecewise graphs of acceleration due to the sinh factor. The similarity is good enough for me to believe that this model contains the essence of the phenomenon.

It is informative to examine the ratio of amplitude to maximum velocity of the plank. Since 'time = distance/velocity' we might expect 'period $\propto$ maximum tilt / maximum velocity'. From Eq 4 this ratio is $\theta_0/(\alpha\xi(\theta))$. It is plotted in Figure 10 for $\alpha = 11\dot{8}9$, $\theta_m = 0 \cdot 2653$ radians, $15 \cdot 2°$. The dimension of the vertical axis is time. Clearly the ratio does not approach a steady value, but decreases almost linearly until, near the origin, it dips sharply, indicating a shudder as the amplitude decays much faster than the velocity.

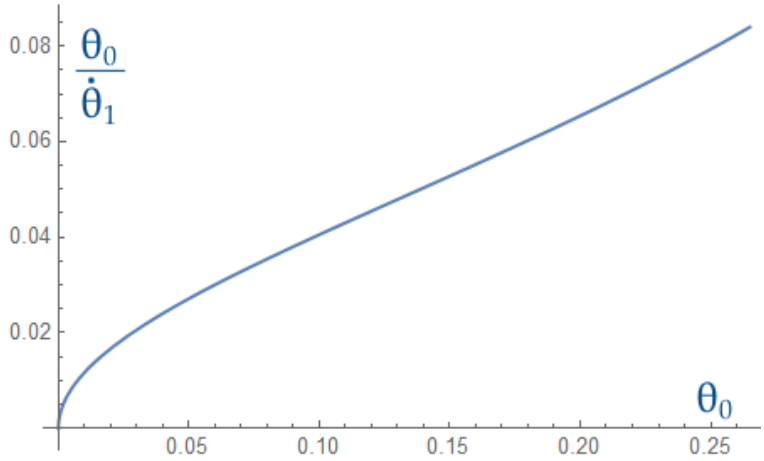

Figure 10: Ratio of maximum tilt to maximum velocity in any quarter cycle of the plank, plotted again initial tilt.

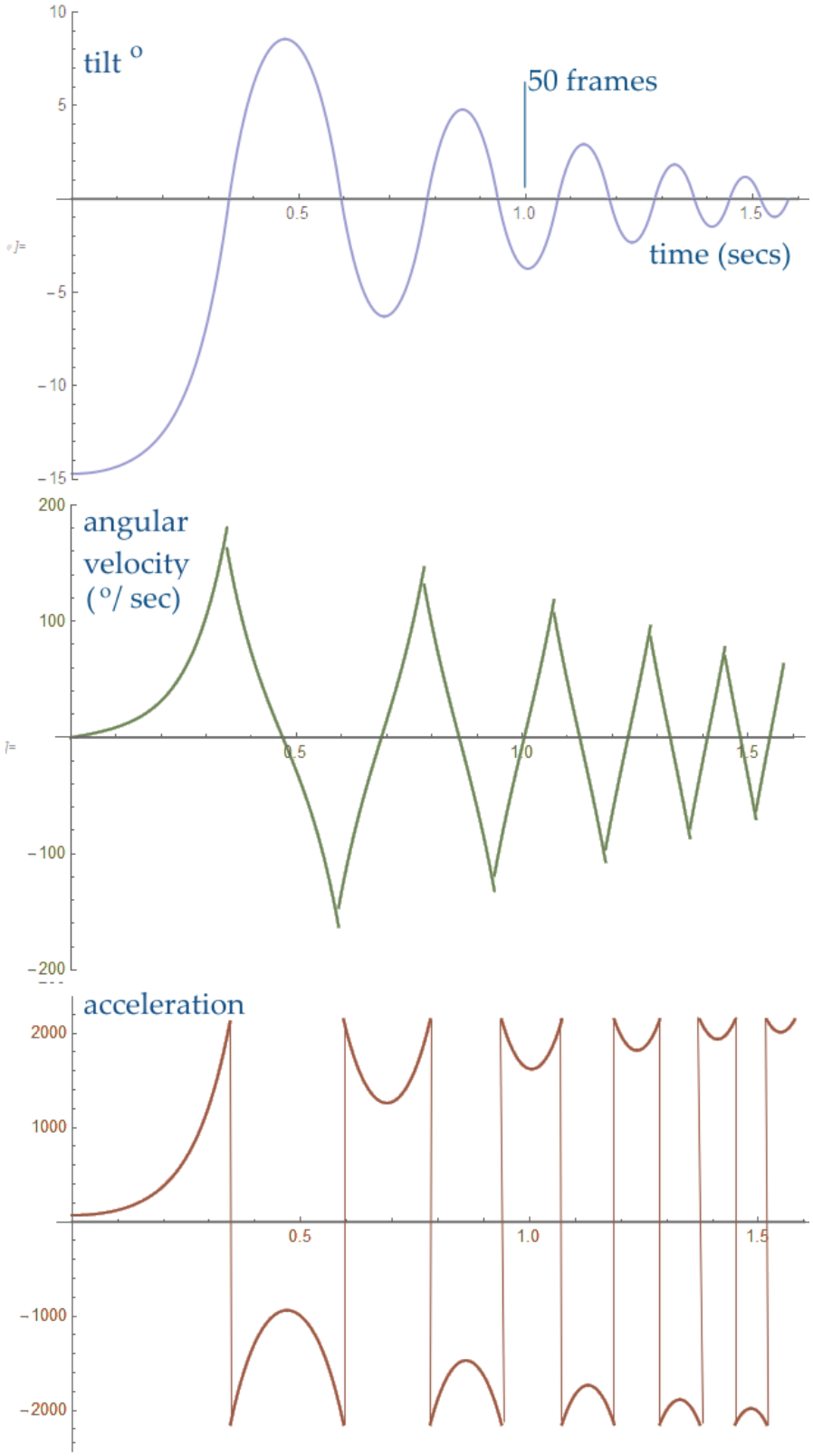

Figure 11: Theoretic pictures of the oscillations of the plank to compare with Figures 5 and 7. Angles in degrees. Velocity is reduced by 10% each time θ passes through 0.

4 The circular tube with eccentric weight

In this section we move to the other extreme of profile and give a 'from first principles' derivation of the exact equation of motion of a circular object with eccentric centre of mass on flat horizontal ground. This is a solvable study in rolling which tries out a method which in principle can be applied to more complicated geometries and to large amplitude oscillations. Experimental results are compared with the theory.

Figure 12: The experimental equipment. The tube rolls on a wooden board. Inside is a steel bar with square section. Oscillations were initially measured with the stop watch but later with a video camera. On the right is a wooden cylinder, flattened along its length.

When an object such as a wheel spins, it turns about a well-defined axis – the axle on which it is mounted. But when an object rolls, there is no unique axis about which it turns. There is a theorem that the system can be replaced by an equivalent simpler one consisting of a mass placed at the centre of mass of the combined tube and bar, turning around its centre of mass which moves both up and down and sideways as the object rolls without slipping on the ground plane. However, this cannot be a unique description. We could instead treat the cylinder and iron bar as two separate objects, and calculate their contributions to the potential and kinetic energy separately. Indeed we see at a glance that the change in potential energy arises solely from the iron bar provided the ground plane is horizontal[3]. I will therefore derive expressions for the potential and kinetic energies from first principles, and thence show how they can be interpreted in terms of at least two models using centre of mass and moment of inertia.

The equipment is photographed in Figure 12. The function of the eccentric steel block is to define a unique equilibrium position. Without such eccentricity the tube would merely roll along the table. In the experiment the block was not glued inside the tube as it was heavy enough not to slip. The parameters are listed in Table 1.

[3] After writing the first version of this article, I found an interesting paper on the internet about a similar object rolling down an inclined plane. 'Rolling of non-axisymmetric cylinders' by A. Carnevali and R. May, Am. J. Phys. Vol.73(10), 2005, p909.

Plastic tube			
	outside diameter, $2r_2$	110	mm
	wall thickness, $r_2 - r_1$	$3 \cdot 5$	mm
	inside diameter, $2r_1$	103	mm
	mass, M_c	503	g
Steel bar			
	height, $2a$	$40 \cdot 0$	mm
	width, $2b$	$40 \cdot 0$	mm
	mass, M_b	2480	g
Oscillation	period	$0 \cdot 57$	secs
	frequency	$1 \cdot 75$	Hz

Table 1: Dimensions and masses of the tube and weight in the experiment.

4.1 A note on Lagrange's equation of motion

Analysis of most of the rocking and rolling cylindrical objects in this article will use Lagrange' formulation of mechanics. In our case there is only one time dependent variable, which for the time being we can take to be the angle θ measured from the equilibrium position. The general Lagrange equation of motion is

$$\frac{d}{dt}\left(\frac{\partial T}{\partial \dot\theta}\right) - \frac{\partial T}{\partial \theta} + \frac{\partial V}{\partial \theta} \;=\; 0\,. \tag{10a}$$

where the total kinetic energy is T and potential energy is V when the system is in general position at tilt θ. This formula ignores energy losses through friction, air resistance, etc., allowing use of a potential to represent the applied force. Of course, friction is necessary to ensure that the cylinder rolls without slipping, and this friction causes a steady loss of energy which makes the amplitude decay. So although this equation of motion cannot be strictly correct, it should be close enough provided the attenuation is small. The equations can be thought of as expressing the condition for the quantity $L = T - V$, sometimes called the 'action', to have a stationary value (usually a minimum) when integrated over the total path of the particles. This means that the kinetic and potential energies have equal effect in determining the whole motion.

We will find that the potential and kinetic energies can be written in terms of two functions, $P(\theta)$ and $Q(\theta)$, which depend only on the geometry of the object.

$$T \;=\; \tfrac{1}{2}MP\dot\theta^2 + \tfrac{1}{2}I\dot\theta^2, \qquad V \;=\; MgQ$$

where M is the mass of the object, I its moment of inertia about its centre of mass and g the acceleration due to gravity. To find the velocity and acceleration we need their derivatives with respect of θ, which will be denoted by the $\hat{}$ superscript, while the dot $\dot{}$ means differentiation with respect to time, t.

$$\hat P \;=\; \frac{\partial P}{\partial \theta} \quad \text{so by the chain rule} \quad \dot P \;=\; \hat P\dot\theta\,.$$

$$\text{Then} \qquad \frac{\partial V}{\partial \theta} \;=\; Mg\hat Q, \qquad \frac{\partial T}{\partial \theta} \;=\; \tfrac{1}{2}M\hat P\dot\theta^2\,, \qquad \frac{\partial T}{\partial \dot\theta} \;=\; (MP + I)\dot\theta\,, \tag{10b}$$

$$\frac{d}{dt}\left(\frac{\partial T}{\partial \dot\theta}\right) \;=\; M(P\ddot\theta + \dot P\dot\theta) \;+\; I\ddot\theta \;=\; (MP + I)\ddot\theta + M\hat P\dot\theta^2\,.$$

Notice that there are two terms in $M\hat{P}\dot{\theta}^2$, one twice the other, and they partly cancel in Lagrange's equation, which is

$$(MP + I)\ddot{\theta} + \tfrac{1}{2}M\hat{P}\dot{\theta}^2 + Mg\hat{Q} = 0\,.$$

There is a mass factor in the moment of inertia so, to cancel M, let $I/M = J$, a purely geometrical function. The general form of the equation of motion is now

$$(P + J)\ddot{\theta} + \tfrac{1}{2}\hat{P}\dot{\theta}^2 + g\hat{Q} = 0\,. \qquad (10c)$$

If i) the middle term in $\dot{\theta}^2$ is known to be small so that it can be ignored, ii) if $\hat{Q}$ is proportional to θ, $\hat{Q} = q\theta$, and iii) if P is not a function of θ, then the remaining terms represent simple harmonic motion (SHM) with radian frequency ω given by

$$\omega^2 = \frac{gq}{P + J}\,.$$

$(P + J)/q$ has the dimension of length. There is the assumption here that P, Q and their derivatives are 'well behaved' functions of the geometry and in particular do not have singularities. However, we have already seen singular behaviour in the rocking plank at the upright position, so we will need to be cautious.

4.2 Theory of the combined tube and bar

Figure 13 shows the composite object when the cylinder is in equilibrium (left picture) and when rolled leftwards (right) – the ghost image shows its original position.At equilibrium the centre line C of the iron bar is distance c below O and the centre of mass, H, of the combined object is h below O. Set up a co-ordinate frame with z horizontal to the right, w vertical, and origin fixed in space where the cylinder rests on the ground in its stable position. Introduce a second co-ordinate system, x, y whose origin is the centre of the iron bar, with x and y parallel to its sides. At equilibrium x is horizontal, y vertical, but this frame rotates with the bar.

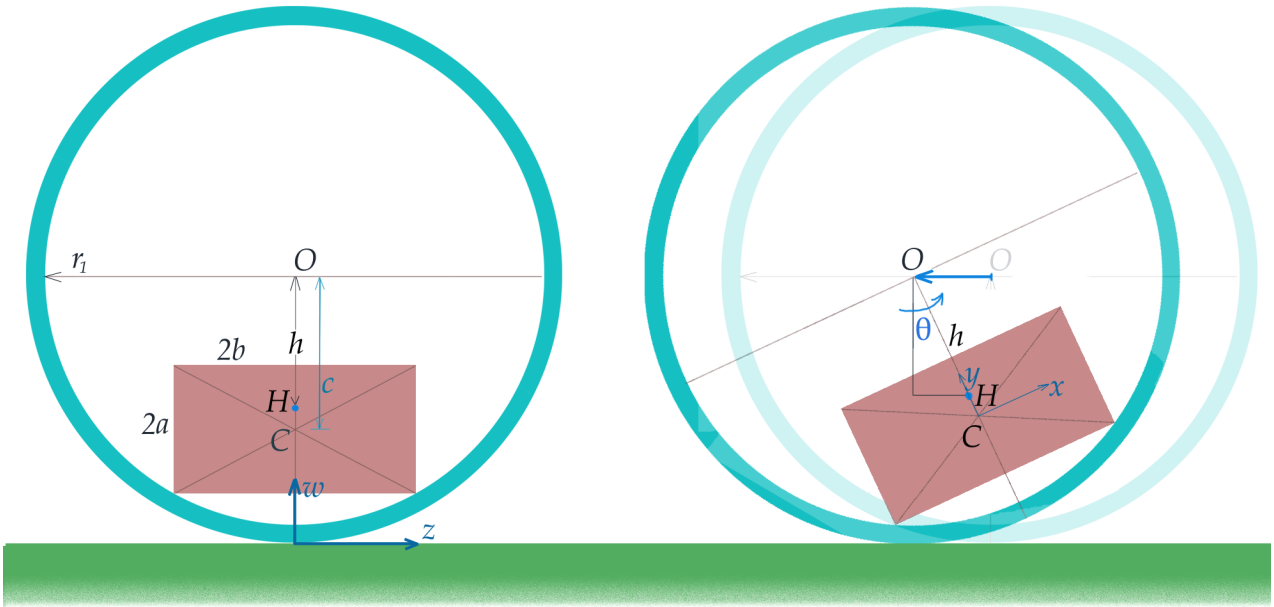

Figure 13: Left: Cylinder and heavy internal bar at equilibrium. Right: Rolled sideways and released.

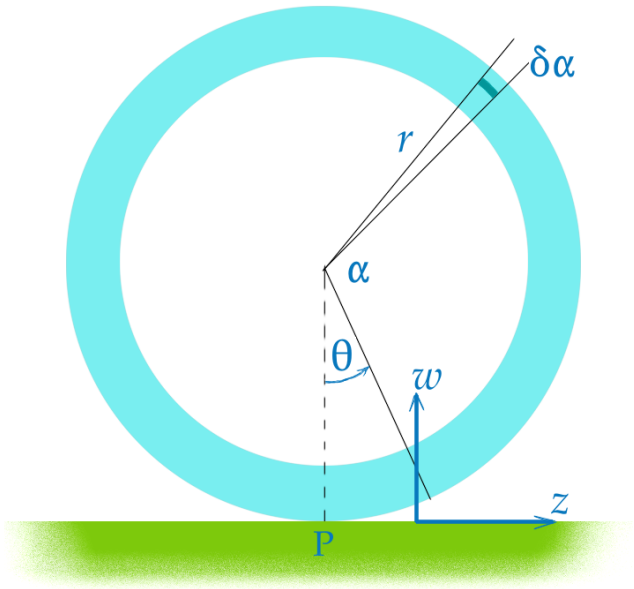

Figure 14: An element of wall of the tube when turned through θ from its reference position.

Consider first the dynamics of the tube alone. In a 'first principles' approach, we find the position of a general element in the tube wall and integrate over the whole tube to determine its kinetic energy. As already noted, the tube as a whole undergoes no change in gravitational potential. Figure 14 shows such an element at radial position r and angle α round from a reference datum on the circumference, when the tube has turned through angle θ. The sign convention is that θ is positive when the object turns anticlockwise and the object rolls to the left, so that the z co-ordinate of the point of contact P becomes increasingly negative. The sectional area of the element is $r\delta\alpha\,\delta r$, its length L and density ρ. The centre O of the tube has rolled in z through $-r_2\,\theta$, placing the element at angle $\theta+\alpha-\pi/2$ anticlockwise from the horizontal. Its position is therefore

$$z \;=\; r\cos(\theta+\alpha-\tfrac{\pi}{2}) - r_2\theta \;=\; r\sin(\theta+\alpha) - r_2\theta,$$

$$w \;=\; r\sin(\theta+\alpha-\tfrac{\pi}{2}) + r_2 \;=\; -r\cos(\theta+\alpha) + r_2\,.$$

Differentiate with respect to time to find the velocity vector to be

$$\boldsymbol{v} \;=\; \dot\theta[\,(r\cos(\theta+\alpha)-r_2)\boldsymbol{e_z} \;+\; r\sin(\theta+\alpha)\boldsymbol{e_w}\,]$$

where $\boldsymbol{e_z}$, $\boldsymbol{e_w}$ are unit vectors. It is worth checking that the rolling condition is satisfied by this formula. The vertical component of velocity is zero where $\theta=-\alpha$, which is at point P. There the horizontal velocity is $(r-r_2)\dot\theta$, and at the surface $r=r_2$. Therefore the local velocity of the tube at P is zero, as required.

The kinetic energy δT of the element whose mass is δm is $\frac{1}{2}|v^2|\,\delta m$.

$$|v^2| \;=\; \dot\theta^2[\,r^2\cos^2(\theta+\alpha) \;-2r\,r_2\cos(\theta+\alpha) + {r_2}^2 + r^2\sin^2(\theta+\alpha)\,]$$

The total kinetic energy is

$$\tfrac{1}{2}\int_0^{2\pi}\int_{r_1}^{r_2}\rho L\,|v^2|\,r\,dr\,d\alpha$$

$$=\; \tfrac{1}{2}\rho L\dot\theta^2\left[\,\tfrac{2\pi}{4}(r_2^4-r_1^4) \;-\; \tfrac{2}{3}(r_2^3-r_1^3)r_2.0 \;+\; \tfrac{2\pi}{2}(r_2^2-r_1^2){r_2}^2\right]. \qquad (11a)$$

The second term is zero because of the periodicity of $\cos\alpha$. In the first $(r_2^4 - r_1^4) = (r_2^2 + r_1^2)(r_2^2 - r_1^2)$ and $\pi(r_2^2 - r_1^2) = 2\pi\frac{1}{2}(r_2 + r_1)(r_2 - r_1)$. $2\pi\frac{1}{2}(r_2 + r_1)$ is the mean circumferential length and $r_2 - r_1$ the wall thickness so $\pi\rho L(r_2^2 - r_1^2) = M_c$, the mass of the cylinder. The conclusion is that the kinetic energy of the cylinder is

$$T_c = \tfrac{1}{2}I_c\dot{\theta}^2 + \tfrac{1}{2}M_c\dot{z}^2, \qquad I_c = \tfrac{1}{2}M_c(r_2^2 + r_1^2), \quad \dot{z} = -r_2\dot{\theta}\,. \tag{11b}$$

I_c is the moment of inertia of the cylinder about its axis of symmetry. The first term in Eq 11b is the energy within the rotation, and the second term is the energy in translation. Of course this is a well known result which could have been written down straight away, but the analysis shows where the model of centre of mass and moment of inertia comes from.

Now examine the dynamics of the iron bar alone. Since it has uniform density, its centre of mass C lie on the geometric centre-line of the bar at distance c from O where

$$c = \sqrt{r_1^2 - b^2} - a \tag{12a}$$

$\sqrt{r_1^2 - b^2}$ is the perpendicular distance from O to the bottom of the steel bar. Clearly any rounding of the corners of the bar would cause it to lie closer to the tube wall. The theoretical value is $27 \cdot 5$ mm which agrees fairly well with 28 mm as measured. C is therefore at general position

$$[-r_2\theta + c\sin\theta]\boldsymbol{e_z} + [r_2 - c\cos\theta]\boldsymbol{e_w}\,. \tag{12b}$$

The vertical component gives the potential energy V of the bar and hence of the combined object. The height through which the centre of mass of the bar is raised on turning is $(r_2 - c\cos\theta) - (r_2 - c) = c(1 - \cos\theta)$, making

$$V = M_b g c(1 - \cos\theta)\,. \tag{13}$$

The curve traced by C was known to renaissance geometers as a species of roulette ('rolling curve') called a curtate hypocycloid[4]. It is the locus of a point attached to a wheel which rolls around the inner surface of a larger circle, graphed in Figure 15 for $r_2 = 55$ mm, $c = 28$ mm. In our case the larger circle has infinite radius since the cylinder rolls on a horizontal plane. Note how the horizontal displacement is much greater when the object is 'upside down' with the bar higher than C ($|\theta| > \pi/2$).

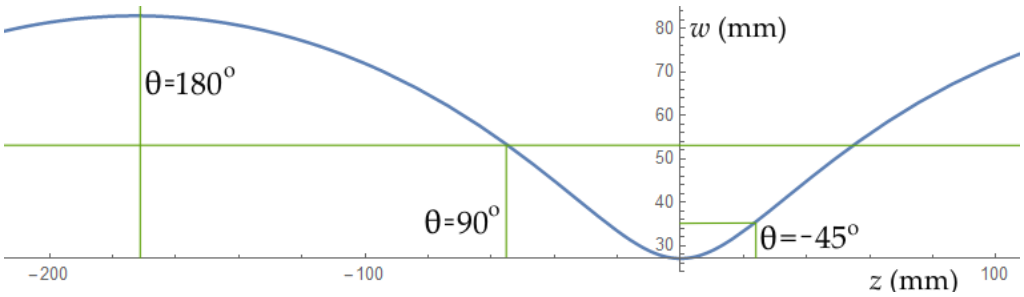

Figure 15: The hypocycloid traced by the centre C of the iron bar as the cylinder turns.

Consider now an element of the bar at (x, y) relative to C, as in Figure 13. When turned through θ, the z and w components of position relative to C become $x\cos\theta - y\sin\theta$ and $x\sin\theta + y\cos\theta$ respectively. The position vector of this element is therefore

$$\boldsymbol{p} = [-r_2\theta + c\sin\theta] + x\cos\theta - y\sin\theta\boldsymbol{e_z} + [r_2 - c\cos\theta + x\sin\theta + y\cos\theta]\boldsymbol{e_w}\,. \tag{14}$$

[4] 'Curtate' means that the point lies within the disc of the rolling wheel. If the point lies on its circumference, the curve is just called a cycloid, and if it is at the end of a rod protruding beyond the rim of the wheel, it is a prolate hypocycloid.

The gravitational potential energy of the element is $\rho L\,dx\,dy[p_w(\theta) - p_w(0)]$ where p_w is the vertical component of $\boldsymbol{p}$. By integrating this over the cross-section, $-a \le x \le a$, $-b \le y \le b$, we find that the potential energy of the bar is indeed correctly given by Eq 13. I will carry out the equivalent integration in full to obtain the kinetic energy. Letting $\boldsymbol{v}$ now denote the velocity of the element, we have

$$\boldsymbol{v} \;=\; \dot\theta\,\{-r_2 + c\cos\theta - x\sin\theta - y\cos\theta\}\,\boldsymbol{e_z} \;+\; \dot\theta\,\{c\sin\theta + x\cos\theta - y\sin\theta\}\,\boldsymbol{e_w}\,. \tag{15}$$

We wish to take the dot product of this with itself and integrate over x and y. Since the cross section of the bar is symmetric about C, any terms in $|v^2|$ which contain either x or y to the first power will integrate to $x^2/2$ from $-a$ to $+a$, $y^2/2$ from $-b$ to $+b$, and contribute zero to the integral. The only terms in $|v^2|$ which contribute are

$$r_2^2 + c^2 + x^2 + y^2 - 2r_c\,c\cos\theta\,.$$

Integrating,

$$|v^2|_{bar} \;=\; 4ab[r_2^2 + c^2 + \tfrac{1}{3}(a^2+b^2) - 2r_2 c\cos\theta]\,.$$

Since $4ab$ is the cross-sectional area of the bar and the mass of the element is $\rho L dx\,dy$, the kinetic energy of the bar is

$$T_b \;=\; \tfrac{1}{2}M_b[r_2^2 + c^2 + \tfrac{1}{3}(a^2+b^2) - 2r_2 c\cos\theta]\dot\theta^2\,. \tag{16}$$

Within this we identify two contributions

1. $\tfrac{1}{2}M_b(r_2^2 + c^2 - 2r_2 c\cos\theta)\dot\theta^2$ is the kinetic energy of a point mass M_b moving at the centre of mass C and can be called the translational contribution. You can obtain this from Eq 5b.
2. $\tfrac{1}{2}M_b\tfrac{1}{3}(a^2+b^2)\dot\theta^2 = \tfrac{1}{2}I_b\dot\theta^2$ is the energy of the bar rotating about its centre of mass at C. The moment of inertia is $I_b = \tfrac{1}{3}M_b(a^2+b^2)$.

Pulling together the various contributions, the total potential energy V is given by Eq 13, and the kinetic energy T by the sum of Eqs 2b and 7.

Before putting these values into Lagrange's equation let us look at an alternative interpretation based on the centre of mass, H, of the combined object. The position h of H is such that the moments of the cylinder and the iron bar balance:

$$M_c\,h \;=\; M_b\,(c-h) \quad \text{making} \quad h \;=\; \frac{M_b\,c}{M_b + M_c} \;=\; 23\cdot 3 \text{ mm}\,. \tag{17}$$

The co-ordinates of H are $z = -r_2\theta + h\sin\theta$, $w = r_2 - h\cos\theta$. From these the potential energy relative to the stable position is $V = (M_b + M_c)gh(1-\cos\theta)$ where M_b is the mass of the bar and M_c that of the cylinder. Substituting for h shows that this is just another way of stating Eq 6. Kinetic energy within the translation of the combined centre of mass is

$$T_{trans} \;=\; \tfrac{1}{2}(M_b + M_c)\left[r_2^2 + h^2 - 2r_2\,h\cos\theta\right]\dot\theta^2\,. \tag{18}$$

This can be recast as

$$\tfrac{\dot\theta^2}{2}M_b(r_2^2 - 2r_2 c\cos\theta) \;+\; \tfrac{\dot\theta^2}{2}M_c r_2^2 \;+\; \tfrac{\dot\theta^2}{2}(M_b + M_c)h^2\,.$$

The first two terms here are the translational energy of the bar and cylinder respectively. Using Eq 6 for h and c, the difference between (Eq 4b + Eq 7) and the above translational energy is

$$\tfrac{\dot\theta^2}{2}[I_b + I_c + M_b c^2 - (M_b + M_c)h^2] \;=\; \tfrac{\dot\theta^2}{2}\left[I_b + I_c + \frac{M_b M_c}{M_b + M_c}c^2\right]. \tag{19a}$$

We suspect that this is rotational energy about the centre of mass. By the theorem of parallel axes, if the cylinder rotates about H its moment of inertia is $I_c + M_c h^2$, and if the iron bar also rotates about H its moment of inertia is $I_b + M_b(c-h)^2$. The sum of these is

$$I_t \;=\; I_b + I_c + M_c h^2 + M_b(c-h)^2 \;=\; I_b + I_c + \frac{M_b M_c}{M_b + M_c} c^2 \qquad (19b)$$

also. We therefore conclude that an alternative representation of the motion is that the combined cylinder+bar rotate about their joint centre of mass H, and this translates in height and horizontal position according to Eq 16.

We now have to put the energy values into Lagrange's equation. I will use the centre of mass representation, and indicate the approximations when θ is small, as when it oscillates just before stopping. Write $M_b + M_c = M_t$, the total mass, and I_t for the total moment of inertia given by Eq 10a, b. The force term is

$$\frac{\partial V}{\partial \theta} \;=\; M_t\, gh \sin\theta \;\approx\; M_t gh\, \theta\,.$$

The inertia terms are

$$-\frac{\partial T}{\partial \theta} \;=\; -M_t\, r_2\, h\, \sin\theta\, \dot\theta^2 \;\approx\; -M_t\, r_2\, h\, \theta\, \dot\theta^2\,.$$

$$\frac{\partial T}{\partial \dot\theta} \;=\; \left[M_t(r_2^2 + h^2 - 2r_2\, h\cos\theta) \;+\; I_t\right]\dot\theta\,,$$

$$\frac{d}{dt}\left(\frac{\partial T}{\partial \dot\theta}\right) \;=\; \left[M_t(r_2^2 + h^2 - 2r_2 h\cos\theta) + I_t\right]\ddot\theta \;+\; 2M_t\, r_2\, h \sin\theta\, \dot\theta^2 \;\approx\; \left[M_t(r_2 - h)^2 \;+\; I_t\right]\ddot\theta\,.$$

The unapproximated equation of motion is

$$\left[M_t(r_2^2 + h^2 - 2r_2 h\cos\theta) + I_t\right]\ddot\theta \;+\; M_t\, r_2\, h \sin\theta\, \dot\theta^2 + M_t\, gh \sin\theta \;= 0\,. \qquad (20)$$

Compare this with the generic form in Eq 10c. The limiting case is when the amplitudes are very small. In simple harmonic motion the velocity will be greatest when $\theta = 0$, and zero when θ is at the limit of its excursion. Therefore one or other factor in $\sin\theta\,\dot\theta^2$ will be small through much of the cycle. It is probably reasonable, therefore, to take $\theta\,\dot\theta^2$ to be negligible. Writing $J = M_t/I_t$, the approximate equation of motion, assumed valid for small displacements without damping, is

$$\left[(r_2 - h)^2 \;+\; J\right]\ddot\theta + gh\,\theta \;=\; 0\,. \qquad (21)$$

This differential equation has already been obtained as Eq A1.2 in Appendix 1, §9 using the principle of conservation of energy. It describes simple harmonic motion with a radian frequency ω of

$$\omega^2 \;=\; \frac{gh}{(r_2 - h)^2 + J}\,. \qquad (22)$$

This can be compared with the frequency of a pendulum of length l for which $\omega^2 = g/l$.

To compare with experiment here are the numerical values and the theoretical frequency and period of oscillation:

M_t :	$2 \cdot 983$	kg
I_c :	$1 \cdot 428 \times 10^{-3}$	kg m^2
I_b :	$0 \cdot 661 \times 10^{-3}$	kg m^2
I_t :	$2 \cdot 417 \times 10^{-3}$	kg m^2
g :	$9 \cdot 814$	m s^{-2}
h :	$0 \cdot 0233$	m
r_2 :	$0 \cdot 055$	m
ω^2 :	$126 \cdot 0$	radians^2 s^{-2}
frequency :	$1 \cdot 786$	Hz
period :	$0 \cdot 560$	s

As with the lead roll, I measured the period of oscillations by taking a video picture of the movement at 50 frames per second, with a stop watch in the view too. By examining this frame by frame and taking measurements of the screen cursor position when it was placed on the image of edge of the tube, the graph in Figure 16 was obtained. This shows that one cycle takes 0.57 ± 0.01 seconds, giving a frequency of $1 \cdot 75 \pm 0.03$ Hz. This is in good agreement with the theoretical value. A correction can be estimated to allow for damping. Damping adds a term $D\dot{\theta}$ to the second order differential equation Eq 21 which imposes an exponential decay

$$\exp\left(-\frac{Dt}{2\left(M_t(h-r_2)^2+I_t\right)}\right).$$

Matching to the observed decay, $D = 0 \cdot 00152$, and the resulting increase in period is negligible.

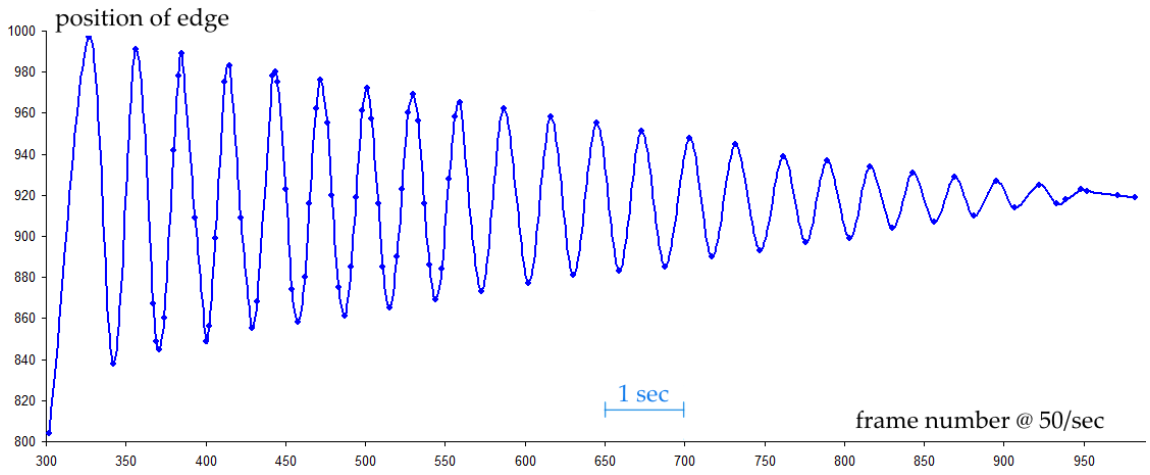

Figure 16: Measured amplitude of oscillations (in arbitrary units) as a function of time.

I used Mathematica to obtain numerical solutions of the exact differential equation, Eq 20, for increasingly large amplitudes. The oscillation remains sinusoidal, but the frequency decreases as the amplitude increases, a fact already noted in §1 for a simple pendulum. While the limiting small amplitude frequency is $11 \cdot 22$ radians/sec, it falls to $9 \cdot 83$ when $\theta(0) = 45°$ and to $7 \cdot 23$ when $\theta(0) = 90°$ before being released. The frequency has then dropped to less than 2/3, so the period has increased by over 50%. This is a significant effect, comparable with that seen with the lead roll, Figure 2, but not enough to explain the shuddering of a mandarin orange.

5 Cylinder rocking with nearly constant acceleration

We now return to the rocking plank. Thinking of it prompts the question 'What profile must the base of an object have for it to rock and roll with constant angular acceleration, or at least under a constant moment causing the acceleration'. Since the acceleration is proportional to the moment about the instantaneous point of contact, the curved base must have the property that the centre of mass maintains a constant perpendicular distance from every normal of the curve. As the cylinder turns, its normals must be tangent to a circle with centre H, the centre of mass. In other words the required curve is the one whose evolute is a circle. The inverse curve, the involute of the circle, is given by the parametric equations

$$x = \pm\sin\beta \mp \beta\cos\beta, \qquad y = -\cos\beta - \beta\sin\beta, \qquad \beta \geq 0. \tag{23}$$

as described in Appendix 2. The curve equation has to be expressed by these parametric relations since they cannot be solved for y in terms of x in closed form. Perhaps by coincidence the shape of this curve is close to the profile of the base of a mandarin orange as Figure 17 shows. The orange is shown stalk upwards. The right panel has superimposed the left and right involutes of a parent circle. Though the mandarin has a dimple in the centre of its base, it rolls through the upright position on the ring of peel around the dimple, so in any study the central inverted V-shaped notch should be filled in.

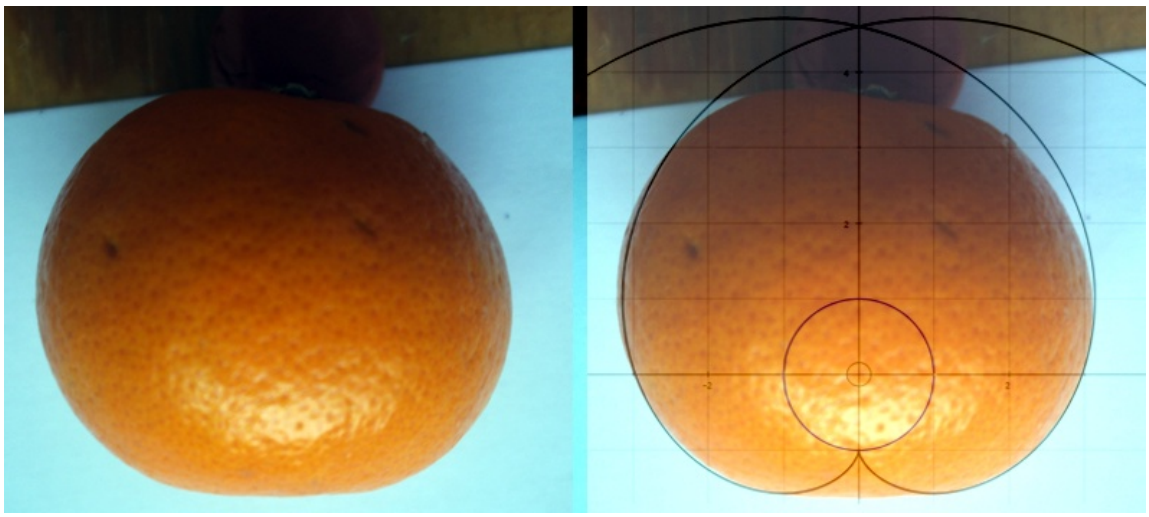

Figure 17: Left: photograph of a mandarin orange. Right: The same photo overlaid with a circle and its involute, showing the similarity of shapes.

5.1 Observations of the involute cylinder

I made a short cylinder with this profile, limiting its height to $y = 2$ units where the circle has unit radius, one unit being 30 mm. We can call it the 'involute cylinder'. It is made from three pieces of 25 mm thick plywood each cut with a jigsaw to this nominal profile around a printed template, then shaped by hand with a plane and abrasive paper. Irregularities were filled with a fibreglass resin mixed with putty and shaped to be as close to the intended profile as could reasonably be achieved by hand. Since the involute itself is re-entrant near where it joins the parent circle, I originally made the block with this V-shaped cut-out, but found that it landed with too much of a bang on the table and bounced before swinging to the opposite side. To promote smooth rolling I filled this cavity with fibreglass resin and profiled it to be almost flat, like the mandarin in the photograph. Consequently

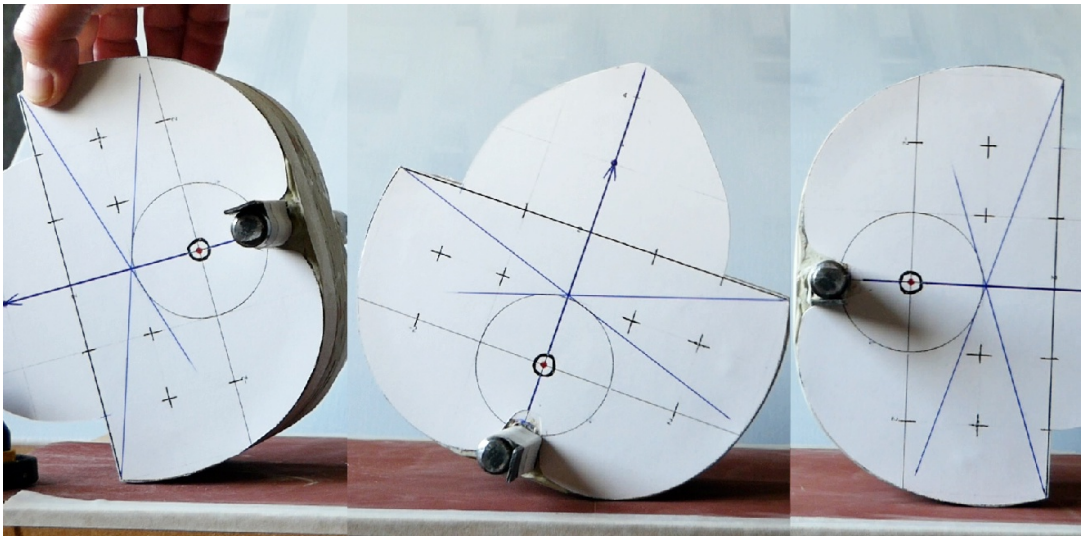

Figure 18: Three positions of the cylinder shaped to the involute of a circle as it rolls from left to right. The centre of mass in marked with a small disc inside the circle to which the curve is involute.

the angular range over which the profile departs from the strict involute is small – probably less than 4°. Also there was so much energy in the moving block that I found it necessary to increase its friction with the table by covering the table with sheets of fine abrasive paper. Figure 18 is a composite of three photographs of the block rolling from left to right. The mitre-shape at the top is only a piece of light card used to extend the y-axis line so as to increase its visibility in the video frames. The wooden block itself ends in a flat top at $y = 2$ units $= 60$ mm. In order for the centre of gravity to be at co-ordinates (0, 0), a steel rod 16 mm diameter has been inserted through the block near the base. The wood itself weighs 790g, the iron bar 300g making the total weight 1090 g.

The pictures show that it was easy to tilt this block to over 90° from its equilibrium position, from where it would quickly roll to about 80° on the other side, and rock to and fro for about 30 half-cycles. Figure 19 plots the tilt angle in degrees, the angular velocity and the angular acceleration for the first few cycles. The pale blue horizontal lines in the acceleration panel (bottom) indicate the left and right values of angular acceleration in each half cycle at about $\pm 2000°\mathrm{s}^{-2}$. With the angular acceleration almost constant the angular velocity must vary linearly with time, and the tilt angle parabolically, not sinusoidally as in simple harmonic motion. The shapes of these graphs are remarkably similar to those for the plank with slightly rounded base in Figure 7. This encourages the view that this object is essentially a plank with rounded base, even though its profile is nothing like a rectangle. It is quite impressive to watch this in motion. Of all objects it may be the one which will roll though the largest range of tilts.

The involute has the interesting property that the arc length from 0 to any value of $\beta > 0$ is $\beta^2/2$. As a result the instantaneous position of the centre of mass is simply related to tilt θ. The arc length on the involute to $\beta = \pi/2$ (at which $\theta = 0$) is $\pi^2/8$, but the arc length along the filled-in curve is only about 1; it would be 1 if the base were exactly flat between $x = \pm 1$. Hence on the as-made cylinder the arc length s_l to the left of the centre of the base (negative θ), or s_r to the right, is

$$s_l = \tfrac{1}{2}\theta(\theta - \pi) - 1\,, \quad \theta < 0, \qquad s_r = \tfrac{1}{2}\theta(\theta + \pi) + 1\,, \quad \theta > 0. \tag{24}$$

As the cylinder rolls to the left, the centre of mass H has co-ordinates $z = s_l{+}1$, $w = -\beta = -\theta{+}\pi/2$ where (z, w) is a co-ordinate frame in the ground surface, z horizontal, w aligned with the y axis where the

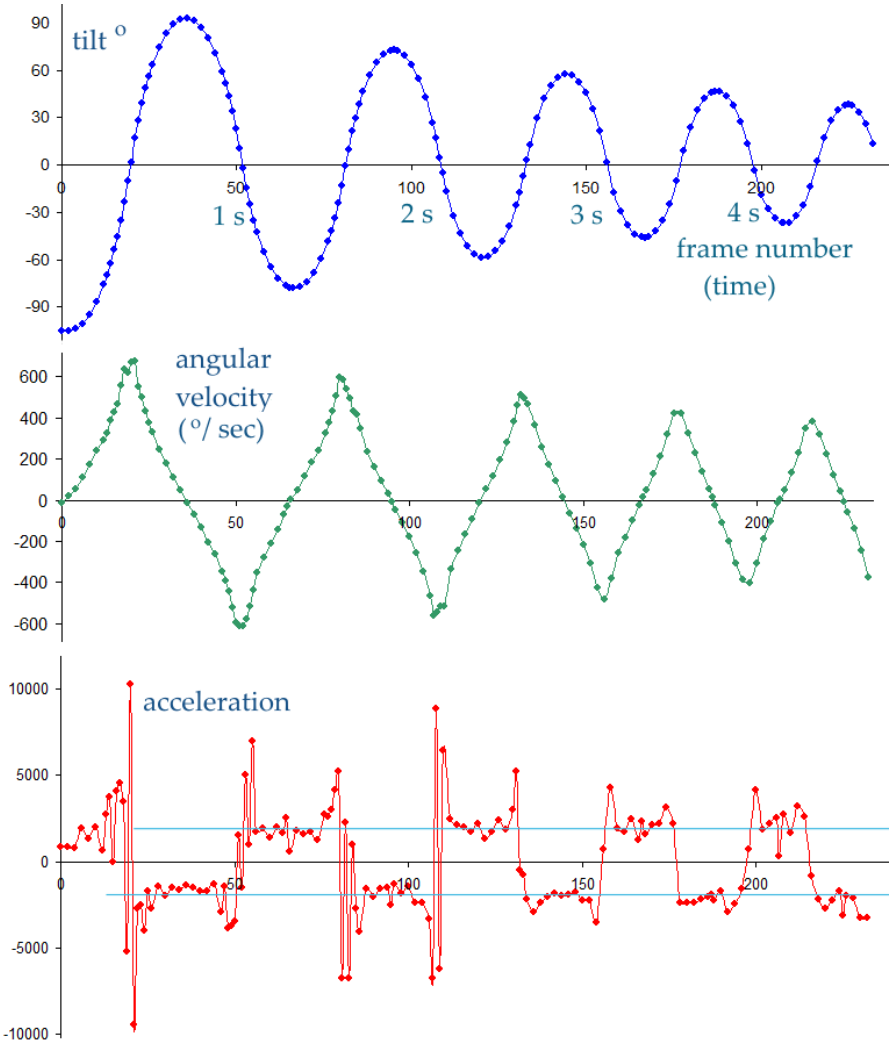

Figure 19: Measurements of the tilt, angular velocity and angular acceleration of the involute cylindrical block in Figure 18. Angles in degrees.

object is stationary. The corresponding position for tilts to the right is $z = s_r - 1$, $w = \beta = \theta + \pi/2$. When at rest, O is $\pi/2$ above the ground, so the potential energy is simply $mg|\theta|$. Figure 20 plots the experimentally measured horizontal and vertical positions of the centre of mass over the cycles observed in Figure 19. The vertical position is recorded here as $w - \pi/2$ which is the increase in height relative to the height at rest.

The reader may care to look at Appendix 3 which describes an experiment to measure the moment of inertia of this block.

5.2 Equation of motion

We now apply Lagrange's equation of motion to this dynamical system. We already have the potential energy $V = mg|\theta|$ and the considerations above, supported by Appendix 2, put us in a position to determine the kinetic energy, T. I will concentrate on $\theta \geq 0$ and use the co-ordinate frame (z, w) in which the position vector of the centre of mass at time t is

$$\boldsymbol{p} = (s_r - 1)\boldsymbol{e_z} + \beta \boldsymbol{e_w} = \tfrac{1}{2}\theta(\theta + \pi)\boldsymbol{e_z} + (\theta + \tfrac{\pi}{2})\boldsymbol{e_w} \tag{25}$$

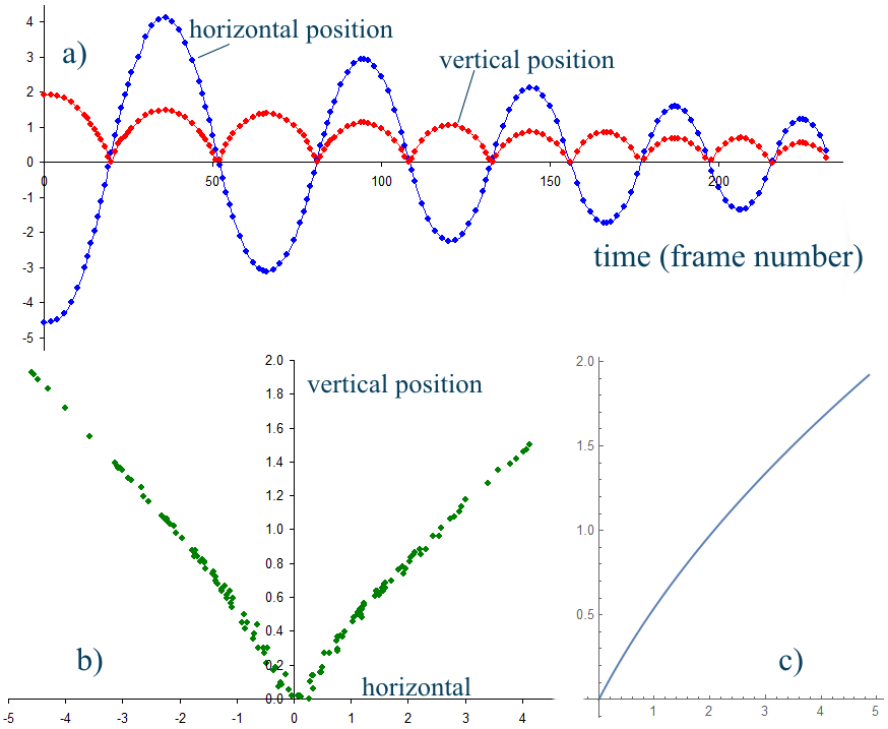

Figure 20: Position of the centre of mass as the involute cylinder rolls on a horizontal plane. Top a): Variation in z and $w - \pi/2$ with time. b) Measured locus of centre of mass over the cycles in a). c) Theoretical locus for $\theta > 0$ derived from the geometry.

where $\boldsymbol{e_z}$, $\boldsymbol{e_w}$ are unit vectors in the positive horizontal and vertical directions respectively. The velocity of the centre of mass is the time derivative of this:

$$\boldsymbol{v}_{trans} = (\theta + \tfrac{\pi}{2})\,\dot{\theta}\,\boldsymbol{e_z} + \dot{\theta}\,\boldsymbol{e_w}\,.$$

Taking the dot product of this with itself, the translational kinetic energy is

$$T_{trans} = \tfrac{1}{2}m[(\theta + \tfrac{\pi}{2})^2 + 1]\dot{\theta}^2\,.$$

The rotational kinetic energy is $\frac{1}{2}I\dot{\theta}^2$. Lagrange's equation, Eq 10, is therefore

$$[(\theta + \tfrac{\pi}{2})^2 + J + 1]\ddot{\theta} + (\theta + \tfrac{\pi}{2})\dot{\theta}^2 + g = 0 \qquad (26a)$$

where $J = I/m$. This can be expressed more succinctly in terms of β by using $\dot{\theta} = \dot{\beta}$:

$$(\beta^2 + J + 1)\ddot{\beta} + \beta\,\dot{\beta}^2 + g = 0. \qquad (26b)$$

This highly non-linear equation has the form of Eq 10c and can only be solved numerically. I am surprised at how complicated this is, considering that only three forces are present: gravity, the upwards reaction from the table, and the horizontal friction which prevent slipping. Of course position is inevitably tangled with velocity and acceleration whenever a body rolls.

In order to compare with experiment it is necessary to make some adjustment to the relatively simple equations of motion above:

1. The quantities g and J must be converted to the same scale of units in which the parent circle has unit radius. Let μ be the scale factor for lengths – actually $0\cdot030$ – which converts 1 unit into metres. Then $w = \mu\beta$, $z = \frac{\mu}{2}\theta(\theta+\pi)$. etc. and the equation of motion in terms of θ becomes

$$[(\theta+\tfrac{\pi}{2})^2 + \hat{J} + 1]\ddot{\theta} + (\theta+\tfrac{\pi}{2})\dot{\theta}^2 + \hat{g} = 0$$

where $\hat{g} = g/\mu = 327$ and $\hat{J} = I/(\mu^2 m) = 3\cdot16$ according to the theory in Appendix 3. However, the experiments also reported in Appendix 3 would place $\hat{J}$ somewhere between $3\cdot2$ and $3\cdot8$. There is therefore scope to pick a value in this range which gives a decent fit between the experimental and computed oscillation waveforms.

2. The computation must deal in some way with attenuation. In modelling the rocking plank, I assumed that a fraction of the velocity was lost in the instant that the plank swung upright. It would not be satisfactory to apply this discontinuous model to the involute cylinder since energy will be lost continuously throughout the motion due to friction. It seems better to add a dissipative term to the equation of motion equivalent to the velocity-dependent damping term added to an equation of simple harmonic motion. There is some discretion in how this is done; I have added a term proportional to the instantaneous velocity at the point of contact. This is $k(\theta+\frac{\pi}{2})\dot{\theta} = \kappa\beta\dot{\beta}$ where κ is a constant chosen to fit the experimentally measured rate of decay.

3. I propose to follow the same calculational scheme as for the rocking plank in §3, by calculating each quarter-cycle separately and concatenating them into motion over several full cycles. Each quarter-cycle ends or begins at $\theta = 0$ which is at either $z = -1$ or $z = +1$. Allowance needs to be made for the brief time that the block moves through the almost flat section between these z values. The video shows that it takes less than one frame at 50 per second to roll through this. The radius here suddenly increases from $\pi/2$ units to some large value, depending on just how flat the profile is. If we take this radius to be 20 units, say, the angle turned is traversing 2 units is 1/10 radian. The time to rock from $z = -1$ to $z = +1$ is therefore $1/(10\,\dot{\theta})$ where $\dot{\theta}$ is the angular velocity as the block enters this flat section. Typically this is less than $\frac{1}{100}$ second.

4. A further refinement would allow for the centre of mass not being precisely at the origin and centre of the parent circle. The as-built wood and steel cylinder had its centre of mass at about $y = -3$ mm, $0\cdot1$ units. This requires the expression for the potential and kinetic energies to have a additional terms dependent on θ. Let h be the distance from 0 to the centre of mass at H = $(0, -h)$. Eq 25 is modified to

$$\boldsymbol{p} = [\tfrac{1}{2}\theta(\theta+\pi) - h\sin\theta]\boldsymbol{e_z} + [\theta + \tfrac{\pi}{2} - h\cos\theta]\boldsymbol{e_w}\,.$$

The potential energy relative to the new zero position is $V = mg[\theta + h(1-\cos\theta)]$ and the translational component of kinetic energy becomes

$$T_{trans} = \tfrac{1}{2}m\left[(\theta+\tfrac{\pi}{2})^2 + 1 + h^2 + 2h\left(\sin\theta - (\theta+\tfrac{\pi}{2})\cos\theta\right)\right]\dot{\theta}^2\,.$$

The elaborated Lagrange equation of motion Eq 26a has the follow terms added to it:

$$\text{Eq 26a plus} \quad \left[h^2 + 2h\left(\sin\theta - (\theta+\tfrac{\pi}{2})\cos\theta\right)\right]\ddot{\theta} + h(\theta+\tfrac{\pi}{2})\sin\theta.\dot{\theta}^2 + gh\sin\theta\,. \qquad (28)$$

I will not copy out the full elaborated equation of motion; it aggregates the above modifications. Compare it with the generic form in Eq 10c.

I have written a computer program to integrate the equation of motion with all the above modifications. Some results are shown in Figure 21, for direct and close comparison with the experimental values in Figure 19. I am pleased with the agreement. To obtain this match the offset h of

the centre of mass below the origin was $0 \cdot 1$ units, or 3 mm in real space. I adjusted the moment of inertia term and the damping coefficient κ to match the waveform. Clearly increasing κ increases the decay rate of the peaks and troughs, but also slightly increases the periods of oscillation. Increasing $\hat{J}$ speeds up the oscillations. Values which give a close match are $\hat{J} = 3 \cdot 3$, $\kappa = 1 \cdot 7$. Here is a brief note on the computer algorithm, which I devised myself. The second order differential equation is solved by stepping forwards from given initial conditions on θ and $\dot{\theta}$. It uses the following algorithm:

1. Rearrange the differential equation to give an analytic expression for the second derivative, $\ddot{\theta}$.
2. Differentiate $\ddot{\theta}$ to find the third and fourth derivatives of θ with respect to time.
3. Assume that locally $\theta(t)$ behaves as a fourth order polynomial in t. Use the derivatives at the given starting point $t = 0$ to fit a fourth order polynomial to $\theta(0)$.
4. Choose a time step δt and evaluate the polynomial for $\theta(t + \delta t)$ and $\dot{\theta}(t + \delta t)$. Determine the 2nd, 3rd and 4th derivatives at $t + \delta t$ from the analytic expressions.
5. Hence step through sequential time steps. As a check on accuracy, evaluate the first and second derivatives across any three adjacent time steps using $\theta'(t) \approx (\theta(t + \delta t) - \theta(t - \delta t))/(2\delta t)$ and $\theta''(t) \approx (\theta(t + \delta t) - 2\theta(t + \delta t) + \theta(t - \delta t))/(\delta t^2)$.

The algorithm was checked extensively against numerical solutions by Mathematica.

I took the calculation out to half period 40 and fitted curves to the length of half-period against both time and against the half-period index number. If Δ is the half period and p the index, Excel gives as best fit $\Delta = 1 \cdot 19 p^{-0.536}$ for $25 < p < 40$. This corresponds roughly to

$$\Delta \approx \frac{6}{5\sqrt{p}} \text{ seconds}.$$

Unlike the rocking plank, this involute cylinder does not speed up in geometric series.

In terms of giving a simple explanation as to why the oscillations speed up, consider the three graphs in Figure 22. They are log plots of i) the amplitude calculated as angle between peak displacements to left and right, ii) the velocity at $\theta = 0$ between these left and right swings, and ii) the half-period time to move between these successive maxima. Note that all three values are decreasing; the object is indeed steadily slowing down. However, the distance travelled between peaks falls more quickly than the velocity. This must be a consequence of the shape of the base, and in particular how much tilt is required to raise the centre of mass to a point where the potential energy equals the kinetic energy in the middle of the swing. Since 'time taken = distance travelled / speed', the time taken decreases and we see the oscillations speed up. It is a paradox that it appears to get faster when it is actually slowing down.

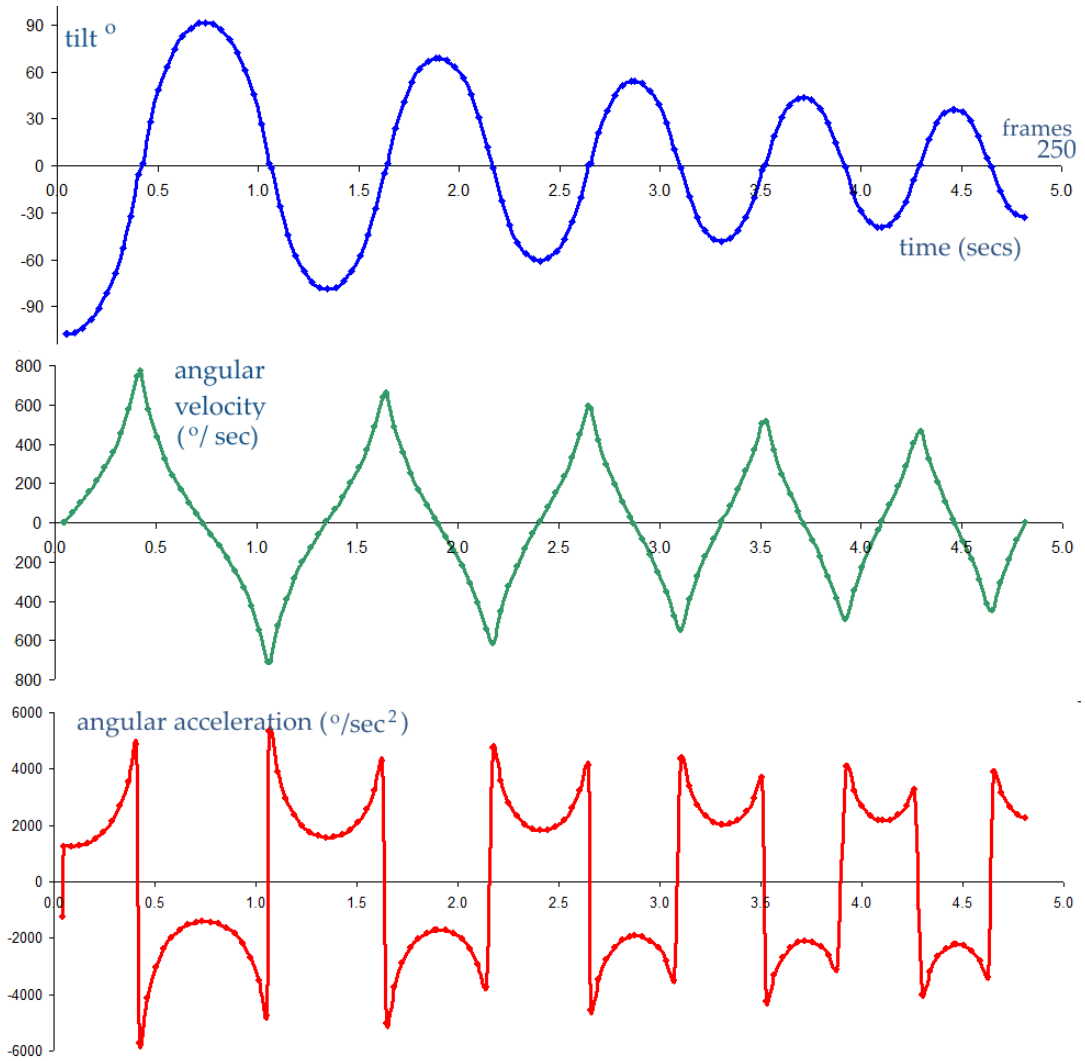

Figure 21: Theoretical graphs for the involute cylinder to compare with Figure 19.

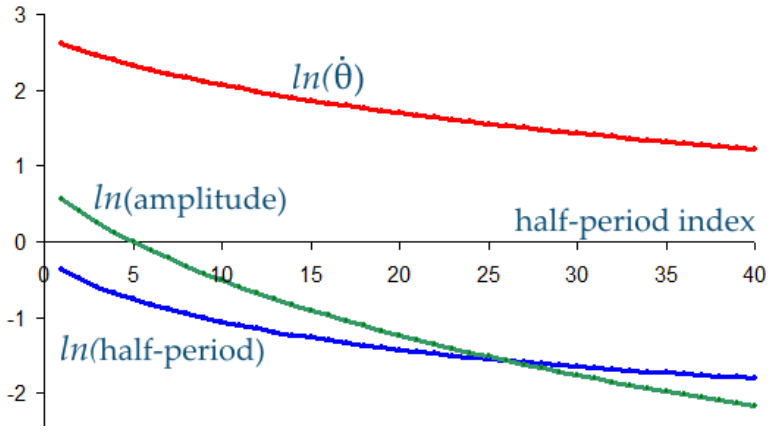

Figure 22: Logarithms of maximum angular velocity, left-to-right amplitude, and half-period plotted against the index number of the half-period for the involute cylinder.

6 The rolling ellipse

We switch our focus back to near-circular cylinders by examining the rolling elliptical cylinder, a generalisation of the circular cylinder with centre of mass H at its geometric centre. Once the symmetry is lost, either by H being displaced or the object becoming elliptical, H will ride up and down as it turns and it will be able to rock. The analysis here is for a case in which the centre of mass is on the vertical axis, distance h below O. In practice this could come about if the upper and lower halves were made of materials with different densities, or if a hole were made in the upper half, or it could be made by inserting a heavy metal bar into the lower half as with the involute cylinder in §5. I have not built such an elliptical cylinder so have no direct knowledge of how it would roll or rock, nor in particular whether its oscillations would speed up.

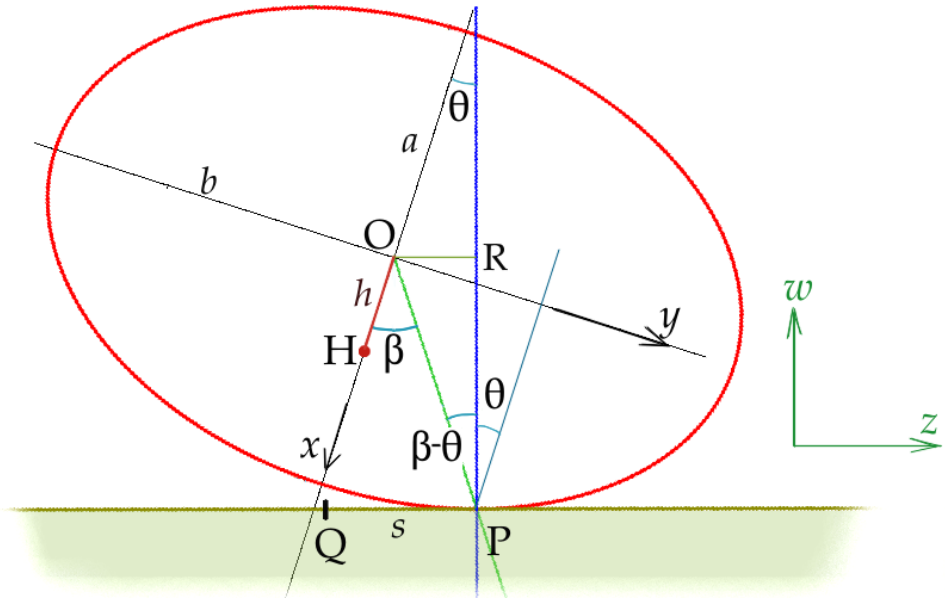

Figure 23: An ellipse, aspect ratio $a/b = 2/3$, rotated by $\theta = 18°$.

Analysis of the rocking eccentric ellipse is a generalisation of that for the tube and iron bar in §4, though the geometry complicates the expressions considerably. We know that we are looking for functions P, Q, $\hat{P}$, $\hat{Q}$ as in Eq 10b, c of §4.1 in terms of which the equation of motion can be stated. P and Q are defined by the geometry, and some formulae for the geometry of an ellipse are given in Appendix 2 at Eq A2.10 to A2.14.

Figure 23 shows an ellipse tilted at angle θ from its stable orientation. The x, y axes are fixed in the object with origin at the centre, O, and rotate with it. The unconventional view, with the x axis vertically downwards when at equilibrium, allows for the object rolling on its flatter surface. The semi-minor axis, therefore, is a, the semi-major b. The radius vector from O to P is at angle β from the positive x axis. As already stated, H is at distance h down the x axis below O. As in the analysis of other rocking objects, (z, w) is a second co-ordinate frame fixed in the ground with origin at Q, the position of P at equilibrium. The distance QP is s, the arc length rolled through.

It will be clear from triangle OPR that the position of O in the (z, w) frame is

$$O_z = s - r\sin(\beta - \theta), \qquad O_w = r\cos(\beta - \theta) \tag{29a}$$

and the position of the centre of mass at H is

$$H_z \;=\; s - r\sin(\beta-\theta) - h\sin\theta, \qquad H_w \;=\; r\cos(\beta-\theta) - h\cos\theta\,. \tag{29b}$$

The (z,w) position of a general point (x,y) after rotation is

$$p_z \;=\; s - r\sin(\beta-\theta) - x\sin\theta + y\cos\theta, \qquad p_w \;=\; r\cos(\beta-\theta) - x\cos\theta - y\sin\theta\,. \tag{29c}$$

We need the arc length s, plus r, β and θ in terms of a single independent variable, which I choose to be θ because of its obvious physical significance. Appendix 2 Eq A2.11 gives a parametrisation of the ellipse in terms of β and a relation between β and θ which allows conversion to θ:

$$x = r\cos\beta, \quad y = r\sin\beta, \quad r^2 = \frac{a^2b^2}{a^2\sin^2\beta + b^2\cos^2\beta}\,.$$

$$\frac{dy}{dx} = m = -\frac{b^2}{a^2\tan\beta}\,, \qquad \tan\theta \;=\; -\frac{1}{m} \;=\; \frac{a^2}{b^2}\tan\beta\,.$$

Let

$$C = a^2\cos\theta, \quad S = b^2\sin\theta, \quad G^2 = a^4\cos^2\theta + b^4\sin^2\theta = C^2 + S^2, \quad H^2 = a^2\cos^2\theta + b^2\sin^2\theta,.$$

G^2 and H^2 can also be written as

$$G^2 \;=\; \tfrac{1}{2}[a^4 + b^4 - (b^4 - a^4)\cos 2\theta], \qquad H^2 \;=\; \tfrac{1}{2}[a^2 + b^2 - (b^2 - a^2)\cos 2\theta]\,.$$

$$\text{Then} \qquad \sin\beta \;=\; \frac{S}{G}, \qquad \cos\beta \;=\; \frac{C}{G}\,, \qquad x \;=\; \frac{C}{H}, \qquad y \;=\; \frac{S}{H}\,.$$

$$r^2 \;=\; \frac{a^4 + b^4\tan^2\theta}{a^2 + b^2\tan^2\theta} \;=\; \frac{a^4\cos^2\theta + b^4\sin^2\theta}{a^2\cos^2\theta + b^2\sin^2\theta} \;=\; \frac{G^2}{H^2}\,,$$

$$\sin(\beta-\theta) \;=\; \frac{(b^2-a^2)}{G}\sin\theta\cos\theta\,, \qquad \cos(\beta-\theta) \;=\; \frac{H^2}{G}\,,$$

$$r\sin(\beta-\theta) \;=\; \frac{(b^2-a^2)}{H}\sin\theta\cos\theta\,, \qquad r\cos(\beta-\theta) \;=\; H\,. \tag{30}$$

To find the velocity we also need their derivatives with respect of θ, which will be denoted by the $\hat{}$ superscript:

$$\hat\beta = \frac{d\beta}{d\theta} \;=\; \frac{a^2b^2}{G^2}\,, \qquad \hat x \;=\; -\frac{a^2b^2\sin\theta}{H^3} \qquad \hat y \;=\; \frac{a^2b^2\cos\theta}{H^3}\,,$$

$$\hat s = \frac{ds}{d\theta} \;=\; \frac{a^2b^2}{H^3}\,, \qquad \hat r \;=\; \frac{a^2b^2(b^2-a^2)\sin\theta\cos\theta}{GH^3}\,.$$

A useful check on these values is that the element of arc length, given by $ds^2 = dx^2 + dy^2$ and equivalent to $\hat s^2 = \hat x^2 + \hat y^2$, can be expressed using an alternative small right-angled triangle formed by the end of the radius vector and the element of arc as:

$$r^2\hat\beta^2 + \hat r^2 \;=\; \hat s^2\,.$$

From Eqs 29b and 30 the potential energy is

$$V \;=\; mg[r\cos(\beta-\theta) \;+\; h(1-\cos\theta) - a]\,. \tag{31}$$

The velocity of a general point has z and w components

$$v_z \;=\; \big[\;\hat{s} \;-\; r(\hat{\beta}-1)\cos(\beta-\theta) \;-\; \hat{r}\sin(\beta-\theta) \;-\; x\cos\theta \;-\; y\sin\theta\;\big]\;\dot{\theta},$$

$$v_w \;=\; \big[\;-r(\hat{\beta}-1)\sin(\beta-\theta) \;+\; \hat{r}\cos(\beta-\theta) \;+\; x\sin\theta \;-\; y\cos\theta\;\big]\;\dot{\theta}\,. \qquad (32)$$

The expressions now can become messy and complicated though the principle is straightforward, and the same as in the previous dynamics cases. It is worth separating the terms which do not depend on x or y from those that do, since the total kinetic energy is obtained by integrating over x and y. Let $\hat{s} - r(\hat{\beta}-1)\cos(\beta-\theta) - \hat{r}\sin(\beta-\theta) = f(\theta)$ and $-r(\hat{\beta}-1)\sin(\beta-\theta) + \hat{r}\cos(\beta-\theta) = g(\theta)$ so that

$$\frac{v_z}{\dot{\theta}} \;=\; f(\theta) \;-\; x\cos\theta \;-\; y\sin\theta\,, \qquad \frac{v_w}{\dot{\theta}} \;=\; g(\theta) \;+\; x\sin\theta \;-\; y\cos\theta\,.$$

The kinetic energy of a particle at (x,y), density ρ, is $\frac{1}{2}\rho\,\dot{\theta}^2\times$

$$(f^2+g^2) \;+\; x^2+y^2 - 2x(f\cos\theta - g\sin\theta) - 2y(f\sin\theta + g\cos\theta)\,.$$

When this is integrated over the cross-section, if the cylindrical object is symmetrical in either x or y, the corresponding linear term will not contribute. In the diagram, Figure 38, the ellipse is symmetric in y. If the density is uniform, the kinetic energy of the whole object is

$$\tfrac{1}{2}\rho\dot{\theta}^2\left\{\;\; \int_{-b}^{b}\!\int_{a}^{-c}(f^2+g^2)\,dx\,dy \;+\; \int_{-b}^{b}\!\int_{a}^{-c} x^2+y^2-2x(f\cos\theta - g\sin\theta)\,dx\,dy \;\;\right\}. \qquad (33)$$

Here $-c$ marks the top surface of the object, the minus sign coming from the upside-down x axis. For a full ellipse $c = a$, while for a semi-ellipse it is 0. Since a complete ellipse is symmetric in x also, Eq 33 integrates to

$$\tfrac{1}{2}M_c\big[\;(f^2+g^2) \;+\; \tfrac{1}{4}(a^2+b^2)\;\big]\,\dot{\theta}^2 \qquad (34)$$

where the mass M has replaced $\rho\times$area, the area being πab.

This brings us to the moment of inertia, I. For a complete homogeneous cylinder of mass M_c this is $\frac{1}{4}M_c(a^2+b^2)$ about O. Eq 34a clearly has two terms, the first being the kinetic energy in moving the centre of mass at H=O, and the second the energy in rotation around it. If the object is only the lower semi-ellipse, mass M_h, its centre of mass is at $h = 4a/(3\pi) = 0\cdot4244a$. Its moment about O would be $\frac{1}{8}M_c(a^2+b^2)$ which is $\frac{1}{4}M_h(a^2+b^2)$ because $M_h = M_c/2$. By the theorem of parallel axes its moment about H is $\frac{1}{4}M_h(a^2+b^2) - 16M_ha^2/(9\pi^2) = 0\cdot07a^2 + 0\cdot25b^2$.

For the semi-ellipse Eq 33 integrates to

$$\tfrac{1}{2}M_h\left[(f^2+g^2) \;+\; \tfrac{1}{4}(a^2+b^2) - 2h(f\cos\theta - g\sin\theta)\;\right]\,\dot{\theta}^2\,. \qquad (35a)$$

We should not be surprised that the position h of the centre of mass appears in this because integration of x over the sectional area is how the position of H is calculated. The second term can be split as $[\frac{1}{4}(a^2+b^2) - h^2] + h^2$ and Eq 35a rewritten as the sum of translational and rotational components about the centre of mass H at $x = h$:

$$T_{trans} + T_{rot} \quad \text{where} \quad T_{trans} \;=\; \tfrac{1}{2}M_h\big[\;(f^2+g^2) + h^2 - 2h(f\cos\theta - g\sin\theta)\;\big]\,\dot{\theta}^2$$

$$\text{and} \quad T_{rot} \;=\; \tfrac{1}{2}M_h\big[\tfrac{1}{4}(a^2+b^2) - h^2\big]\,\dot{\theta}^2 \;=\; \tfrac{1}{2}I_H\,\dot{\theta}^2\,.$$

where I_H is the moment of inertia about H. Clearly, for any other design of ellipse in which the centre of gravity has been displaced downwards, the kinetic energy is given by

$$T \;=\; \tfrac{1}{2}M_h\big[\;(f^2+g^2) + h^2 - 2h(f\cos\theta - g\sin\theta)\big]\,\dot{\theta}^2 \;+\; \tfrac{1}{2}I_H\,\dot{\theta}^2\,. \qquad (35b)$$

The quantities in f, g are

$$f^2+g^2 \;=\; \hat{s}^2 \;+\; r^2(\hat{\beta}-1)^2 \;+\; \hat{r}^2 \;-\; 2\hat{s}\left[\, r(\hat{\beta}-1)\cos(\beta-\theta) \;+\; \hat{r}\sin(\beta-\theta)\,\right]. \tag{36}$$

$$\text{and} \qquad -f\cos\theta + g\sin\theta \;=\; r(\hat{\beta}-1)\cos\beta + \hat{r}\sin\beta - \hat{s}\cos\theta\,.$$

We now have all the building blocks of the problem and can formulate Lagrange's equation of motion. For a circular section, $b = a$, there is much simplification and we obtain the relations which led to Eq 20 in §4.2 for the tube with the steel bar inside. For $b \neq a$ the equation of motion is complicated so I will present it in terms of the functions P and Q in the generic Lagrange equation, Eq 10b, c of §4.1. For reference

$$T \;=\; \tfrac{1}{2}MP\dot{\theta}^2 + \tfrac{1}{2}I\dot{\theta}^2, \qquad V \;=\; MgQ$$

$$\frac{\partial V}{\partial\theta} \;=\; Mg\hat{Q}, \qquad \frac{\partial T}{\partial\theta} \;=\; \tfrac{1}{2}M\hat{P}\dot{\theta}^2\,, \qquad \frac{\partial T}{\partial\dot{\theta}} \;=\; (MP+I)\dot{\theta}\,, \qquad \textit{copy of } (10b)$$

$$\frac{d}{dt}\left(\frac{\partial T}{\partial\dot{\theta}}\right) \;=\; (MP+I)\ddot{\theta} + M\hat{P}\dot{\theta}^2\,.$$

Writing $I/M = J$ the equation of motion is

$$(P+J)\ddot{\theta} \;+\; \tfrac{1}{2}\hat{P}\dot{\theta}^2 + g\hat{Q} \;=\; 0\,. \qquad \textit{copy of } (10c)$$

From Eq 29b

$$Q \;=\; r\cos(\beta-\theta) \;+\; h(1-\cos\theta) - a, \qquad \hat{Q} \;=\; -r(\hat{\beta}-1)\sin(\beta-\theta) \;+\; \hat{r}\cos(\beta-\theta) \;+\; h\sin\theta\,, \tag{37}$$

$$P \;=\; f^2+g^2+h^2-2h(f\cos\theta - g\sin\theta), \qquad \tfrac{1}{2}\hat{P} \;=\; f\hat{f}+g\hat{g}+h[(f+\hat{g})\sin\theta - (\hat{f}-g)\cos\theta]\,.$$

These relations are enough for computer software to determine numerical solutions.

In looking for evidence of shuddering there are three variables to be examined: the ratio b/a, h, and the initial displacement, θ_0. I have used Mathematica to carry out a sample. The six panels in Figure 24 shows results for an elliptical cross section with ratio 3/2 for various values of h. This is for a notional wooden ellipse with $a = 10$ cm, $b = 15$ cm, 10 cm thick with specific gravity $0{\cdot}6$, so the mass is $2{\cdot}83$ kg and moment of inertia $I = 0{\cdot}023$ SI units. Starting with $h = 0$ (centre of mass in the centre, O), h is incremented in 25 mm stages but the mass and moment of inertia remain constant. This is rather contrived, but allows ready theoretical comparisons; it could be achieved in practice with suitable uneven distributions of mass. θ_0 is the initial displacement in radians, which is the amplitude of oscillation as the assumption is of no attenuation. As with the plank, the maximum velocity $\dot{\theta}_1$ occurs when $\theta = 0$. In all panels the horizontal axis is the amplitude/initial tilt. A uniform ellipse with centre of mass at $h = 0$ is in unstable equilibrium position when $\theta = \pi/2$ radians, when it stands on its pointed end. If $h > 0$ so the centre of mass is off-centre, it can balance precariously at tilt greater than $\pi/2$. At this position there is no moment of the centre of mass from the vertical, but the slightest displacement will cause the block to accelerate and roll. Clearly this first quarter cycle will take a relatively long time because the driving torque is near zero to start. For smaller initial tilts the centre of mass has a larger offset from the vertical and so there is a larger torque causing angular acceleration. This in broad terms accounts for the shape of the curves in panels a and b. These show the same information since frequency is just the reciprocal of period. The frequency changes almost linearly over most of its range. The highest frequency is when the motion has become simple harmonic and is given by

$$\omega^2 \;=\; \frac{g(b^2-a^2+ah)}{a[J+(a-h)^2]}\,. \tag{38}$$

The lower four panels in Figure 24 show the effect of increasing h as the centre of mass moves towards the base of the resting ellipse. These cover a smaller range of initial tilts, up to $1 \cdot 2$ radians, 69°. Panel c plots the half period, which approaches a constant for each h, and d is the corresponding frequency plot. In all cases for small amplitudes the frequency tends to a constant, but this constant terminal frequency is highest when the centre of mass is low, as we might expect. The graphs clearly show that the frequency does not continue to increase as the amplitude decreases towards zero; instead it becomes settled and the ellipse undergoes simple harmonic motion with frequency given by Eq 38. Panel e shows that the velocity falls almost linearly with amplitude, and panel f shows that their ratio approaches a constant for each value of h. The graphs in panel f are similar to those in c, and in fact the limiting values in c are π times those in f. This is in line with 'time = distance /velocity'.

Would we observe that an ellipse seemed to shudder before coming to rest? Clearly the frequency does steadily increase towards a limiting value, and if the initial tilt were close the 90°, the first cycles would be slow, so enhancing the impression of much speeding up. I have not built an ellipse to see for myself. Perhaps the question can be answered by comparing the graphs in Figure 24 with similar graphs for other rocking cylinders which we do feel speed up to a closing shudder. Figure 24 f for the ellipse is very different from the equivalent plot for the plank in Figure 10. The plank does not undergo SHM and has no limiting frequency.

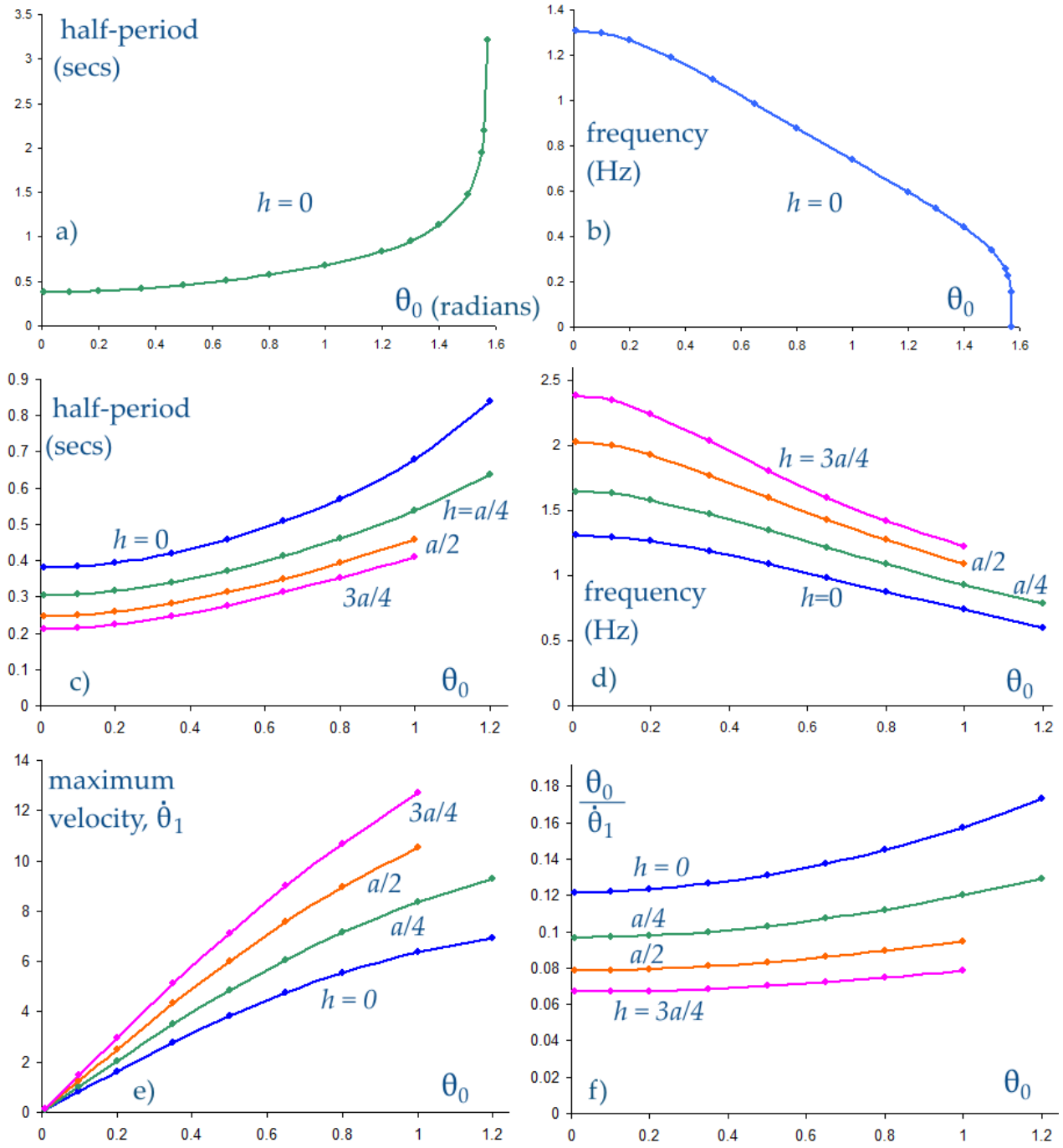

Figure 24: The period and frequency of oscillations of an elliptical cylinder, $b/a = 3/2$, for various positions h of the centre of mass. Panel a): half-period versus initial tilt from 90° starting tilt. b): frequency versus initial tilts up to $\pi/2$ radians for $h = 0$. c), d): half period and frequency v initial tilt for four h. e): maximum velocity at the upright position, f): ratio $\theta_0/\dot{\theta}_1$.

7 Observations of cylinder with flattened base: $y = Ax^4$

This and the next section deal with profiles of the form $y = Ax^4 + Bx^2$ which span the range of shapes from parabola to circle, to ellipse and to cylinders with increasingly flattened base. By varying the coefficients A and B it should be possible to study the transition from SHM to shuddering and thereby identify the conditions at which the rocking behaviour changes from one type to the other.

In this section I give an account of experiments on the oscillation of a specially made object with a flattened curved base, photographed in Figure 25. In shape this is somewhere between the plank of §3 and the involute cylinder of §5 in that it has a flattened base and steep side, and is stable lying on either. I made the profile to be close to $y = x^4$ because this is almost flat near $x = 0$ and as a mathematical function I hoped it would be not be too complicated to manipulate. By having a carefully defined base shape it should be possible to study the oscillations as they become very small. This is not possible with the involute block because of its relatively ill-defined central section.

7.1 Construction of the cylinder

This constant cross-section block is made from four pieces of thick plywood cut with a jig-saw to a guide curve and glued together to a thickness of 96 mm. As with the involute block, a thin coating of resin mixed with fibreglass putty was applied to fill small irregularities around the edge, and the whole profiled by hand with abrasive paper to fit as closely as I could judge to the paper template plot of $y = x^4$, with 1 unit = 69 mm. The section extends in x (width) to $\pm a$ and so has height $W = Aa^4$, which is 2 units in this case, being 138 mm in the model. The block is 149 mm wide at the top and weighs 930 g. Subsequent measurements showed that the overall profile was closer to $1 \cdot 5x^4$ and the base closer to $1 \cdot 2x^4$, as I had made the sides slightly too steep. In the photograph H marks the axis containing the centre of gravity which is at 5/9 of the height. Appendix 2 gives more detail on the geometry.

Figure 26 shows the cylinder at tilt θ from its stable position, and defines the variables. The sign convention is that θ is positive if the object rolls clockwise to the right so that P, the point of contact, moves in the positive sense. The shape is defined in terms of the (x, y) co-ordinate system,

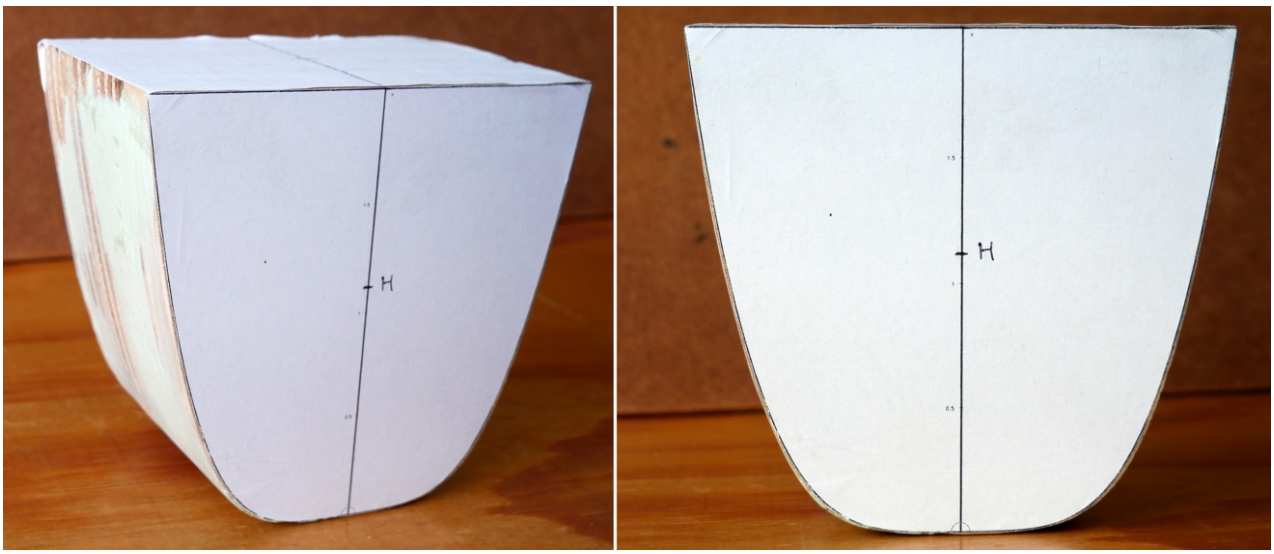

Figure 25: A wooden block cut to the profile $y = 1 \cdot 5\, x^4$.

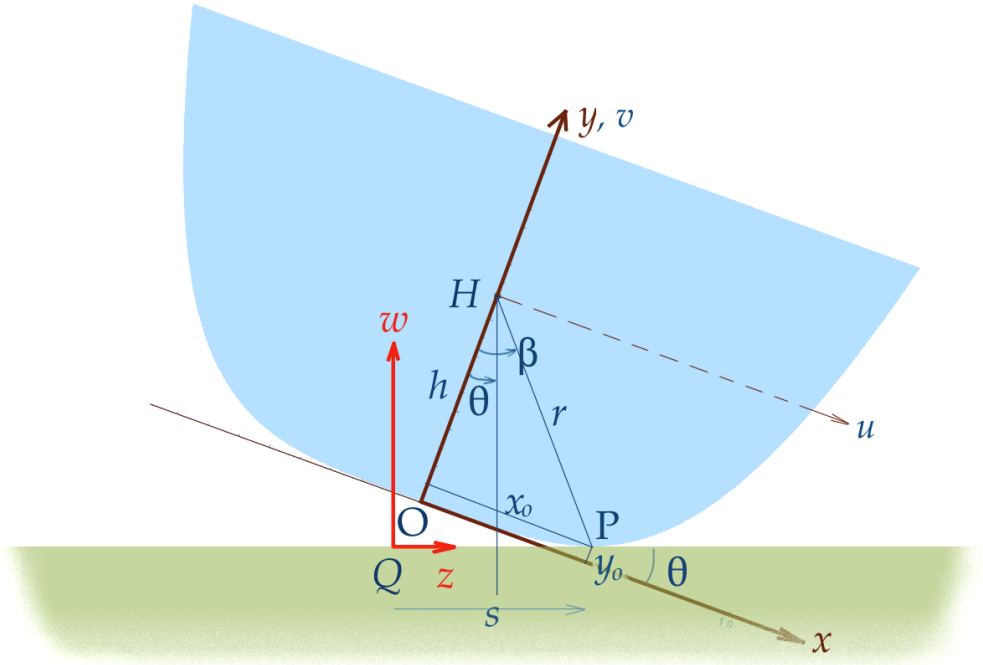

Figure 26: The cylinder with a flat-bottomed sectional profile tilted from its equilibrium position.

origin O in the centre of the base and symmetrical about the y axis. The (x, y) frame turns with the cylinder. The centre of mass at H is at distance h up the y axis from the base, so h = OH. Note the change in axes and in the definition of h from the ellipse. A separate fixed co-ordinate system, (z, w), is defined in the ground plane. Its origin is Q which is where the origin O of (x, y) would be when there is no tilt. The normal at the instantaneous contact point P = (x_0, y_0) is vertical. The arc length s from O to P equals the linear distance QP through which it has rolled.

I measured the as-made cross-sectional profile of the block in two ways. The overall shape was found by scanning the block's front and back faces on an A4 digital scanner and measuring about 50 points around the image of its edge in pixels using the on-screen cursor monitor. The overall profile was found to correspond quite closely to $y = 1 \cdot 5\,x^4$. The second method was to measure the base over which the cylinder rocks. The block was turned upside down with the flat face on a smooth

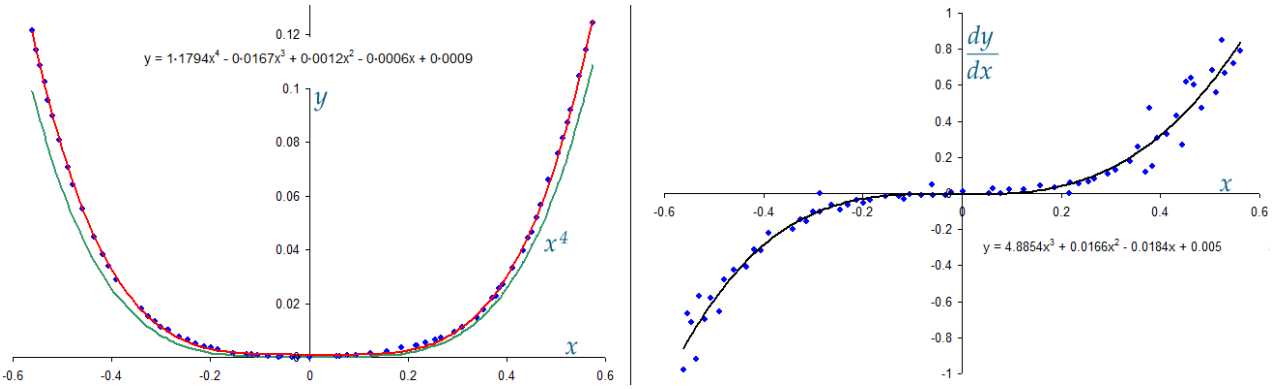

Figure 27: Left: measured sectional shape of the wooden block compared with $y = x^4$. Right: derivative with fitted cubic curve.

horizontal table. Above was fixed a dial gauge reading vertical displacement to $0 \cdot 01$ mm. The block was pushed along the table in small increments and a point reading of height taken at each from the dial gauge, and a precise measurement of the horizontal position relative to a reference position, equivalent to x_0, using an engineer's vernier calliper reading to $0 \cdot 1$ mm. At first the base profile corresponded to $y = x^4 + x^2/10$. I had already started making measurements on the oscillations by this time, and a few of these are described below. I subsequently made a concerted effort to reshape it to $y = Ax^4$ by gently flattening the base even more. Very little material was removed in this reshaping, leading me to the see how sensitive the oscillations are to the precise shape. Measurements of the final base are plotted in the left panel of Figure 27, while the right panel is the divided difference which approximates the gradient. The trend line fitted by the Excel spreadsheet is a close fit to $y = 1 \cdot 18x^4$, while integrating the fitted cubic on the right gives $y = 1 \cdot 22x^4$. In comparisons with theory we can take $A = 1 \cdot 2$. So the base profile is slightly different from the overall one.

7.2 Measurement of oscillations

To measure the oscillations I used the same technique as before, namely, photographing it either from above or from the side at 50 frames per second with a digital camera. The three graphs in Figure 28 show how the half-period becomes shorter. The horizontal axis in a) and b) is the time since the start of the oscillations indexed by the video frame number. Panel a) plots the half period and b) its reciprocal. The green trend line is close to $\Delta t = 8400/(t + 125)$ where Δt is the half period and t the time. This means that if the first $2\frac{1}{2}$ sec are ignored and time t' counted from frame 125, the half period is inversely proportional to t' with $\Delta t \approx 8400/t'$. When the block is released, it first seems to balance with almost no movement, then totters into a swing to and fro before speeding up as the amplitude decreases until coming to a stop when the half period is about $7 \cdot 5$ frames, corresponding to a full period of $0 \cdot 30$ secs and frequency $3 \cdot 3$ Hz. In panel c) the left-to-right peak amplitude of z_h is plotted against its half-period – the time between left and right excursions. This shows a trend to a linear relation for small amplitudes and half-periods. A straight line fitted to these points is 'half-period $= 0 \cdot 53\times$ amplitude $+ 0 \cdot 13$ secs'.

The waveform, as represented by the horizontal displacement of point H, is plotted in the three panels of Figure 29. The two upper panels show the first 400 frames from the block's ungainly, asymmetric start. The lower left shows a mid-motion sample, and lower right some cycles close to settling. The unit of displacement is the same unit used in drawing $y = Ax^4$, being 69 mm on the wooden block. Despite my earnest efforts in shaping the base, the motion shows significant asymmetry near its start.

While videoing the oscillations the ground plane was a thick sheet of glass, and the initial tilt of the block, to the left, was close to the limit beyond which it would fall onto its side. Motion was measured frame by frame in the video editor with positions and angles on the screen measured point by point by placing the cursor on the images of O, H, and also P as far as P could be recognised. As before, tools were an on-screen pixel position ruler and on-screen protractor. The on-screen co-ordinates were scaled to 1 unit = 69 mm, and shifted to allow for a 2° misalignment of the camera from vertical. The horizontal position of H, z_H, swings through a relatively large distance and is quite easy to measure from the screen, so I focused on this. Over the first few cycles I measured O, H and P and found relations amongst them so that for later cycles it was necessary only to determine z_H; other co-ordinates could be deduced from this alone. For example, the tilt was measured directly with an on-screen protractor, and also calculated from the positions of O and H, since OH is the y axis. The graph of these two values of θ is $\theta_{OH} = 1 \cdot 005\,\theta_{direct} - 0 \cdot 02$ degrees; that is, almost exact agreement. In contrast, judging the point of contact, P, was not precise. It involved a by-eye estimate of where the tangent to the curved base was parallel to the edge of the glass plate. Because

the object rocks quickly through the resting position at $\theta = 0$, there are few points there, and they are also the least accurate. The graph of x_0 direct against $((\tan\theta)/4 \cdot 8)^{1/3}$ has a gradient of only $0 \cdot 93$ instead of 1. However, considering the imprecision of the direct measurement, I consider this adequate and will use the formula to derive x_0 in the graphs below.

Empirical approximate relationships between z_H and some other parameters are as follows:

- Figure 30 plots w_H, the vertical displacement of H, against its horizontal displacement, z_H. This is a shallow V-shaped curve; w_H departs only slightly from zero, though this height change provides the gravitational potential energy to drive the motion. This curve is determined entirely by the shape of the block. The graph is higher to the left because that was the initial displacement, but there is intrinsic asymmetry in the unequal angles of the V-shape. For what they are worth, the fitted parabolas are

$$\begin{cases} z_H \le 0: & w_H = -0 \cdot 202\, z_H^2 - 0 \cdot 230 z_H + 1 \cdot 111, \\ z_H \ge 0: & w_H = -0 \cdot 133\, z_H^2 + 0 \cdot 124 z_H + 1 \cdot 111. \end{cases}$$

- The position of origin O is charted in Figure 29. By combining the positions of O and H angle θ is given by $\tan\theta = (z_H - z_O)/(w_H - w_O)$.

- A simpler direct empirical formula relates $\tan\theta$ to z_H, namely $\tan\theta \approx 0 \cdot 899 z_H - 0 \cdot 011$. This agrees well with the values calculated from H and O using the fitted polynomials above; a linear

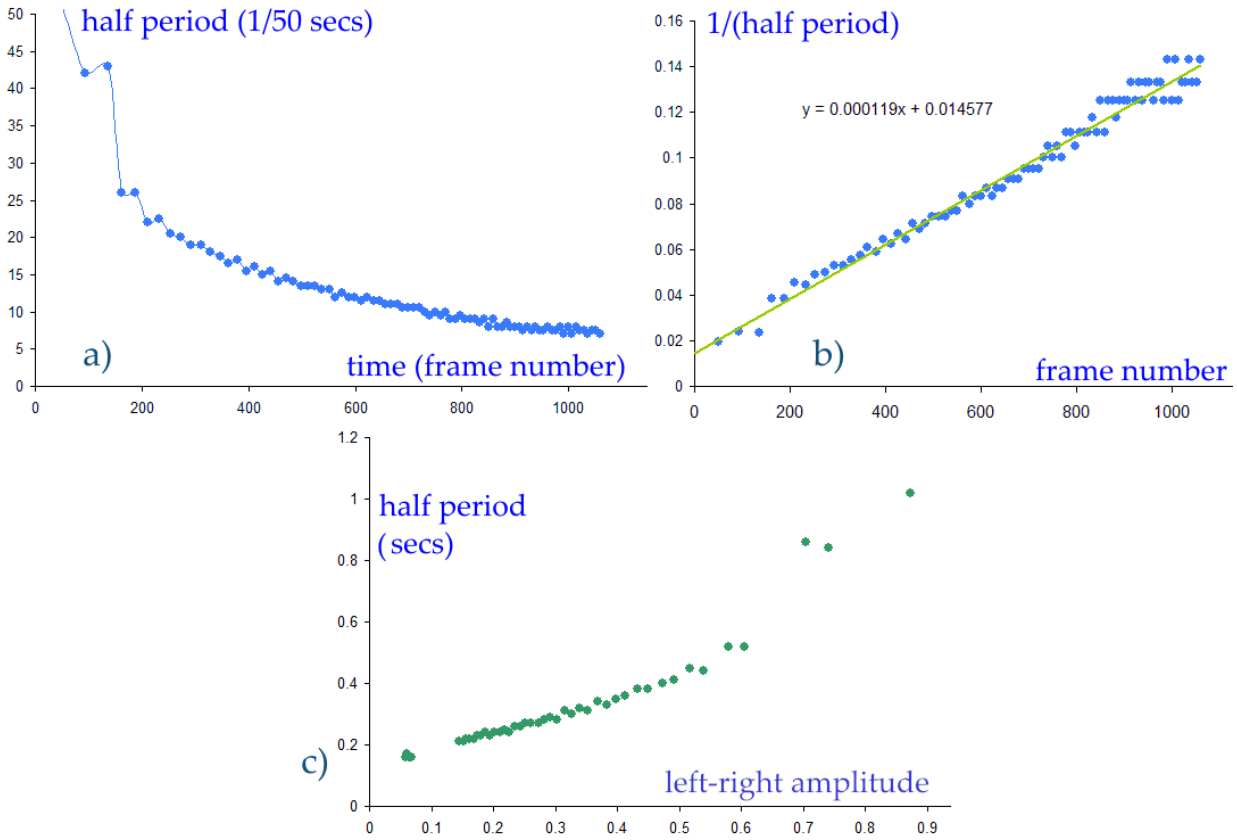

Figure 28: The shortening half period of oscillations of the block in Figure 23. a) half periods against time. b) their reciprocal. c) amplitude of z_h versus half-period.

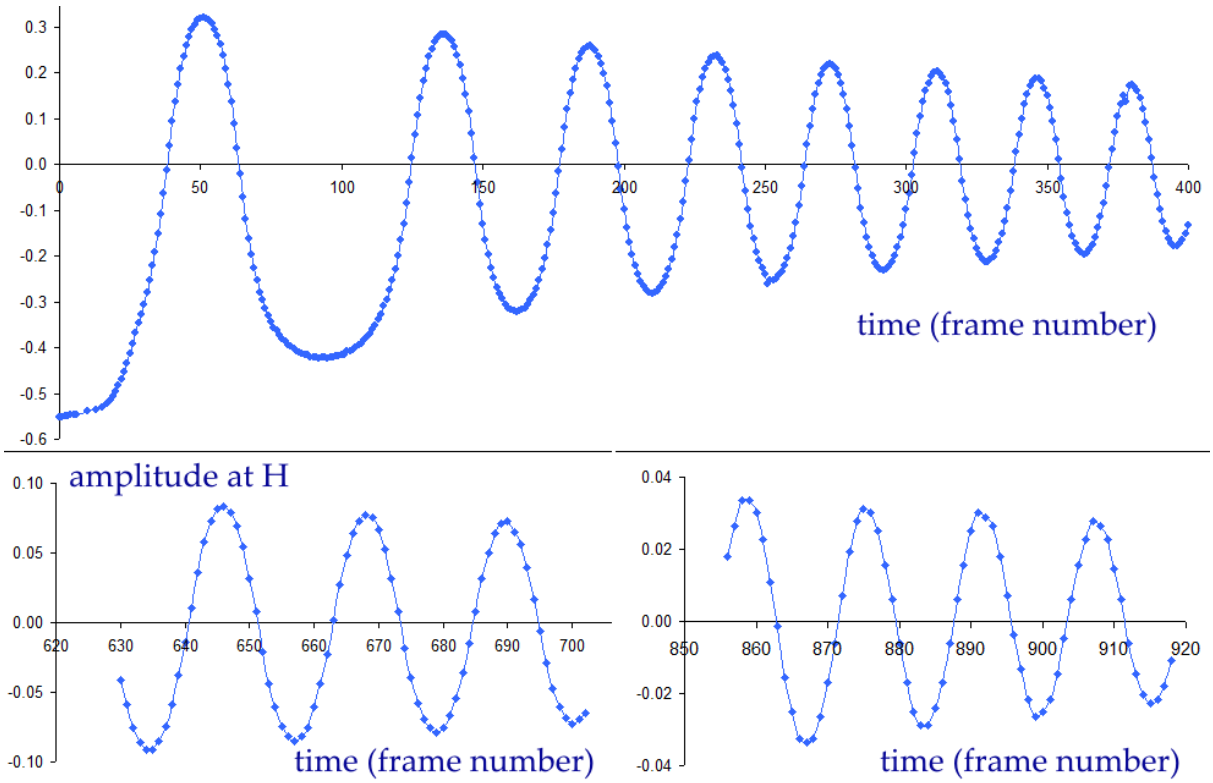

Figure 29: Waveforms of the oscillations in terms of the horizontal displacement of H from equilibrium, at three stages of the motion.

relation is found with $\tan\theta \approx 0\cdot896 z_H \pm 0\cdot014\, z_H$. As a working value, therefore, we can take $\tan\theta \approx 0\cdot9 z_H$. Reversing this relation gives $z_H \approx 1\cdot11\tan\theta$ which empirically is $z_H = h\tan\theta$, where h is the distance of the centre of mass from the origin O.

- For $z_H > -0\cdot5$ there is an almost equally good linear fit of $\sin\theta$ to z_H: $\sin\theta \approx 0\cdot841 z_H - 0\cdot007$.
- The contact point P is at (x_0, y_0) where $x_0 = ((\tan\theta)/4\cdot75)^{1/3}$. The relation with z_H is $x_0 \approx 0{\cdot}5755\sqrt[3]{z_H}$. This is quite a good fit to the data, though a better one is $x_0 \approx 0{\cdot}5755\sqrt[3]{z_H} - 0{\cdot}005$. The small constant here arises from errors in measurement and small asymmetries in the wooden block itself. I have used the latter formula to convert z_H values to x_0.

In the analysis of this oscillating object in §8 below I have used x_0 as the principal co-ordinate because it seems to feature most fundamentally in the expressions which arise. Our interest must focus, therefore, on the time variation of x_0. Using the measured values of z_H I have calculated x_0 according to $x_0 \approx 0\cdot5755 z_H^{1/3} - 0\cdot005$ and hence its first and second time derivatives. The derivatives of z_H are plotted in Figure 32 for the three episodes in the motion whose horizontal position has already been plotted in Figure 29. These two figures correspond directly. As with the plank and the involute cylinder, it is striking that $dz_H/dt = \dot{z_H}$ follows a zigzag of almost piecewise straight lines. There is some softening of the locus in the lower right panel towards the end of the motion, but it is still more angular than the sine curve of simple harmonic motion. Numerical approximations to the second derivative d^2z_H/dt^2 are plotted in Figure 31 for the same three episodes. The earlier episode in the top panel has a clearly discernible square-like wave. These mean that z_H itself varies not in a sinusoidal manner but in a series of piecewise parabolas. The later episode looks rather more like a sine wave, showing a tendency towards simple harmonic motion at vanishingly small amplitudes.

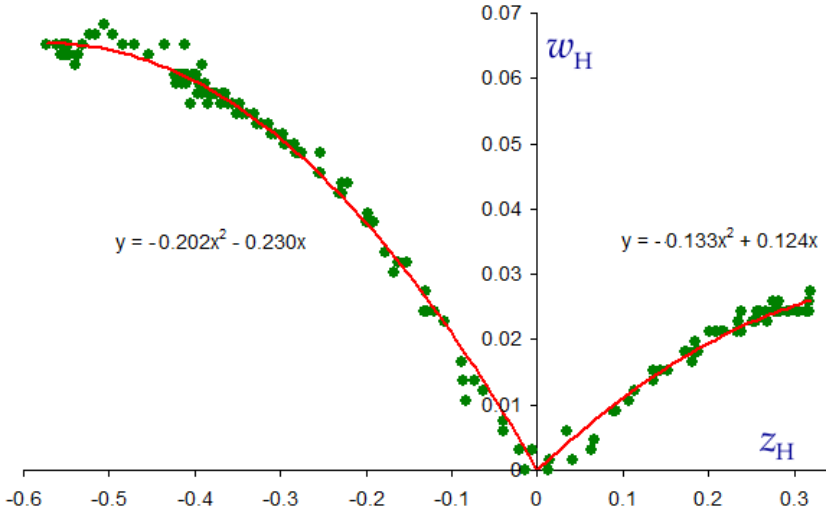

Figure 30: The height w_H of the centre of mass, H, in relation to its horizontal displacement, z_H for the block with profile $y = 1 \cdot 19x^4$. w_H is measured here from its equilibrium height $h = 10/9$.

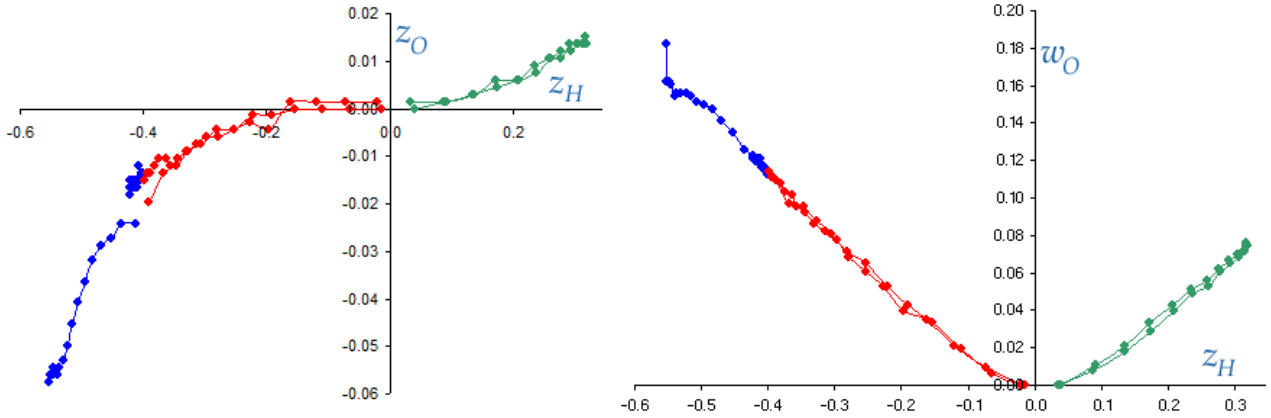

Figure 31: Variation in position of the (x, y) origin 0 with z_H. Left: horizontal component. Right: Vertical component.

The corresponding plots of x_0, $\dot{x_0}$ and $\ddot{x_0}$ (on two scales) for the first episode only are in Figure 35. The near singularities as the block moves rapidly through its equilibrium position are striking, and probably plays a significant role in the mathematical analysis. This singularity probably occurs because the cylinder is flat at $x_0 = 0$: the radius of curvature here is infinite so all points within the neighbourhood of 0 are arrived at at the same time.

I mentioned that initially the profile of this wooden cylinder corresponded to $y = x^4 + \frac{1}{10}x^2$. Its dynamical behaviour was very similar to the reshaped block described above. As an example, the left panel in Figure 34 plots the half-period against time, measured in frames at $\frac{1}{50}$ sec intervals. The right panel is a search for some relation between half period and amplitude. The initial displacement was close to the largest possible without the object tipping over onto its side, and from there the amplitude decayed over about 30 cycles. The first half period was long – $\frac{48}{50}$ s – but subsequent ones decreased steadily as 27, 26, 24, etc. frames per half cycle. Compare this with Figure 3 for the lead roll – they are similar. The decrease in half-period is not linear, nor is it logarithmic. The full period decreased from just over 1 second to about 1/4 second. The right panel in Figure 34 is in

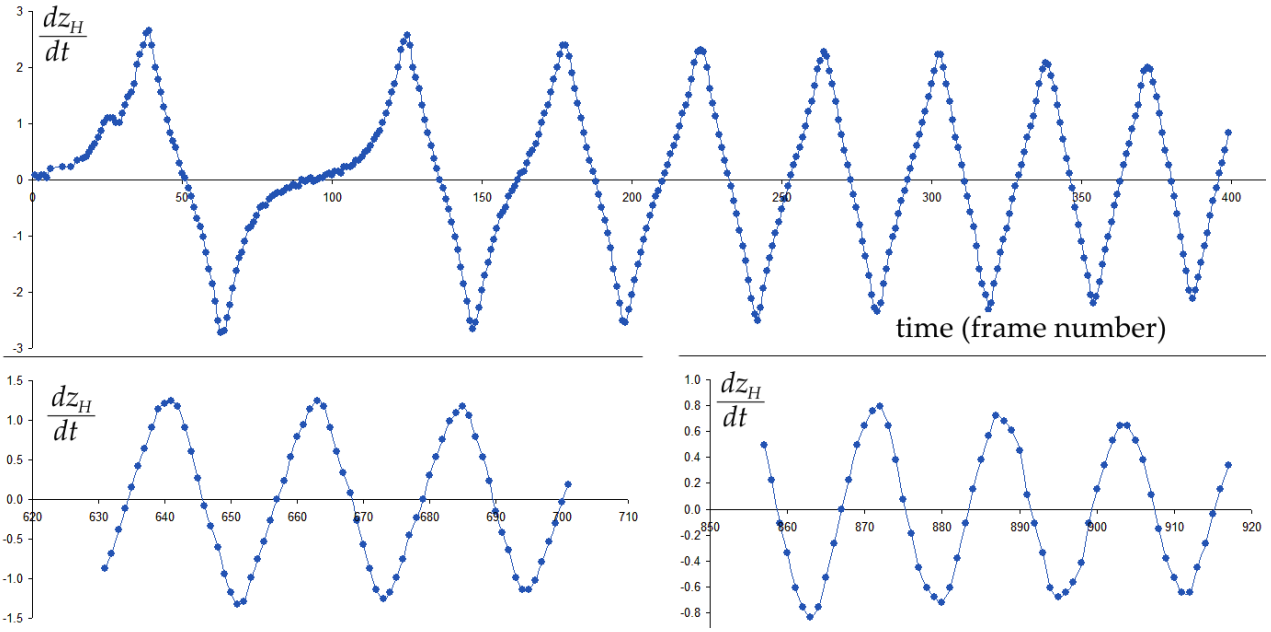

Figure 32: Velocity of the centre of mass at H. Plots of dz_H/dt over three episodes in the motion.

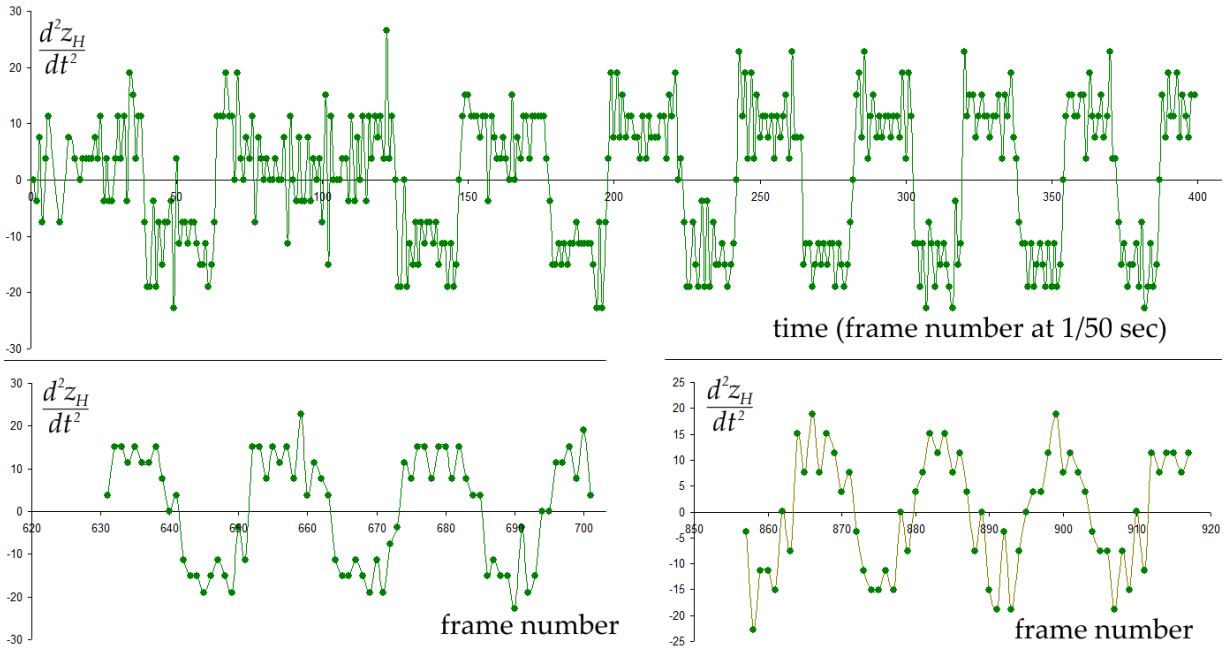

Figure 33: Acceleration of the centre of mass. d^2z_H/dt^2 versus time.

response to the question 'How is the period related to the amplitude?'. The three graphs show the peak-to-trough amplitude of each half cycle (blue), the half-period (red) and the ratio of the two (green), with the blue and green graphs scaled in height for easy comparison. The amplitude decays more quickly than the period.

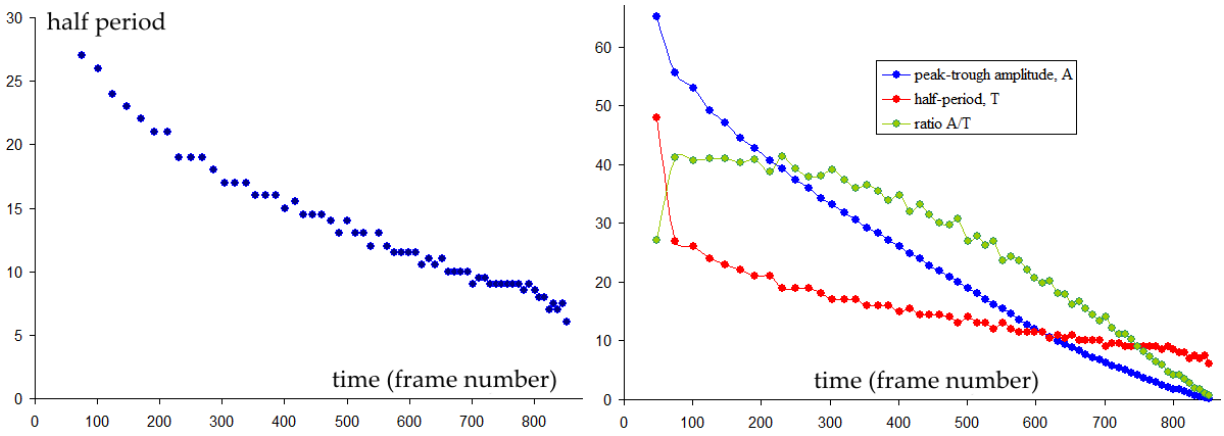

Figure 34: Profile $x^4 + x^2/10$: Left: half-period of block in Figure 25 before re-profiling. Right: amplitude compared with half-period. Time units of $\frac{1}{50}$ sec.

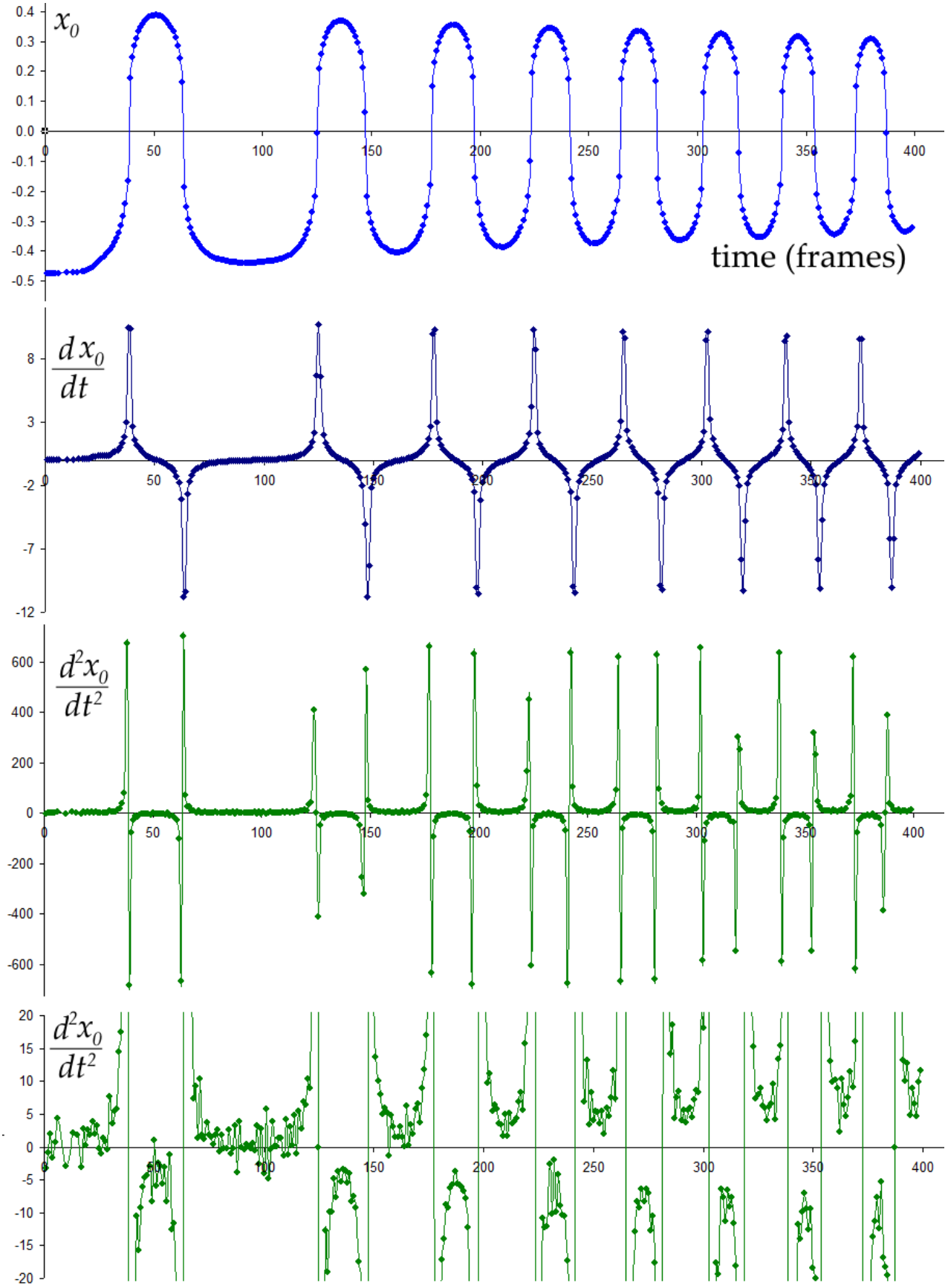

Figure 35: Profile $y = 1 \cdot 2x^4$. Time variation of x_0 and its derivatives at the start of oscillation.

8 Theory of the cylinder $y = f(x)$

8.1 Formulae for a general profile

The dynamics of the plank (§3) and involute cylinder (§5) were derived in terms of the tilt angle θ. With this new cylinder the independent variable will be changed to x_0, the x coordinate of the point of contact P with the ground. When the base is almost flat, distance is more meaningful than angle. To a large extent the calculation can be stated for a general function $y(x)$ describing the cross-section, and derivation of the equation of motion follows the formulae Eq 10a, 10b of §4.1. The expressions become cumbersomely complicated if converted too early to a specific curve such as $y = Ax^4$, so I will keep things general for as long as is reasonable.

Consider, therefore, the cylindrical object in Figure 26, reproduced in Figure 36. Using the notation in the figure the values of some variables can be given in terms of x_0 and h.

$$r^2 = x_0^2 + (h - y_0)^2,$$

$$\tan\theta = m = \frac{dy}{dx}|_{x_0}. \qquad \text{Let } K = \sqrt{1+m^2} \quad \text{so} \quad \cos\theta = \frac{1}{K}, \quad \sin\theta = \frac{m}{K},$$

$$\tan\beta = \frac{x_0}{h-y_0}, \qquad \sin\beta = \frac{x_0}{r}, \qquad \cos\beta = \frac{h-y_0}{r},$$

$$ds^2 = \left(1 + \left(\frac{dy}{dx}\right)^2\right) dx^2, \qquad ds = K\,dx, \qquad s = \int_0^{x_0} ds, \tag{39}$$

$$H_z = s - r\sin(\beta-\theta) = s - \frac{x_0 - m(h-y_0)}{K}.$$

$$H_w = r\cos(\beta-\theta) = \frac{mx_0 + h - y_0}{K},$$

where (H_z, H_w) are the co-ordinates of H relative to the ground. The maximum angle of tilt is where $\theta = \beta \neq 0$ at which the centre of mass is vertically above P; any further tilt and the object will topple onto its side.

We will also need the time derivatives of these quantities. Let a dot $\dot{}$ denote the time derivative, $\dot{x_0} = dx_0/dt$, and a $\hat{}$ sign denote differentiation with respect to x_0, so, for example, $dK/dt = \hat{K}\dot{x_0}$ by the chain rule. Then with $K^2 = m^2 + 1$

$$\hat{\theta} = \frac{\hat{m}}{K^2} \qquad K\hat{K} = m\hat{m}, \qquad K\hat{m} - \hat{K}m = \frac{\hat{m}}{K} = \frac{\hat{K}}{m}, \qquad \hat{s} = K. \tag{40}$$

We could be purists and follow the method in §4 which considers the element E, area $dy\,dx$, at a general point (x, y) relative to O, and carries out integration over the object to find the potential and kinetic energies. Alternatively, we can use the theorem that the dynamics can be described by translation of H, the centre of mass, plus rotation about H, and determine the moment of inertia in a separate calculation. For the first approach it is helpful to introduce a third sets of axes, (u, v) which have H as origin, and u parallel to x. E has co-ordinates $(x, y-h)$ in the (u, v) frame. When turned through θ, the u and v components of E relative to H become $u\cos\theta + v\sin\theta$ and $-u\sin\theta + v\cos\theta$ respectively. The position vector $\boldsymbol{E}$ of E in the stationary (z, w) frame is therefore

$$\boldsymbol{E} = [s - r\sin(\beta-\theta) + x\cos\theta + (y-h)\sin\theta]\boldsymbol{e_z} + [r\cos(\beta-\theta) - x\sin\theta + (y-h)\cos\theta]\boldsymbol{e_w}$$

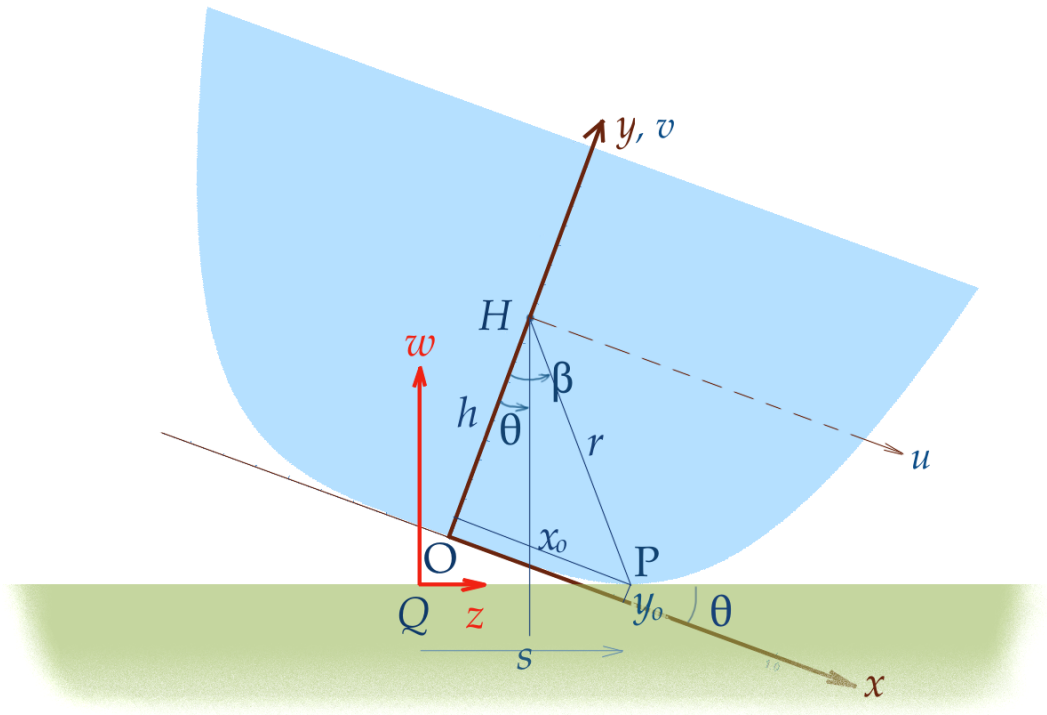

Figure 36: Copy of Figure 26 for easier reference.

$$= \left[s + \frac{1}{K}((u-x_0) + m(v-y_0))\right]\boldsymbol{e_z} + \frac{1}{K}\left[-m(u-x_0) + (v-y_0)\right]\boldsymbol{e_w} \tag{41}$$

where $\boldsymbol{e_z}$, $\boldsymbol{e_w}$ are horizontal and vertical unit vectors. This element has mass $\rho L\, dy\, dx$ where L is the length of the cylinder and ρ its density. Integrating over the object gives the potential energy due to gravity relative to the stable position as

$$V = Mg[r\cos(\beta-\theta) - h] = \frac{Mg}{K}[mx_0 - y_0 + h(1-K)]\,. \tag{42}$$

Referring back to §4.1 the function Q (now $Q(x_0)$) and its derivative are

$$Q = \frac{1}{K}[mx_0 - y_0 + h(1-K)]\,, \qquad \hat{Q} = \frac{\hat{m}}{K^3}[x_0 - m(h-y_0)]\,.$$

The velocity of the particle is the time derivative $d\boldsymbol{E}/dt$. Its components are

$$v_z = \frac{\hat{m}}{K^3}[\,-m(u-x_0) + (v-y_0)\,]\,\dot{x_0}\,, \tag{43a}$$

$$v_w = -\frac{\hat{m}}{K^3}[\,(u-x_0) + m(v-y_0)\,]\,\dot{x_0}.$$

The squared velocity is

$$v^2 = \frac{\hat{m}^2}{(m^2+1)^2}\left[(u-x_0)^2 + (v-y_0)^2\right]\dot{x_0}^2\,. \tag{43b}$$

Using the function P from Eq 10, the squared velocity of the centre of mass is

$$P\dot{x_0}^2 = \frac{\hat{m}^2}{(m^2+1)^2}\left[x_0^2 + (h-y_0)^2\right]\dot{x_0}^2 = \frac{\hat{m}^2}{(m^2+1)^2}\,r^2\,\dot{x_0}^2\,. \tag{43c}$$

Since $d\theta/dt = \frac{\hat{m}}{m^2+1}\dot{x_0}$, we see that P is simply the squared angular velocity as point H turns about the local point of contact with the ground, with instantaneous radius r.

It is worthwhile checking that the rolling condition is satisfied, namely that the velocity at P $= (s, 0)$ in the (z, w) frame be zero. Solving the z and w components of Eq 41 simultaneously for the values of u, v which make $\boldsymbol{E}$ = P gives $u = x_0$, $v = y_0$ as expected. Putting these into Eq 43a does indeed make the $\boldsymbol{v_E} = (0, 0)$ exactly. Therefore the rolling condition is satisfied. A second special position is the instantaneous centre of curvature vertically above the point of contact, P. In the case of $y = Ax^4$ discussed below its position is given by Eq A2.7 in Appendix 2. Substituting its co-ordinates into Eq 42 gives the velocity $(K\dot{x_0}, 0) = (\frac{ds}{dt}, 0)$. This confirms that the centre of curvature moves parallel to the ground and at the same instantaneous rate as P.

Eq 43b for the squared velocity can be integrated over the surface with respect to v then u. We would find, as with the tube and iron bar in §4, that the integral is made of two terms, one describing translation of the centre of mass and the other rotation about it. Knowing this outcome, and being able to determine the moment of inertia in a separate calculation, we can write down the kinetic energy. Since H is at $(0, h)$ the kinetic energy of translation is

$$T_{trans} = \tfrac{1}{2} M P \dot{x_0}^2 . \qquad (44a)$$

The energy in rotation is $\frac{1}{2}I\dot{\theta}^2$ but we require $\dot{\theta}$ in terms of x_0:

$$T_{rot} = \tfrac{1}{2} I \frac{\hat{m}^2}{(m^2+1)^2} \dot{x_0}^2 . \qquad (44b)$$

Again write $I/M = J$, where J has the dimensions of area. The total kinetic energy is written succinctly as

$$T = \tfrac{1}{2} M \frac{\hat{m}^2}{(m^2+1)^2} [r^2 + J] \dot{x_0}^2 = \tfrac{1}{2} M H(x_0, J) \dot{x_0}^2 . \qquad (45)$$

The derivative of the multiplying factor in function H, just defined, is

$$\frac{d}{dx_0} \frac{\hat{m}^2}{(m^2+1)^2} = \frac{2\hat{m}}{(m^2+1)^3} \left[(m^2+1) \frac{d^3 y_0}{dx_0^3} - 2m\hat{m}^2 \right] .$$

Clearly the contribution to d^3y_0/dx_0^3 from the quadratic term in the Taylor series of the profile of the cylinder will be zero; only the 'flatter' 4th order term can contribute and its contribution will be proportional to x_0.

Eqs 42 and 45 allow us to form Lagrange's equation of motion for a cylinder of general profile $y(x)$, but it will only be possible to solve it numerically. The mass M cancels and the three contributions to Eq 10 are

$$\frac{\partial V}{\partial x_0} = g\hat{Q} , \qquad \frac{\partial T}{\partial x_0} = \tfrac{1}{2}\hat{H}\dot{x_0}^2 ,$$

$$\frac{\partial T}{\partial \dot{x_0}} = H\dot{x_0} , \qquad \frac{d}{dt}\left(\frac{\partial T}{\partial \dot{x_0}}\right) = H\ddot{x_0} + \hat{H}\dot{x_0}^2 ,$$

$$\boxed{H\ddot{x_0} + \tfrac{1}{2}\hat{H}\dot{x_0}^2 + g\hat{Q} = 0.} \qquad (46)$$

The algorithm and code I wrote to solve this differential equation for the involute cylinder can in principle be used for these more general shapes. It requires rearranging the equation to express the second derivative $\ddot{x_0}$ in terms of x_0, $\dot{x_0}$ and any constants, and then differentiating to find the third and fourth derivatives.

8.2 Expressions for $y = Ax^4 + Bx^2$

The overall shape of the cylindrical block in Figure 25 is $y = Ax^4$ – only the base is shaped to $Ax^4 + Bx^2$. I will therefore take the dimensions and moment of inertia to be those of $y = Ax^4$, and limit the additional Bx^2 term to analysis of rocking and rolling. The object is truncated at half width a and at $W = A\,a^4 = 2$ units at the top. Appendix 2 gives details of the geometry. By integrating $y(x)$ the sectional area is found to be $8A\,a^5/5 = 8Wa/5$, 80% of the area of the enclosing rectangle. The centre of mass at H is the point around which moments balance; H is on the y axis at height $h = 5W/9$. The moment of inertia, I_H about an axis through H and parallel to the axis of the cylinder is

$$I_H \;=\; \frac{5M}{7371}\,a^2(351 + 112A^2\,a^6) \;=\; (0\cdot238a^2 + 0\cdot076\,W^2)M\,. \tag{47}$$

where M is the mass of the cylinder. As a numerical check on this formula, for $A = 1$, $W = 2$ and $a = \sqrt[4]{2}$, this evaluates to $0\cdot641\,M$. With these dimensions the section looks not too dissimilar from a square. The square with the same area has side $1\cdot95$ units, and this would have a moment of inertia about a perpendicular axis through its centre of $0\cdot976^2 \times 2/3 = 0\cdot634\,M$. For $A = 1\cdot2$, $I_H = 0\cdot6113\,M$ normalised units.

The equation of motion is Eq 46. Here are some of the quantities introduced in §7.1 evaluated for $y = Ax^4 + Bx^2$:

$$y_0 = Ax_0^4 + Bx_0^2, \qquad r^2 \;=\; x_0^2 + (h - y_0)^2\,,$$

$$\frac{d}{dx_0}r^2 \;=\; 2x_0 - 4Bhx_0 + 4B^2x_0^3 - 8Ahx_0^3 + 12ABx_0^5 + 8A^2x_0^7\,,$$

$$m = 4Ax_0^3 + 2Bx_0, \qquad \hat{m} = 12Ax_0^2 + 2B,$$

$$\hat{Q} \;=\; \frac{2x_0}{(m^2+1)^{3/2}}\,(6Ax_0^2 + B)(1 - 2Bh + 2B^2x_0^2 - 4Ahx_0^2 + 6ABx_0^4 + 4A^2x_0^6)\,,$$

$$H \;=\; \frac{\hat{m}^2}{(m^2+1)^2}\,[r^2 + J]\,.$$

$\hat{H}$ is a complicated expression involving a polynomial in x_0 of order 15, odd powers only:

$$\hat{H} \;=\; \frac{8}{(m^2+1)^3}\,[a_1x_0 + a_3x_0^3 + a_5x_0^5 + \ldots - 192A^5Bx_0^{15}\,]$$

where $\quad a_1 = B^2 - 2B^3h + 12ABh^2 - 8B^4h^2 + 12ABJ - 8B^4J\,,$

$$a_3 = 24AB - 2B^4 - 52AB^2h + 8B^5h + 72A^2h^2 - 112AB^3h^2 + 72A^2J - 112AB^3J\,,$$

$$a_5 = 108A^2 - 6AB^3 - 288A^2Bh + 96AB^4h - 672A^2B^2h^2 - 672A^2B^2J,$$

$$a_7 = -76A^2B^2 + 24AB^5 - 288A^3h + 608A^2B^3h - 2112A^3Bh^2 - 2112A^3BJ,$$

$$a_9 = -924A^3B + 200A^2B^4 + 2624A^3B^2h - 2304A^4h^2 - 2304A^4J,$$

$$a_{11} = -1512A^4 + 336A^3B^3 + 4608A^4Bh, \qquad a_{13} = -32A^4B^2 + 2304A^5h\,.$$

The two extremes of form are when $A = 0$ and $B = 0$. In these limiting cases:

Case $A = 0$: parabolic base:

$$y_0 = Bx_0^2, \qquad m \;=\; 2Bx_0, \qquad \hat{m} \;=\; 2B\,,$$

$$\hat{Q} = \frac{2Bx_0}{(m^2+1)^{3/2}}\left[1-2B(h-Bx_0^2)\right].$$

$$H = \frac{4B^2}{(m^2+1)^2}\left[h^2+J+x_0^2-2Bh_0^2+B^2x_0^4\right].$$

$$\hat{H} = \frac{8B^2x_0}{(m^2+1)^3}\left[(1-2Bh-8B^2h^2-8B^2J)+(-2B^2+8B^3h)x_0^2\right].$$

The Taylor approximation to the equation of motion, Eq 46, up to the power x_0^1 is

$$4B^2(h^2+J)\ddot{x_0} + \tfrac{1}{2}[4B^2(2-4Bh)-64B^4(h^2+J)]\dot{x_0}^2 x_0 + 2Bg(1-2Bh)x_0.$$

Assuming that numerical calculations justify taking $\dot{x_0}^2 x_0 \to 0$ as $x_0 \to 0$, this equation reduces to simple harmonic motion with radian frequency ω gives by

$$\omega^2 = \frac{g\,(1-2Bh)}{2B(h^2+J)}. \tag{48}$$

The B in the denominator predicts that the frequency will rise rapidly as $B \to 0$. Also $2Bh < 1$ sets a limit to the height of the centre of mass. For fixed B the fastest oscillation will be when H is in the centre of the base, $h = 0$.

Case $B = 0$: quartic base:

$$y_0 = Ax_0^4, \qquad m = 4Ax_0^3, \qquad \hat{m} = 12Ax_0^2,$$

$$\hat{Q} = \frac{12A\,x_0^3}{(m^2+1)^{3/2}}\left[1-4Ahx_0^2+4A^2x_0^6\right].$$

$$H = \frac{144A^2\,x_0^4}{(m^2+1)^2}\left[h^2+J+x_0^2-2Ahx_0^4+A^2x_0^8\right].$$

$$\hat{H} = \frac{288A^2\,x_0^3}{(m^2+1)^3}\left[2(h^2+J)+3x_0^2-8Ahx_0^4-64A^2Jx_0^6-42A^2x_0^8+64A^3hx_0^{10}\right].$$

I carried out numerical solution of the equation of motion using both Mathematica and a program of my own, already used for the involute cylinder and described at the end of §5.2. For the quartic case, $B = 0$, Mathematica reports a singularity and so I adjusted my own method of solution to deal with this case. The algorithm requires finding $\ddot{x_0}$ using

$$\ddot{x_0} = -\frac{1}{H}\left[\tfrac{1}{2}\hat{H}\dot{x_0}^2 + g\hat{Q}\right]$$

and then differentiating this to get the 3rd and 4th derivatives. In the above equation a common factor of $12Ax_0^3(m^2+1)^3$ can be cancelled, but H in the denominator retains x_0 as a factor which has been cancelled from the other functions. This places a singularity like $1/x_0$ in $\ddot{x_0}$ at $x_0 = 0$. This almost certainly arises from the geometry because here the curve is flat, with zero second derivative. Like the square-cornered plank, a whole neighbourhood of the central point is in contact with the ground for an instant, so velocity momentarily ceases to have a meaning. A probable consequence is that the contribution from the acceleration to Lagrange's equation disappears near the upright position and the equation of motion there, in so far as one can be defined, is non-linear and first order. A Taylor expansion of Lagrange's equation about 0 has leading terms

$$12A(J+h^2)(x_0\ddot{x_0}+2\dot{x_0}^2)+g=0, \quad \text{with the form} \quad C(x\ddot{x}+2\dot{x}^2)+g=0.$$

Mathematica declares that this does not have a closed form solution. If the acceleration were zero at 0, as the physics would require, $\dot{x_0}$ would be constant, v say, and we would have $2Cv^2 + g = 0$. However, but this does not have a real solution since all quantities are positive. We just have to accept that attempts at solving the differential equation for the quartic cylinder must stop just before the upright position is reached. Therefore numerical solutions for $B = 0$ have been obtained only for a single quarter cycle, starting with the cylinder tilted to some chosen x_0 and tracing its fall to the upright position. I used exact expressions for the second and third derivatives, but retained only terms to x^4 in the fourth derivative, as it involves many higher powers which contribute little. For all other cases in which $B \neq 0$ Mathematica has provided the solutions.

8.3 Comparison with experiment for $y = 1 \cdot 2x^4$

The independent quantity x_0 was derived from the measurement of tilt in §7.2 and its value and derivatives are shown in Figure 35 for the first few cycles of the motion. The sharp peaks in $\dot{x_0}$ and $\ddot{x_0}$ would be consistent with a singularity at $x_0 = 0$ as the theory predicts. Equivalent plots in terms of the tilt θ are in Figures 29, 32 and 33. Another set of graphs to review is Figure 28 which shows the decreasing period against elapsed time and, more significantly, against amplitude of swing.

Let us take the theoretical equivalent of Figure 28 first. Figure 37 plots on both a linear and a log-log scale the change in the duration of one quarter cycle versus the starting position of the object x_0, from where it is released with zero velocity. Bear in mind that there is no damping in the theory. This curve mimics the effect of attenuation on the speed of oscillation. The straight line section of the log-log plot (right panel) has equation 'quarter period = $1 \cdot 006 \times$ initial $x_0 - 0 \cdot 984$'. In words, the time for the cylinder to roll from rest to the upright position is proportional to the starting displacement x_0. Figure 28c also shows an almost linear relationship for half-periods less than about $0 \cdot 3$ secs., though the experimental amplitude is of the horizontal position of the centre of mass, whereas x_0 is the point of contact with the ground. The theory shows a strong decrease in half-period with amplitude and therefore models the increasingly rapid oscillations which appear as a shudder. Figure 38 replots the theoretical curve of Figure 37a in terms of initial tilt angle and compares it with the experimental values previously reported in Figure 28c. The agreement is encouraging.

The actual waveform or trajectory – position against time – is plotted in Figure 39 for a

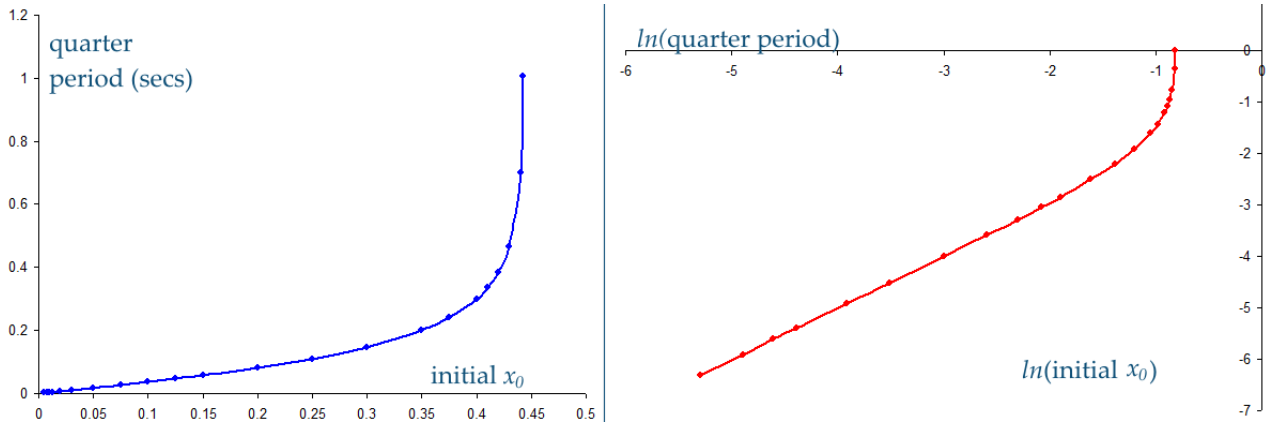

Figure 37: Model of the shudder. Theoretical relation between amplitude and period of oscillation of $y = 1 \cdot 2x^4$ cylinder.

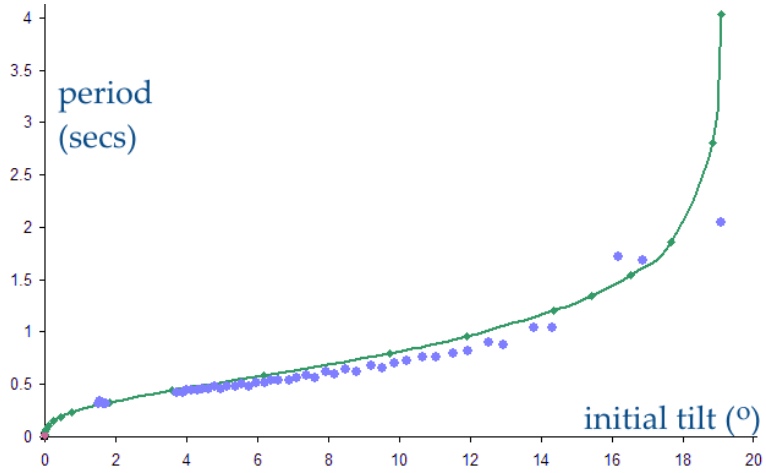

Figure 38: Comparison of theoretic period-amplitude graph with experimental measurements on the $y = 1 \cdot 2x^4$ constant cross-section block.

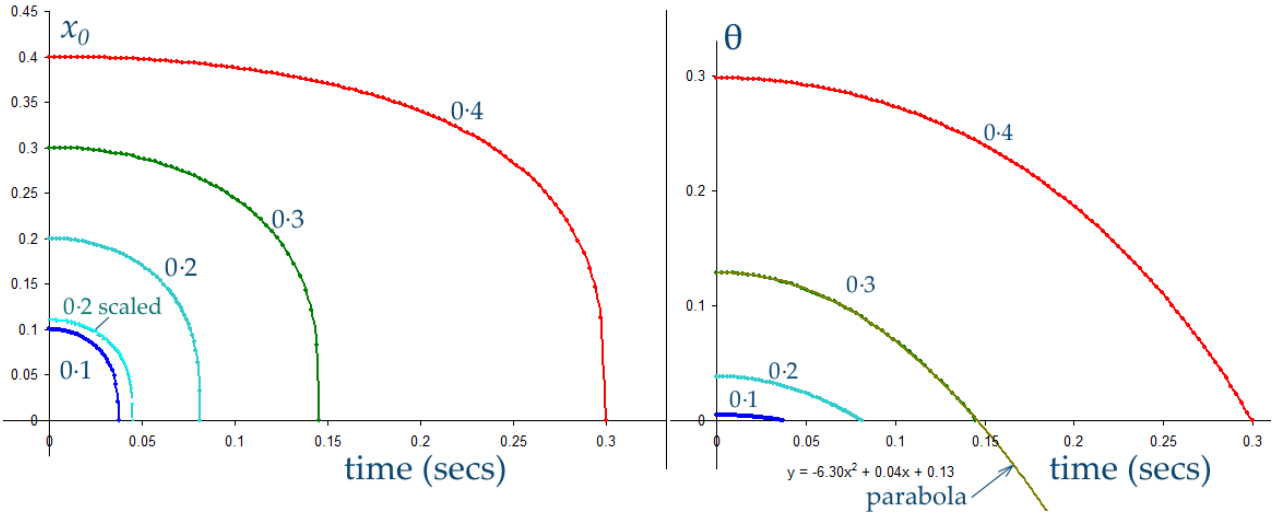

Figure 39: The waveform of the rolling cylinder over one quarter-cycle. Left: in terms of x_0. Right: in terms of tilt θ. Starting values of x_0 are labelled on each curve.

single quarter-cycle during which the cylinder rolls from rest to the upright position. In the left panel the vertical axis is x_0 and in the right the tilt angle θ. These are related through $\tan\theta = 4Ax_0^3$. The left panel can be compared with the experimental results at the top of Figure 35, and the right panel with Figure 29. Struck by the linear zig-zag shape of the experimental velocity curves in §7.2, I surmised there that the position of the object must vary almost as a parabola. This conjecture is vindicated by the parabola fitted to the right hand curve labelled $x_0 = 0 \cdot 3$. In the left panel I have added a fifth curve labelled '$0 \cdot 2$ scaled'. This is the curve for $0 \cdot 2$ scaled in both axes to 55% in order to compare its shape with the $0 \cdot 1$ curve. The close fit is another illustration of the proportionality between amplitude and period seen in Figure 37.

To aid comparison I have reproduced a single cycle of the measurements in Figure 40. These are from video frame 162 to 210 in Figure 29, here renumbered from 0. I have scaled the experimental results slightly in amplitude to remove the attenuation and make all four quarter-cycles appear the same except for symmetry, but have made no adjustment to the time scale. These are in panels a),

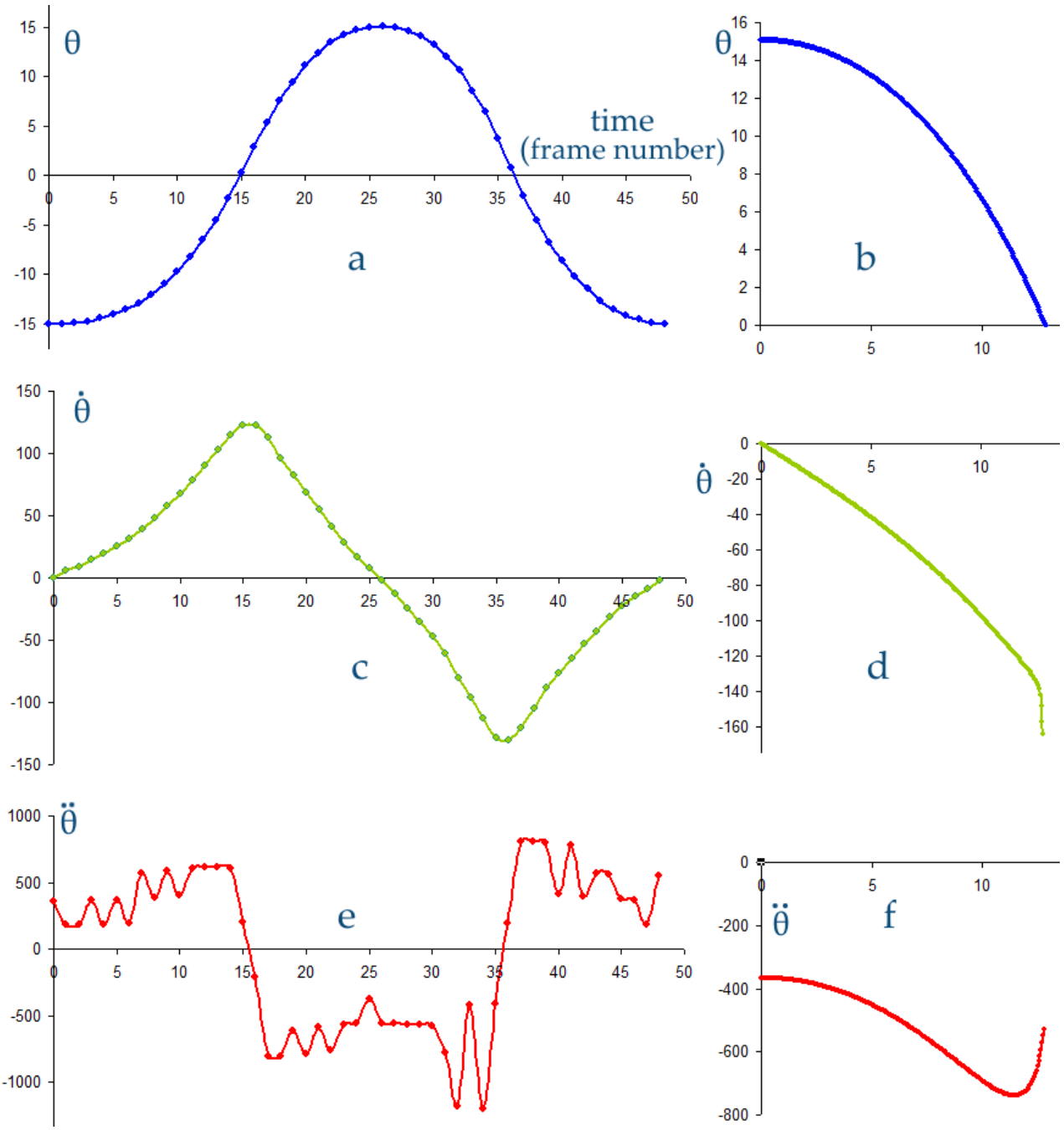

Figure 40: Comparison of theory with experiment over a single cycle. Left panels: experimental values of tilt angle, angular velocity and acceleration. Right: theory for the 3rd quarter-cycle, other quarter cycles being in symmetry.

c), e). The initial tilt is 15°, equivalent to $x_0 = 0 \cdot 38$, so the computer program has been run for this value to produce the quarter-cycle curves in the three right hand panels b), d), f). The whole cycle is observed to last for 48 frames at $\frac{1}{50}$ sec, and the theoretical quarter-cycle for $12\frac{1}{2}$ frames so this is quite good agreement. The values of angular velocity $\dot{\theta}$ and acceleration $\ddot{\theta}$ are also in good agreement. The theory reproduces the slight departure from a straight line in the velocity curve, while the hook-shaped theoretical acceleration curve can, with a generous allowance for experiment

error, fit the measurements on the left. It seems not possible to define a final velocity or acceleration as the cylinder reaches the upright position because of the singularity in the differential equation. This is not seen so strikingly in the measurements, probably because in practice energy loss through friction damps out the discontinuities. Overall I consider the agreement satisfactory.

8.4 Calculations for general $y = Ax^4 + Bx^2$

Calculations point to the equation of motion tending to SHM as the amplitude tends to zero in all cases except $B = 0$. The limiting form of Lagrange's equation is

$$2B(h^2 + J)\ddot{x_0} + 2Fx_0\dot{x_0}^2 + g(1 - 2Bh)x_0 = 0 \qquad (49)$$

$$\text{where} \qquad F = B - 2B^2h + 4(3A - 2B^3)(h^2 + J)\,.$$

This gives the same formula, Eq 48, for ω^2 as when $A = 0$. The role of A, therefore, must be through the polynomial F to govern the rate at which this limiting SHM is approached. The dependence on A cannot be strong; if $3A << 2B^3$, its role is negligible. In looking for shuddering motion, the focus needs to be on the rate at which SHM is approached as x_0 decreases, and on behaviour around $A \approx B^3$. To give a picture of what this condition means, consider a circular cylinder, radius a, rolling on a horizontal table. The Taylor series to order 4 around the point of contact is

$$y = a - \sqrt{a^2 - x^2} \approx \frac{x^2}{2a} + \frac{x^4}{8a^3}\,.$$

So $A > B^3$ means that the base is more flat than a circle.

One comparison which can readily be made is with the oscillation of the tube-plus-bar object studied in §4.2, for which there is experimental verification. The table on page 22 lists the parameters[5] in SI units:

$$g = 9\cdot814, \qquad J = 2\cdot417 \times 10^{-3}/2\cdot983, \qquad h = 0\cdot055 - 0\cdot0233, \qquad r_2 = 0\cdot055$$

from which $B = 1/(2 \times 0\cdot055)$. In Eq 48 this gives $\omega^2 = 126\cdot0$ in exact agreement with Eq 22.

It would be a tedious task to chart the amplitude-frequency relation for cylinder profiles with many combinations of A and B, plus position of the centre of mass. Figures 41 plots a selection of graphs of whole period against initial tilt amplitude θ. All have $h = 10/9$ and $J = 0\cdot6113$ which are the values of the wooden block in Figure 25 and reported in the opening paragraph of §8.2. Keeping these parameters constant helps us see the trend as the quadratic component B is changed. The graph marked $A = 1\cdot2$, $B = 0$ and the companion experimental results are a replotting of Figures 29c and 38. All the other curves are for notional cylinders with $A = 1$ and various B from $1/100$ to $0\cdot42$ which is the highest B value for which oscillations can occur while h is fixed at $10/9$. In all cases $A >> B^3$. As the arrow on the figure indicates, decreasing B means that the base of the cylinder is becoming flatter.

These graphs are much same shape though with increasing flatness they are drawn out to the right (larger initial tilt) and move down (shorter period). No step change strikes us; rather the graphs show gradual change. The horizontal gradient close to $\theta = 0$ means that the period and frequency have become essentially constant, and here the cylinder is in SHM. The only graph which looks different is that for $A = 1\cdot2$, $B = 0$ where, near $\theta = 0$, the period decreases toward zero and

[5] h in Eq 22 is measured from the centre downwards, whereas in Eq 48 it is from the circumference upwards.

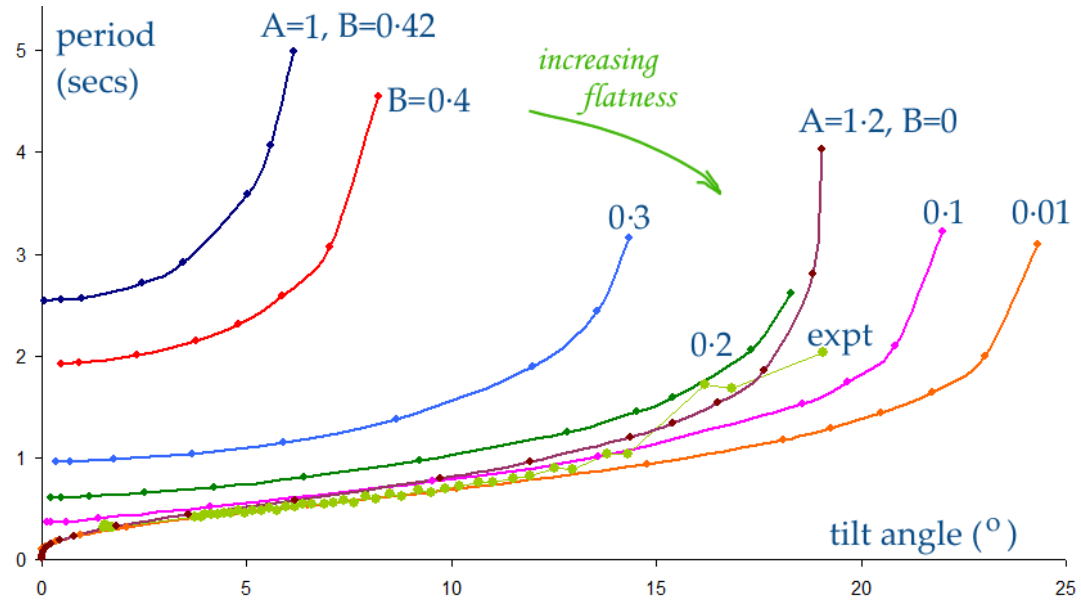

Figure 41: Theoretical dependence of period on initial amplitude of oscillation for various profiles $y = Ax^4 + B^2$. The experimental values are for $A = 1 \cdot 2, B = 0$ (see Figure 38).

there is no SHM. This block really is shuddering. In general the flatter profiles let the cylinder accommodate a larger initial displacement and this means that the person viewing it sees it decay through a larger range of angles. The observer sees enough cycles of rocking to perceive that the block is speeding up from a slow (long period) start to increasingly rapid oscillations. When there is friction causing decay in amplitude, the observer would not see enough cycles at any one frequency to recognise SHM, even damped SHM. The impression is left that the cylinder has speeded up to a shudder before coming to rest.

The three panels in Figure 42 show frequency in Hertz against initial tilt in degrees– the reciprocal presentation of period. In these the quartic component A is constant at 1 and the quadratic element B has values $0 \cdot 4$ (top), $0 \cdot 2$ middle and $0 \cdot 1$ (bottom); that is, the base of the cylinder is more flat as we look down the page. In each panel the effect of changing h from 10/9 to 1 to $0 \cdot 8$ is illustrated by the blue, green and red graphs. The vertical scales are not quite the same, but sufficiently close to see that the terminal frequency (left edge) is much larger for the cylinder with the flattest base and the lowest centre of gravity. This is as we might expect. Changing B changes the shape of the curves. They are all similar at the largest tilts, near 20, 25 and 40°, but for low B it seems as if the left edge of each curve has been grasped by an invisible hand and dragged upwards. The two end points of each graph are readily calculated from two formulae. On the left edge the limiting frequency is given by Eq 48 whilst the rightmost point is where $\beta = \theta$, equivalent to $m = x_0/(h - y_0)$, Eq 39. Here the graphs drop sharply to zero frequency since in this position the cylinder is balanced precariously. Between these limits each curve can be fitted well by a 4th order polynomial $f = c_0 + c_1\theta + c_2\theta^2 + c_3\theta^3 + c_4\theta^4$, not that I am claiming this is more than a coincidence.

The velocity of the block as it swings through the upright position is plotted in Figure 43 for the same values of quadratic component B as in the previous figure. The variable here is x_0 and the logarithm of its maximum rate of change forms the vertical axis. The horizontal axis is the initial displacement x_0. A, h and J are the same for all curves. We see again the much wider range of displacements possible with a flat bottomed block and with that come far higher velocities when the

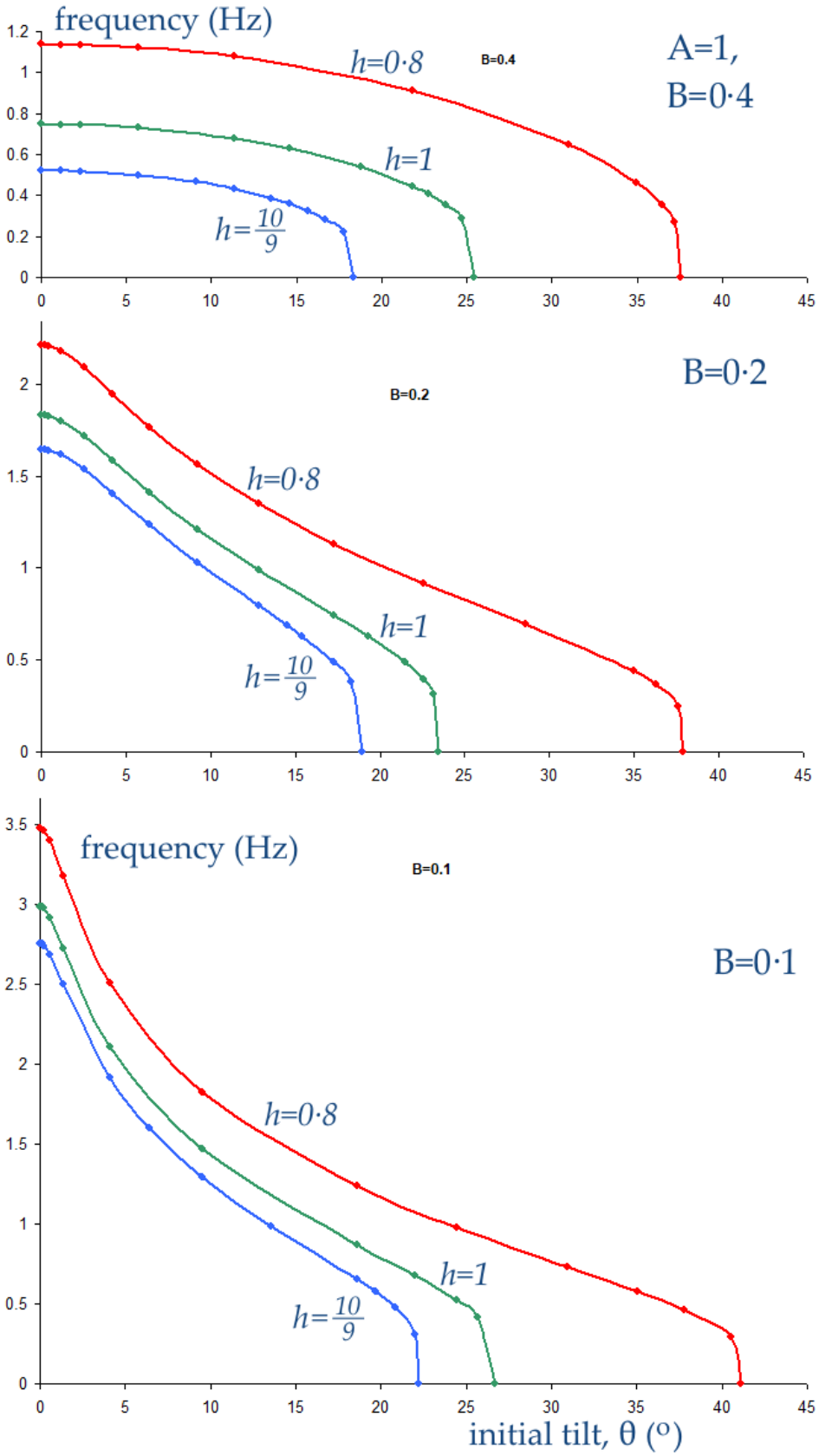

Figure 42: The effect of changing the quadratic component of the profile (coefficient B), and of changing the position h of the centre of mass of cylinder with profile $y = Ax^4 + Bx^2$. Frequency (Hz) plotted against tilt angle (°).

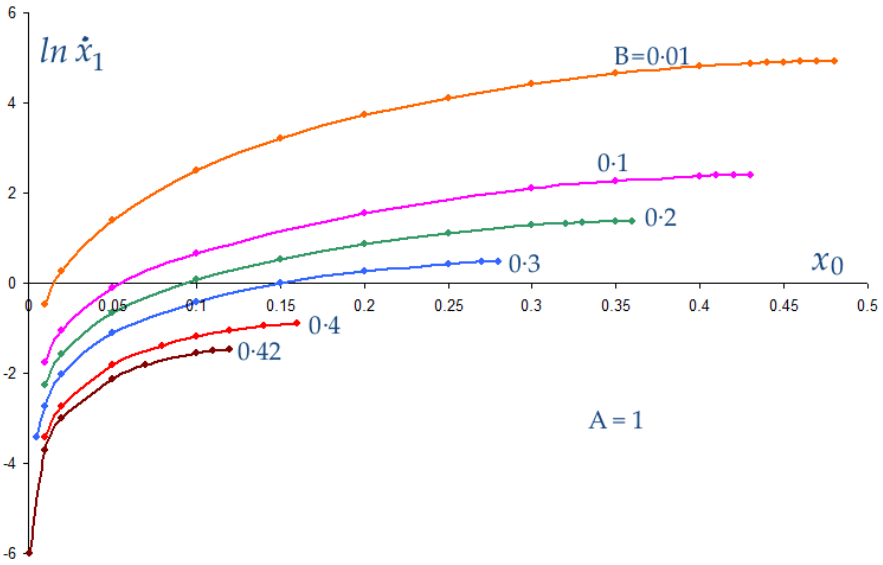

Figure 43: Variation of maximum velocity with initial tilt. Log plot of $\dot{x_0}$ at the central position versus the initial displacement x_0. $A = 1$, $h = 10/9$ for all curves.

block is rocking past $x_0 = 0$. These high velocities, even near the upright position, contribute to the observed sensation of the block shuddering as it comes to rest. They are the main reason that the period becomes shorter. Given equal initial displacements, a block with a flatter base (low B) will achieve higher central velocity than one with a rounded, more circular base.

8.5 Profiles $y = x^n, n > 2$

Functions $y = x^n$ for n an even positive integer become more square-bottomed and hence more like a plank as n increases. For $n \geq 4$ the period of oscillation continues to decrease. The cases $n = 4$ to 10 are plotted in Figure 44. The left panel is a linear plot of the quarter-period, that is, the time for the object to roll from its initial displacement to the upright position. Displacement along the horizontal axis is measured as x_0. This panel can be compared with Figure 41 for the $y = x^4 + Bx^2$ cylinders where the shapes are similar except that the curves tend to constant values at 0. For $n > 2$ the curves continue to decrease as the log-log plots in the right panel of Figure 44 show. Indeed, the gradients of these graphs for exponent $n = 4$, 6, 8 and 10 are 1, 2, 3, 4 respectively. Since for $y = x^2$ the curve tends to a constant given by Eq 48, the gradient for $n = 2$ is 0. Therefore

$$\text{the period of } y = x^n \text{ decreases as } x_0^{\frac{n}{2}-1} \text{ as } \; x_0 \to 0\,, \qquad n \text{ even.} \tag{50}$$

Shuddering, therefore, is the norm for smoothly based symmetric objects, and SHM occurs only where a quadratic component is present. By forming the Taylor series for the equation of motion in $x_0(t)$ about 0 we obtain approximate non-linear differential equations for vanishingly small x_0:

$$\text{for } n = 4: \qquad 12(h^2 + J)\, x_0\ddot{x_0} + 24(h^2 + J)\dot{x_0}^2 + g = 0\,, \tag{51}$$

$$\text{for } n = 6: \qquad 30(h^2 + J)\, x_0^3\ddot{x_0} + 120(h^2 + J)x_0^2\dot{x_0}^2 + g = 0\,,$$

$$\text{for } n = 8: \qquad 56(h^2 + J)\, x_0^5\ddot{x_0} + 336(h^2 + J)x_0^4\dot{x_0}^2 + g = 0\,,$$

$$\text{for } n = 10: \qquad 90(h^2 + J)\, x_0^7\ddot{x_0} + 720(h^2 + J)x_0^6\dot{x_0}^2 + g = 0\,.$$

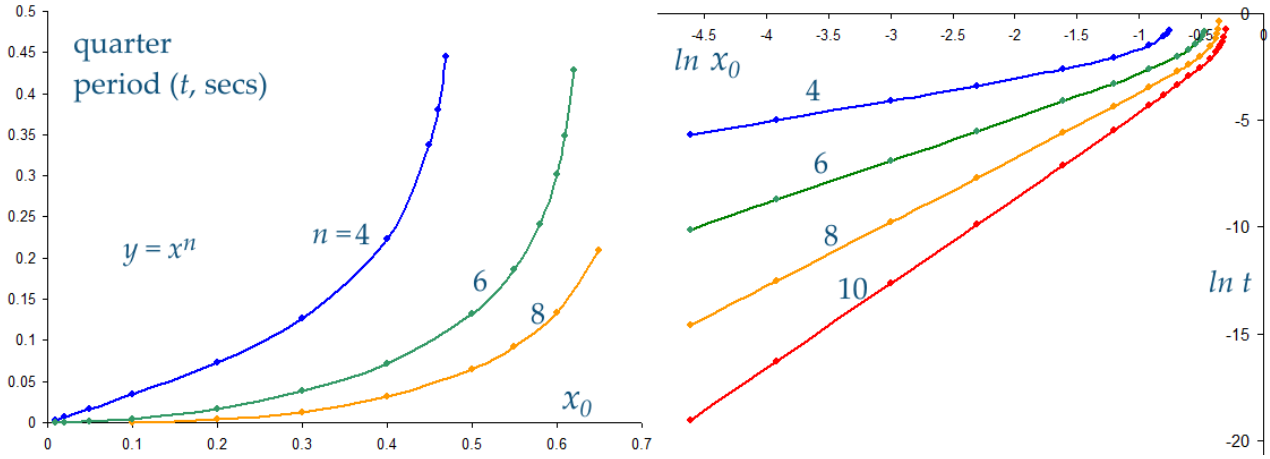

Figure 44: Quarter period (time to upright) for constant cross-section blocks with profile $y = x^n$ for $n = 4$, 6, 8 and 10. Left: linear graphs. Right: log-log graphs. $h = 10/9$, $g = 142$, $J = 0 \cdot 6113$.

9 Some conclusions

There are a lot of graphs and equations in this article, all trying to answer the question 'why does a tilted mandarin orange rolls with increasingly fast oscillations before coming to rest?'. I showed that this phenomenon is shared by many cylindrical or near-spherical objects which have a flattened bottom and/or low, eccentric centre of gravity. All such objects speed up to some extent as the initial displacement is decreased. When tilted to their maximum, so that the centre of mass is almost vertically above the point of contact with the ground plane, the time to fall to the upright position is the longest of all quarter-cycles because the moment causing angular acceleration is initially almost zero. At smaller tilts, the moment is larger and the acceleration greater, and to this extent all objects speed up. However, whether an observer sees the object vibrate so fast as to be called a shudder depends on the extent to which the frequency of oscillations increases as attenuation due to friction causes the amplitude to decrease towards zero. Friction is essential to rolling; without it the object would slip and slide on the table. With friction, it must slow down and come to rest. The crucial result is Eq 50: when attenuation is small, the period of a cylinder with base profile $y = x^n$ decreases as $x_0^{\frac{n}{2}-1}$ as $x_0 \to 0$, x_0 being the initial displacement.

The symmetric curve which describes the profile of the base can be expanded as a Taylor series in the co-ordinate x around the upright position at $x = 0$. Flatness can be quantified in terms of the coefficients in this Taylor expansion. If the profile contains a non-zero quadratic component (in x^2) with weighting B, the cylinder will execute simple harmonic motion for sufficiently small x at a frequency given by Eq 48:

$$\omega^2 = \frac{g\,(1 - 2Bh)}{2B(h^2 + J)}\,. \tag{48}$$

The value of x at which SHM sets in depends on the relative weights of the x^2 and x^4 terms in the Taylor expansion; the smaller $BtoA$ in $y = Bx^2 + Ax^4$, the smaller the x below which there is SHM. This means that if the quadratic component is small compared with the x^4 term, SHM will not set in until the oscillations are already rapid and of small amplitude, so some observers may then judge the cylinder to shudder. However, if the quadratic component in absent, there is no limiting frequency to which the oscillations tend, and shuddering will be certainly be seen.

The position of the centre of mass has a significant effect. If it is too high above the ground,

the object may not rock, but instead fall on its side when displaced. In general, lowering the centre of mass increases the maximum possible tilt angle and, for bases with a quadratic term, increases the frequency of the terminal SHM.

Flatness of the base is essential to shuddering. The clue to understanding what is happening comes from a plank of wood rocking on its narrow face. This is the limiting form of blocks with the profile $y = x^n$ as $2n \to \infty$. The plank pivots first about the left corner then the right, so each period of oscillation is made of four quarter-cycles in which the plank falls from a position of maximum tilt to the central upright position, or rises from the upright to a new maximum tilt on the other side. When the base face of the plank is slightly smoothed, the bump as it passed through zero tilt is softened and less energy lost, so the oscillations run on for longer. Much the same smoothed fall or rise in quarter-cycles is shown by object such as the specially made involute cylinder, §5, and the $y = Ax^4$ cylinder of §7, 8. Indeed, the equations of motion I have derived for these apply only to one quarter-cycle at a time. A mandarin has a very similar shape to the involute cylinder, as the photographs in Figure 17 show. Perhaps the simplest explanation of the speeding up is found in Figure 12 for the plank and Figure 22 for this involute cylinder, and I reproduce both below. As the motion continues, the amplitude, the period and the maximum velocity all decrease. However, the amplitude reduces more quickly than the velocity. Since time (period) is distance (amplitude) divided by velocity, the period must decrease. In other words, the oscillations speed up in the sense that their frequency increases even though the maximum velocity is decreasing – something of a paradox.

To close let us review the conditions necessary for an object of constant cross section to rock to and fro, and perhaps to shudder as it comes to a halt:

1. the object need to be symmetric left to right,
2. it needs a low centre of gravity so that it has an upright equilibrium position,
3. when it is tilted, there must be a moment causing it to right itself under gravity. This excludes the homogeneous circular cylinder.
4. there must be friction with the ground so that it turns and rolls without slipping.
5. for oscillations to speed up the base must be flatter than a circle. For shuddering to occur the quadratic component to the shape must be small or, better still, absent.

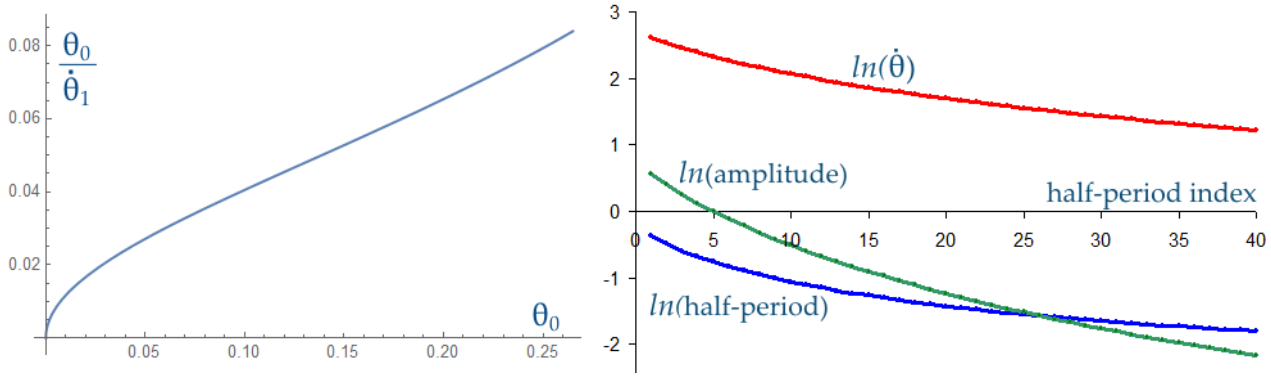

Figure 45: Evidence of amplitude decaying faster than velocity. Left: Figure 10 for rocking plank. Right: Figure 22 for involute cylinder. Logarithms of maximum angular velocity, left-to-right amplitude, and half-period plotted against the index number of the half-period.

10 Appendix 1: Small oscillations using conservation of energy

10.1 Oscillations on a flat table

All the theory in this article will assume that the object and ground are rigid. We start in the limit of small oscillations. Several textbooks show that the equation of motion for small-amplitude oscillations can be obtained by writing down an expression for the total kinetic and potential energy, then differentiating it with respect to time. Assuming no energy loss, this produces the equation of motion in a form similar to Newton's second law, 'force = mass × acceleration'. Where the potential energy is due to gravity, it is proportional to m, the mass of the object. In this case m cancels from the equation of motion, meaning that small oscillations are governed by gravity and length dimensions only. Using the approximation that the angle of tilt θ, or other parameter which measures the displacement from equilibrium, is small – specifically such that $\cos\theta \approx 1$, or $\theta^2/2 \approx 0$ – one obtains the equation of motion

$$\ddot{\theta} + \omega^2\theta = 0\,. \qquad (A1.1)$$

Eq 1 is the characteristic equation of undamped simple harmonic motion with radian frequency ω and period $2\pi/\omega$.

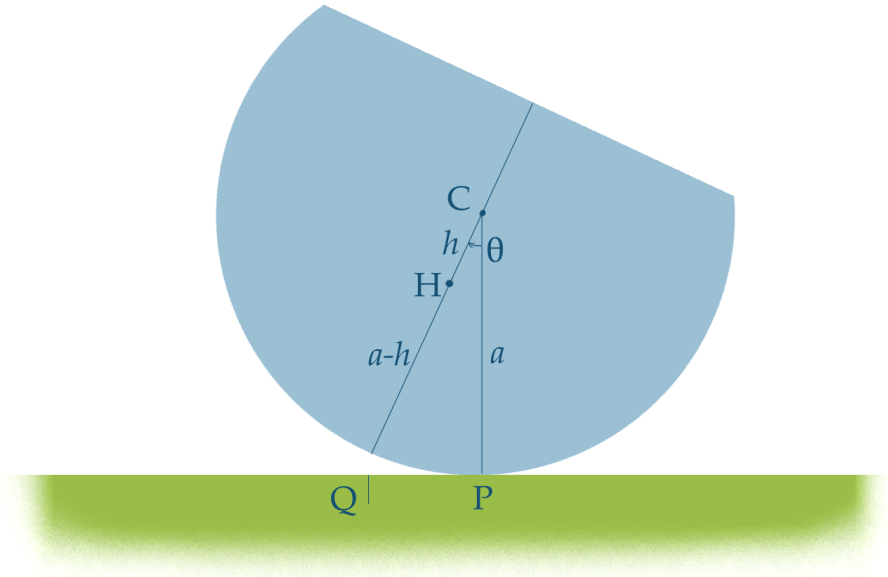

Figure 46: Section through a cylindrical object with centre of mass at H, and circular profile where it rolls on the ground.

The method is based not just on the principle of conservation of energy, but on the theorem that the motion of any rigid body is equivalent to translation of its centre of mass plus rotation around the centre of mass. I will apply this now to obtain the frequency of small oscillation of a locally circular object with eccentric centre of mass rocking on a flat horizontal ground. The geometry is shown in Figure 46. The centre of mass is at H and at equilibrium H and C are vertically about Q. Clearly H is not higher than C for stable equilibrium. At tilt angle θ the instantaneous point of contact is P. The potential energy relative to the equilibrium position is

$$V = mgh(1-\cos\theta) \geq 0.$$

The kinetic energy has two contributions, one from translation of H and the other from rotation around H. Let v_H be the speed of the centre of mass relative to axes fixed at Q, and v_C the velocity

at the centre of curvature, C. The arc length through which the object has rolled is $a\theta$ so this is also the distance through which C has moved parallel to the ground and to the right. Relative to C point P is spinning at the rate $a\dot{\theta}$ to the left. So the velocity at P relative to Q is $v_c - a\dot{\theta}$. However, since there is no slipping, the relative velocity of object and ground at P is zero. Therefore $v_c = a\dot{\theta}$, consistent with $d/dt(a\theta) = a\dot{\theta}$. Points up the vertical line above P will have speeds in proportion to their height relative at C. For instance, it the object were a full circle, the point instantaneous at the top would have speed $2a\dot{\theta}$. The speed at H when it is near to its lowest position is close to $(a-h)\dot{\theta}$. Therefore the kinetic energy of translation is

$$T_{trans} \approx \tfrac{1}{2}m(a-h)^2\,\dot{\theta}^2\,.$$

The energy in rotation is $\frac{1}{2}I_H\,\dot{\theta}^2$ where I_H is the moment of inertia about H, which depends on the particular geometry of the object. Adding these together the energy conservation equation is

$$\tfrac{1}{2}\left[m(a-h)^2 + I_H\right]\dot{\theta}^2 \;+\; mgh(1-\cos\theta) \;=\; \text{a constant}\,.$$

Differentiating with respect to time

$$\left[m(a-h)^2 + I_H\right]\dot{\theta}\,\ddot{\theta} \;+\; mgh\sin\theta\,\dot{\theta} \;=\; 0$$

and the $\dot{\theta}$ cancel. For small angles $\sin\theta \approx \theta$, giving Eq 1. The frequency is given by

$$\omega^2 \;=\; \frac{gh}{(a-h)^2 + \frac{I_H}{m}}\,. \qquad (A1.2)$$

Note that I_H/m has dimensions of Length^2; the mass has cancelled out. For the special case of a semicircle with uniform density, $h = 4a/(3\pi)$ and $I_H = m(a^2/2 - h^2)$, making

$$\omega^2 \;=\; \frac{8g}{a(9\pi-16)}, \quad \text{and so the period is } \pi\sqrt{\frac{a(9\pi-16)}{2g}}\,.$$

For a hemisphere rocking in a plane $h = 3a/8$ and $I_H = 83ma^2/320$. The method can be extended to curved ground surfaces, as illustrated next.

10.2 Oscillations on a concave ground

Here I use the energy method to obtain the frequency of small amplitude oscillations of a locally circular object on a locally circular ground, both concave and slightly convex. 'Locally' means that profiles of both object and ground around the equilibrium position are arcs of circles. To start take the simplest case of a uniform cylinder or sphere, radius a, centre C, rolling on the inside of a hollow cylinder or sphere whose radius is b, as shown in Figure 47. The angle rolled through from the equilibrium position at Q is θ. Since the density is constant the centre of the object coincides with its centre of mass H.

The height increase of the centre of mass at angle β is $(b-a)(1-\cos\beta)$ so the potential energy is $mg(b-a)(1-\cos\beta)$. The kinetic energy in translating the centre of mass is $\frac{1}{2}mv^2$ where $v = (b-a)\dot{\beta}$. The energy in rotation is $\frac{1}{2}I_C\dot{\theta}^2$ where I_C is the moment of inertia about C. To find $\dot{\theta}$ in terms of $\dot{\beta}$ we use the rolling condition that the relative velocity between ground and object at P, the instantaneous point of contact, is zero. The element of cylinder's (or ball's) rim at P is moving to the left relative to C on account of it turning, but C is moving to the right at the rate $(b-a)\dot{\beta}$. The sum of these velocities is $-a\dot{\theta} + (b-a)\dot{\beta} = 0$. The energy conservation equation is therefore

$$\tfrac{1}{2}m(b-a)^2\dot{\beta}^2 \;+\; \tfrac{1}{2}I_C\tfrac{(b-a)^2}{a^2}\dot{\beta}^2 \;+\; mg(b-a)(1-\cos\beta) \;=\; \text{a constant}\,.$$

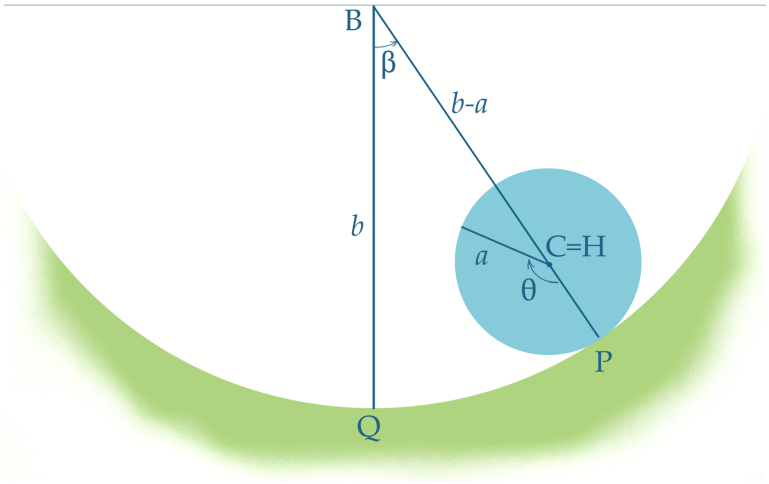

Figure 47: A circular cylinder or ball with uniform density rolling inside a hollow cylinder.

Differentiating with respect to time gives the equation of motion

$$(b-a)\left[m+\frac{I_C}{a^2}\right]\ddot{\beta} + mg\sin\beta = 0\,. \qquad (A1.1)$$

No approximations have been made in deriving this. For small amplitudes of oscillation $\sin\beta \approx \beta$ and we obtain an equation of the form of Eq 1 where

$$\omega^2 = \frac{mg}{(b-a)\left[m+\frac{I_C}{a^2}\right]}\,.$$

For a uniform cylinder $I_C = \frac{1}{2}ma^2$ and for a sphere it is $\frac{2}{5}ma^2$, making

$$\text{rolling cylinder:}\quad \omega^2 = \frac{2g}{3(b-a)}\,, \qquad \text{sphere:}\quad \omega^2 = \frac{5g}{7(b-a)}\,.$$

Eq A1.3 is also obtained from Lagrange's equation, Eq 10, §4. The term $\partial T/\partial\beta$ is zero because there is no β dependence of the kinetic energy – it depends only on $\dot{\beta}$ which Lagrange treats as an independent variable. Similarly $\partial T/\partial\dot{\beta}$ has no explicit dependence on β. In more general geometries where the centre of mass H does not coincide with the centre of curvature, these simplifications are not likely to occur.

Having an eccentric centre of mass obviously creates complications but does allow the object to roll on a slightly convex surface, provided H is sufficiently close to the ground. The concave geometry is essentially that of Figure 47. Energy is defined in relation to H, not C. The height of C relative to its stable position is $(b-a)(1-\cos\beta)$ as above, and the position of H relative to C is $-h\cos(\theta-\beta)$. If β is our chosen co-ordinate, we need θ in terms of β. The arc length $s =$ QP rolled through is $a\theta$ around the cylinder and $b\beta$ along the ground, so $\theta = b\beta/a$. Putting this together, the potential energy increase at angle β is

$$V = mg\left[(b-a)(1-\cos\beta) + h\left[1-\cos\left(\beta(\tfrac{b}{a}-1)\right)\right]\right]\,.$$

To obtain the velocity of H the assumption is that H has moved only a small distance from equilibrium so its velocity is almost parallel to the ground. As above, the velocity of C is $v_C = (b-a)\dot{\beta}$, and the

rolling condition requires that $\dot\theta = (b-a)\dot\beta/a$. Relative to C, H is moving to the left at speed $h\dot\theta$. The kinetic energy in translation of H is therefore

$$T_{trans} \approx \tfrac{1}{2}m(b-a)^2\left(1-\tfrac{h}{a}\right)^2\dot\beta^2\,.$$

Writing I_H for the moment of inertia around H, the conservation of energy equation is

$$\tfrac{1}{2}m(b-a)^2\left(1-\tfrac{h}{a}\right)^2\dot\beta^2 + \tfrac{1}{2}I_H\tfrac{(b-a)^2}{a^2}\dot\beta^2 + mg\left[(b-a)(1-\cos\beta)+h\left[1-\cos\left(\beta(\tfrac{b}{a}-1)\right)\right]\right] = \text{ constant}\,.$$

Differentiating with respect to time gives the equation of motion

$$(b-a)\left[(a-h)^2+\frac{I_c}{m}\right]\ddot\beta + g[a^2\sin\beta + ha\sin\left(\beta(\tfrac{b}{a}-1)\right)] = 0. \qquad (A1.4)$$

As $h\to 0$ this reduces to Eq A1.1. However, it presents the problem that even when β is small, $\beta(b-a)/a$ need not be small, so it seems that h also must be small to obtain an equation like Eq 1 characteristic of simple harmonic motion (SHM). This implies that a light weight hoop with a single heavy weight fixed near its rim will not show SHM when rocking inside a hollow cylinder. SHM is so common that this seems rather implausible, but it could be worth testing experimentally.

It is possible to recover Eq A1.2 from this, it being the equation of SHM for a cylindrical object with locally circular section and eccentric centre of mass rocking on a flat horizontal surface. First swap the co-ordinate from β to θ by $\beta\to a\theta/b$, $\ddot\beta\to a\ddot\theta/(b-a)$ before letting $b\to\infty$. The awkward nature of this limit suggests that, when modelling oscillation on a gently curved surface, a better choice of co-ordinate might be s, the arc length or a similar measure of distance to the instantaneous point of contact.

11 Appendix 2: Curvature and evolute

This appendix sets out the formula for the radius of curvature, the position of the centre of curvature, and the equation of the evolute of a plane curve given in polar co-ordinates r, ϕ.

Take the curve to be defined by the independent variable ϕ which determines the length of the radius vector $r(\phi)$. The centre of curvature Q corresponding to ϕ_0 is the limiting point of intersection of two closely adjacent normals at ϕ_0 and $\phi_0+\delta\phi$ as $\delta\phi\to 0$. I will attempt to find Q by following this definition. We need to find the gradient of the curve at ϕ_0 and hence the cartesian equation of the normal there. Using Taylor's theorem the equation of an adjacent point can be found. That will give two simultaneous equations whose solution determines the point of intersection of these infinitesimally close normals. To check the maths at each stage I will apply the formulae to an ellipse whose cartesian and polar equations are

$$\frac{x^2}{a^2}+\frac{y^2}{b^2}=1\,,\qquad \frac{r^2\cos^2\phi}{a^2}+\frac{r^2\sin^2\phi}{b^2}=1,\qquad r^2(\phi)=\frac{a^2b^2}{a^2\sin^2\phi+b^2\cos^2\phi}=\frac{a^2b^2}{E}\,. \qquad (A2.1)$$

In discussing the ellipse it will be useful to abbreviate $a^2\sin^2\phi+b^2\cos^2\phi=E$. Here ϕ is the angle which the radius vector makes with x axis, and so has physical significance. Though we are not studying the ellipse *per se*, I should point out that there is an alternative parametrisation which leads to simpler formulae for the evolute. The parameter is γ, defined so that the ratio of x co-ordinate to the semi-major axis is $\cos\gamma$ and the ratio of y co-ordinate to the semi-minor axis is $\sin\gamma$. In symbols

$$\frac{x}{a}=\cos\gamma,\quad \frac{y}{b}=\sin\gamma,\quad r^2=a^2\sin^2\gamma+b^2\cos^2\gamma. \qquad (A2.2)$$

ϕ and γ are related by $b\tan\gamma = a\tan\phi$. For some purposes it is convenient to use the eccentricity e of the ellipse, defined by $e^2 = (1 - b^2/a^2)$. This measures how for the ellipse differs from a circle.

Gradient and normal : The gradient m_0 at (x_0, y_0) is defined to be $dy/dx|_{x_0}$. Working in polar co-ordinates this is

$$m = \frac{\frac{dy}{d\phi}}{\frac{dx}{d\phi}}.$$

$$m = \frac{dy}{dx} = \frac{r\cos\phi + r'\sin\phi}{-r\sin\phi + r'\cos\phi} \quad \text{where} \quad r' = \frac{dr}{d\phi}. \tag{A2.3}$$

The normal at (x_0, y_0) is

$$v = y_0 - \frac{1}{m}(u - x_0) \tag{A2.4}$$

where I am using (u, v) for the co-ordinates of points on the normal line, as this will save confusion with points on the parent curve. For the ellipse $m = -b^2x_0/(a^2y_0) = -b^2/(a^2\tan\phi)$. Figure 48 shows five normals to the ellipse with aspect ratio $3b = 2a$. The two at $\phi = -0\cdot2,\ -0\cdot22$ intersect near $(0\cdot8, 0)$.

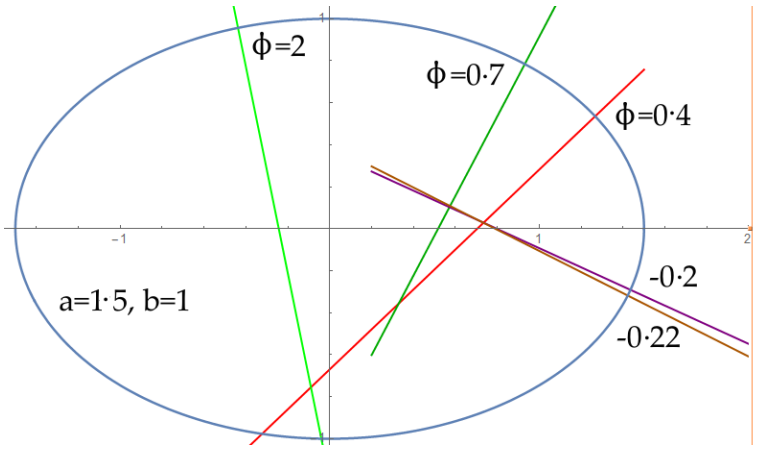

Figure 48: An ellipse with $a = 3/2$, $b = 1$ showing several normals each with gradient $a^2\tan\phi/b^2$.

Intersection and evolute : The equation of the adjacent normal at $\phi + \delta\phi$ is found by replacing m, x_0 and y_0 from Eq A3 by the first two terms of their Taylor expansions.

$$v = \frac{1}{m + m'\,\delta\phi}\left[x_0 + x_0'\,\delta\phi - u\right] + y_0 + y_0'\delta\phi \approx \frac{1}{m}\left(1 - \frac{m'}{m}\delta\phi\right)\left[x_0 + x_0'\,\delta\phi - u\right] + y_0 + y_0'\delta\phi. \quad (A2.5).$$

The prime $'$ denotes differentiation with respect to ϕ. Dropping the subscripts $_0$,

$$m' = \frac{d}{d\phi}\left[\frac{dy/d\phi}{dx/d\phi}\right] = \frac{x'y'' - y'x''}{(x')^2}.$$

The lines in Eqs A3, A4 intersect where their v values are equal, which is where

$$\left(\frac{x'}{m} - \frac{m'}{m^2}(x - u) + y'\right)\delta\phi = 0.$$

Therefore the point of intersection has co-ordinates

$$u_{int} = x - \frac{m}{m'}(x' + my'), \qquad v_{int} = y + \frac{1}{m'}(x' + my') . \tag{A2.6}$$

This is a parametric equation for the evolute with parameter ϕ. Again dropping the subscripts, $(u(\phi), v(\phi))$ is the centre of curvature of the curve at $(x(\phi), y(\phi))$, and the distance between these points is the radius of curvature $\rho(\phi)$.

Geometry of a cylinder with cross-section $y = Ax^4$: A short cylinder with this nominal profile is measured in §6 and the theory of its oscillations developed in §7. It is shown with its evolute and smallest radius of curvature in Figure 49 for $A = 1$. The curve is cut off at height $y = W = Aa^4$ to

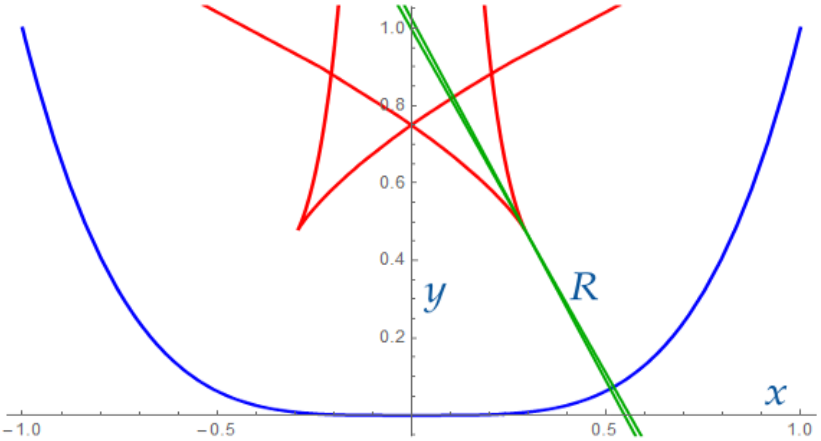

Figure 49: The curve $y = x^4$, $A = 1$, (blue) and its evolute (red). The two normals in green are at the position of greatest curvature.

form a flat top, as in Figures 23, 24. In the wooden model $A \approx 1{\cdot}2$ and $W = 2$ making $a = 1{\cdot}136$. The enclosed area is then $8Aa^5/9$, and (for uniform density) the centre of mass is at point H at $x = 0$, $y = h = 5Aa^4/9 = 5W/9$. The gradient at the point of contact P $= (x_0, y_0)$ is $m = 4Ax_0^3$ and the normal there is $y = y_0 - (x - x_0)/(4Ax_0^3)$. The evolute has co-ordinates

$$x_e = \frac{2}{3}x_0(1 - 8A^2 x_0^6), \qquad y_e = \frac{1 + 28A^2 x_0^6}{12A x_0^2} . \tag{A2.7}$$

The distance from (x_0, y_0) on the curve to its corresponding point on the evolute is the radius of curvature, R, which is given by

$$R = \frac{(1 + 16A^2 x_0^6)^{3/2}}{12Ax_0^2} . \tag{A2.8}$$

For $A = 1$ the least value of this occurs at $x_0 = 1/\sqrt[6]{56} = 0{\cdot}51125$ and is $R_{min} = 0{\cdot}4648$. Two closely adjacent normals here converge on the cusp of the evolute at $(0.2921, 0.4782)$. The normal at a general point (x_0, Ax_0^4) intersects the y axis at

$$Y = x_0^4 + \frac{1}{4Ax_0^2} .$$

If $Y = h$ the centre of mass is vertically above P. Since this is a cubic equation in x_0^2, the three symmetric roots correspond to positions of some type of stability. For $h = 10/9$, the roots at $x_0 = 0$, and at $0{\cdot}957$ for $A = 1$, $0{\cdot}922$ for $A = 1{\cdot}2$, are stable positions about which the object can oscillate,

one on its flattened base and the other lying on its side. The intermediate position of $0\cdot487$ for $A=1$, $0\cdot44224$ for $A=1\cdot2$, is a precarious balance; any tiny deviation will cause the object the roll either onto its base at $P=0$ or its side. This therefore corresponds to the largest angle of tilt which this study need consider.

The normal at (x_0, y_0) cuts the y axis at $Ax_0^4 + 1/(4Ax_0^2)$. Let R be the position of the instantaneous centre of curvature, always vertically above P(x_0). The significance of R is that, as the cylinder turns, it appears to turn about R, and the element of arc length ds rolled on the flat ground is equal to the element of distance parallel to the ground by which R advances. With a circular cylinder, of course, this is constant; here is varies continually. R_c tends to infinity at $x_0=0$ because $y=x^4$ is flatter than any finite circle at this point. R_c is plotted in the right hand panel of Figure 50. There is a limit to the tilt of the cylinder if it is not to fall over onto its side. This critical orientation is where H is vertically above P and here the angles θ and β are equal. Since $h=5W/9$, P is then at $x_0=\pm0\cdot487$ for $A=1$.

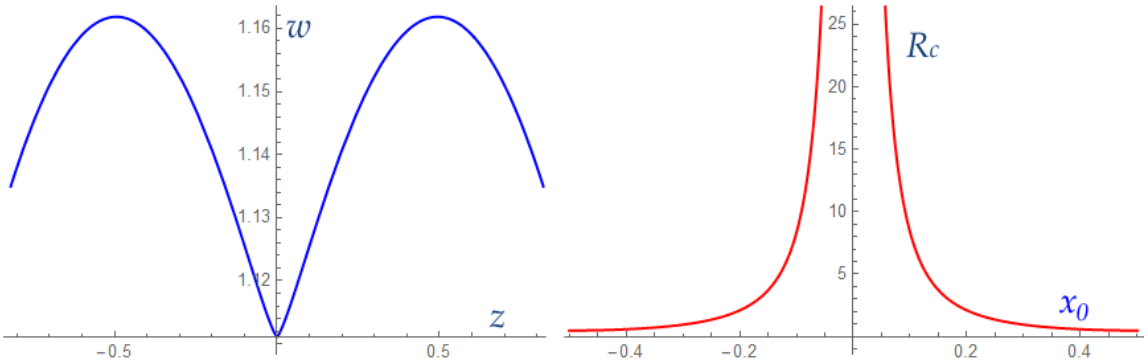

Figure 50: Left: position of centre of mass H relative to the equilibrium position Q for a $y=x^4$ cylinder with height $W=a^4=2$. Central value is 10/9. Right: Variation of radius of curvature with position.

Involute of a circle §5 posed the question 'What profile shape must the base of a cylinder have for precisely constant angular acceleration'. Since the acceleration is proportional to the moment about the instantaneous point of contact, the curve must have the property that its centre of mass maintains a constant perpendicular distance from every normal of the curve. As the cylinder turns, the envelope of its normals is a circle, centre H, the centre of mass. The required curve is therefore the one whose evolute is a circle. The inverse curve, the involute of the circle, is given by the parametric equations

$$x = \pm\sin\beta \mp \beta\cos\beta, \qquad y = -\cos\beta - \beta\sin\beta \tag{A2.9}$$

and illustrated in Figure 51. β is the angle around the parent unit circle to the point of tangency, with $\beta=0$ on the negative y axis. Three tangents to the circle are shown in pale green; note how each is normal to the involute. The distance of a point from the origin is $\sqrt{x^2+y^2}=\sqrt{\beta^2+1}$, so the distance from (x,y) on the involute to its point of tangency on the parent circle is simply β. As shown, the normal at $\beta=\pi/2$ is vertical. If the curve were rotated clockwise on its right involute through angle θ, the normal to the involute at $\beta=\theta+\pi/2$ would be vertical, so $\beta-\pi/2$ is identical with the angle of tilt, θ. The curve has the interesting property in that the arc length from $\beta=0$ to any value $\beta_0>0$ is $\beta_0^2/2$. The reason is that the radius of curvature, being the distance to the parent circle, is β, so the arc length element around the involute is $\beta\,d\beta$, and the integral of this is $\beta_0^2/2$.

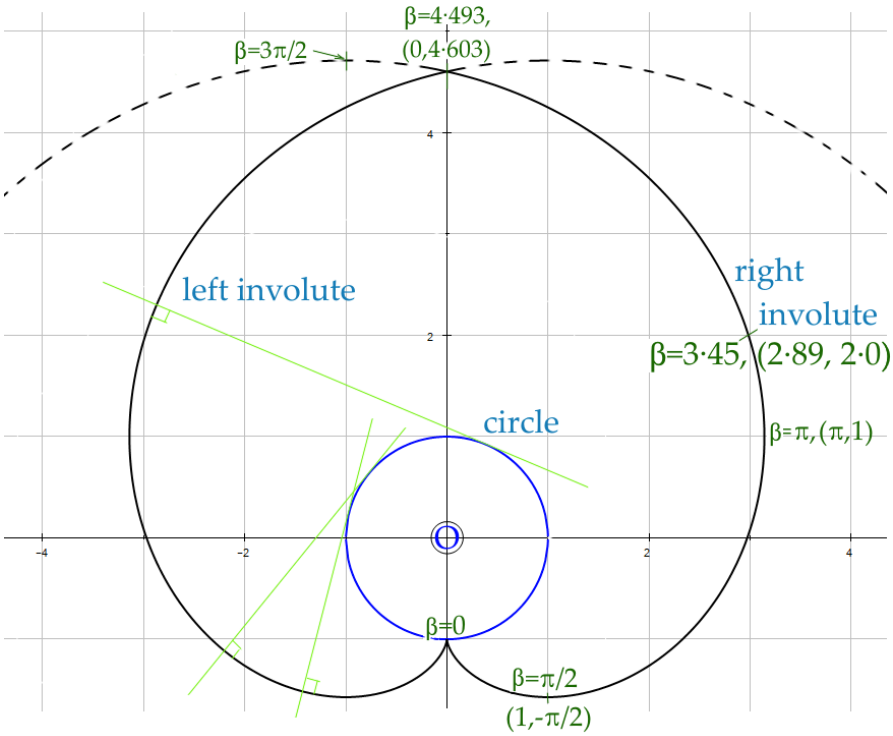

Figure 51: A circle, unit radius and centre (0, 0) and its left and right involutes.

Geometry of ellipse In §8 we need the geometry of the ellipse. Refer to Figure 52 which is drawn with the x axis, semi-length a, shorter than the y axis, semi-length b. This figure is therefore a rotation of Figure 38 in §8. For any general point $\mathrm{P} = (x, y)$

$$\frac{x^2}{a^2} + \frac{y^2}{b^2} = 1\,, \qquad x^2 + y^2 = r^2\,. \tag{A2.10}$$

The gradient $m = dy/dx$ is negative in the diagram, but we are more interested in the inclination of the normal from the x axis, which will become the angle of tilt of the ellipse. If this is θ, then $\tan\theta = -1/m$.

Two parametrisations are illustrated. In one the controlling parameter is β, the angle which the radius vector (green, length $r(\beta)$) from O to P makes with the x axis. The other uses γ, essentially a length ratio defined such that $x/a = \cos\gamma$, $y/b = \sin\gamma$. In the γ parametrisation circles of radii and a and b are involved as shown. Introduce the abbreviations E and F, and from Eq A2.10 we deduce that the two schemes are related as follows:

$$x = r\cos\beta, \quad y = r\sin\beta, \quad r^2 = \frac{a^2b^2}{a^2\sin^2\beta + b^2\cos^2\beta} = \frac{a^2b^2}{E}, \quad m = -\frac{b^2}{a^2\tan\beta}\,,$$

$$x = a\cos\gamma, \quad y = b\sin\gamma, \quad r^2 = a^2\cos^2\gamma + b^2\sin^2\gamma = F, \quad m = -\frac{b}{a\tan\gamma}$$

$$b\tan\gamma = a\tan\beta\,, \qquad \frac{d\gamma}{d\beta} = \frac{a\cos^2\gamma}{b\cos^2\beta} = \frac{ab}{a^2\sin^2\beta + b^2\cos^2\beta} = \frac{ab}{E}\,, \tag{A2.11}$$

$$\frac{d\beta}{d\gamma} = \frac{ab}{a^2\cos^2\gamma + b^2\sin^2\gamma} = \frac{ab}{F}\,, \qquad \text{eccentricity } e = \frac{\sqrt{a^2 - b^2}}{a}\,.$$

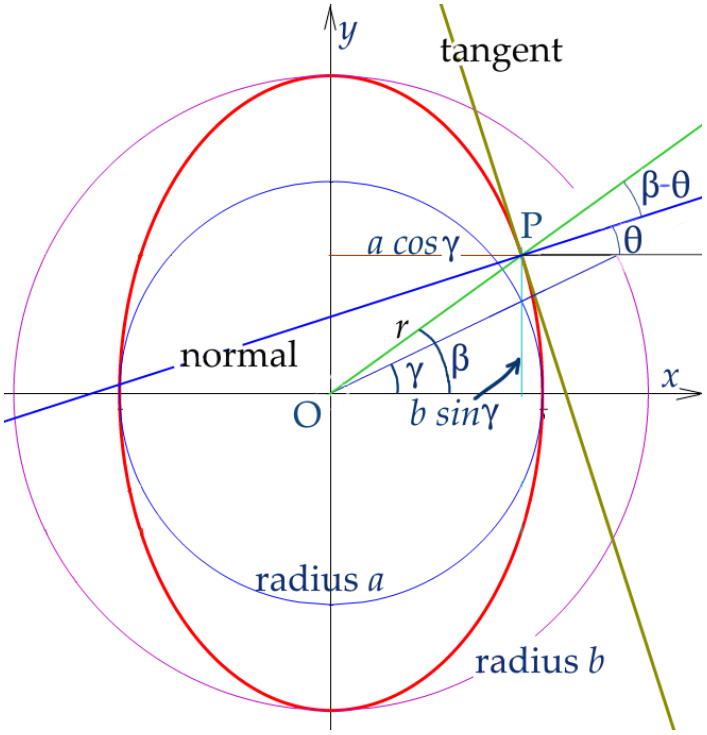

Figure 52: Geometry of an ellipse.

The element of arc length, ds, is given by

$$ds^2 = dx^2 + dy^2 = \left(1 + \left(\frac{dy}{dx}\right)^2\right) dx^2 = (1 + m^2)\, dx^2$$

$$= \left(\frac{a^4 \sin^2\beta + b^4 \cos^2\beta}{a^4 \sin^2\beta}\right) dx^2 = \frac{dx^2}{\sin^2\theta}\,. \qquad (A2.12)$$

This appears to be singular at $\theta = 0$ but there $dx = 0$. The limit for small β and θ is that $r \to a$ and $s \to a\beta = b^2\theta/a$.

Formulae for the evolute of the ellipse in terms of the radius angle β are :

$$\frac{dm}{d\beta} = \frac{b^2}{a^2 \sin^2\beta}, \qquad \frac{dx}{d\beta} = -\frac{a^3 b \sin\beta}{E^3}, \qquad \frac{dy}{d\beta} = \frac{ab^3 \cos\beta}{E^3}.$$

$$x' + my' = \frac{b}{2a \sin\beta\, E^3}\left[a^4 \sin^2\beta + b^4 \cos^2\beta\right], \qquad E = a^2 \sin^2\beta + b^2 \cos^2\beta$$

$$u = \frac{b^3(a^2 - b^2)\cos^3\beta}{a\, E^3}, \qquad v = -\frac{a^3(a^2 - b^2)\sin^3\beta}{b\, E^3}\,. \qquad (A2.13)$$

Figure 53 shows this ellipse and its evolute. The two adjacent normals show how the evolute is the envelope of these lines, each of which is tangent to the evolute. For completeness I will give the formula for the alternative parametrisation in terms of the ratios $\cos\gamma$, $\sin\gamma$.

$$u = \frac{a^2 - b^2}{a}\cos^3\gamma, \qquad v = -\frac{a^2 - b^2}{b}\sin^3\gamma = \frac{a^2 - b^2}{b}\sin^3(-\gamma)\,.$$

This formulation readily allows γ to be eliminated to produce the cartesian equation

$$\left(\frac{ua}{a^2-b^2}\right)^{2/3} + \left(\frac{vb}{a^2-b^2}\right)^{2/3} = \cos^2(\gamma) + \sin^2(-\gamma) = 1\,. \qquad (A2.14)$$

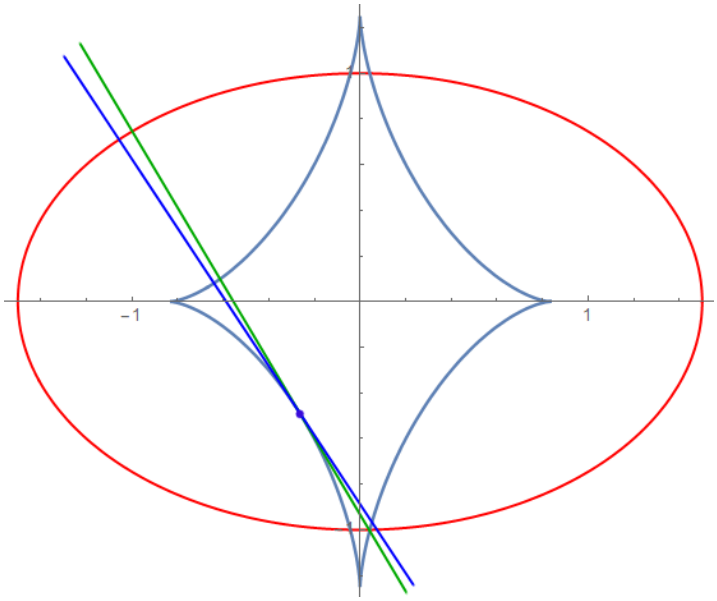

Figure 53: Ellipse, $a = 1\cdot5$, $b = 1$ (red) with evolute. The two normals at $\beta = 2\cdot5$, and $2\cdot55$ intersect at $(-0\cdot246, -0\cdot519)$.

12 Appendix 3: Moment of inertia of the involute cylinder

This appendix describes my efforts to determine the moment of inertia I of the cylindrical block studied in §5 and pictured in Figure 18 (ignore the mitre-shaped piece of card). Though I is readily understood as 'the sum of all terms mr^2 over the object', where r is the distance from axis of rotation, I have found it awkward to fix confidently on a value. Uncertainty arises from its complicated shape and the fact that it is made of two components: the wooden block with resin infill and the steel bar. I have tried to determine a value theoretically from the formula and by experiment.

12.1 Theory

The wooden cylinder measured in §5 has a profile conforming to the involute of a unit circle except in the re-entrant section in the centre of the base between $x = -1$ and $+1$ where it is almost flat. It is cut off at $y = 2$ units where $\beta = 3\cdot45$ (see Appendix 2), making the maximum tilt possible $1\cdot88$ radians or $107\cdot7°$. Take the wooden block first. One unit of distance in (x, y) space corresponds to 30 mm in real space and its mass is 790 g. It is clear from Figure 51 in Appendix 2 that it is about 6 units wide in x and a little over 3 in y. By numerical integration, the area of the face up to $y = 2$ is $19\cdot93$ square units or $0\cdot0179$ m^2. The first moment of area about the origin is $7\cdot02$ units, so the centre of mass of the wooden part is at $y = 0\cdot352$ units, $10\cdot6$ mm. Its moment of inertia about a horizontal axis through O is $3\cdot868m$, $m = 0\cdot78$ kg, equivalent to $27\cdot5\times10^{-4}$ kg m^2. This is close to the moment of inertia of a rectangular block 6 units in x, $3\cdot1$ in y about a similarly placed axis.

The steel cylinder, mass 300g, 16 mm diameter, was inserted to lower the centre of gravity towards the origin. The centre of this rod should have been at $10 \cdot 6 \times 790/300 = 29$ mm below O. For practical reasons the rod as built centres at $y = -36$mm, which places the centre of gravity of the combined object at $y = -4$ mm. By balancing the block on a steel straight edge I found −3mm to be a better estimate. This small offset, though undesirable, probably makes little difference to the dynamics. One day in the future when I am feeling compelled to do so, I may shift the centre of gravity up to $y = 0$ by adding a small weight (≈ 30g) – such as a piece of the lead sheet – to the flat top surface and remeasure the dynamics; the effect of the lower centre of mass is to increase the moment for large angles of tilt, the increase falling to zero with θ. However the offset is small and should not make any marked change from the results in §5. The theorem of parallel axes allows us to calculate the moment of inertia of the wood with its centre of mass moved from $y = 0$ to $y = -3$mm, but the increase is only to $27 \cdot 58 \times 10^{-4}$ kg m^2. The moment of inertia of the rod about its own axis is small: $ma^2/2 = 0 \cdot 1 \times 10^{-4}$ kg m^2. However, it contributes significantly by virtue of being offset by $36 - 3 = 33$ mm from the true centre of gravity. By the theorem of parallel axes the offset increases its contribution to $3 \cdot 46 \times 10^{-4}$ kg m^2. The conclusion is that the moment of inertia of the completed object is $31 \cdot 0 \times 10^{-4}$ kg m^2. In §5 this is needed in dimensionless normalised form $I/(\mu^2 m)$ where m is its total mass, $1 \cdot 09$ kg, and $\mu = 0 \cdot 030$ is the length of 1 unit in metres. This evaluates to $3 \cdot 16$.

12.2 Experiment

As an amusing aside, and something to do in the winter while locked down during the prevailing covid19 pandemic, I rigged up some equipment to measure the moment of inertia of this wood and steel cylinder. The concept was to support the cylinder on an axis through its centre of gravity so that it could turn freely, and to fit a light weight spool on the same axis around which a light weight chord is wrapped. The cylinder's support frame is clamped to a ceiling beam and a weight attached to the free end of the chord; this is allowed to fall under gravity, so unwinding the chord from the spool and turning the cylinder. The angular acceleration is proportional to the linear acceleration during the descent of the weight, and the moment of inertia I is calculated from the formula

$$I = \frac{mgr}{\ddot{\theta}}$$

where m is the mass of the falling platform, g the acceleration due to gravity, r the radius of the spool and $\ddot{\theta}$ the angular acceleration in radians per second.

The equipment was improvised from wood and other materials to hand, shown in the photos of Figure 54. The spindles on which the specimen turned were two screws, one either side, screwed into the wood at the axis (3 mm below the origin). These screws had smooth rims to their heads, 10 mm diameter, and turned inside a sleeve made of hard plastic tube. The contact areas would be very small, and I hoped this would limit the frictional drag. The spool was an empty tuna fish can. The first chord used was 2mm diameter nylon braid used for hanging paintings, but later I replaced it with fine nylon fishing line. The weight was a small plastic pot with pebbles placed inside. The photographs show the equipment clamped to a ceiling beam from where the pot would fall through about $1 \cdot 9$ metres (7 feet). The descent was photographed with a digital video camera at 50 frames per second. Calibration pictures were recorded so that distances in metres could be determined from the video frames. By making on-screen measurements frame by frame in a video editor (blender 2.90) I determined the height of a fiducial mark on the pot as a function of time. The data was analysed in an Excel spreadsheet. The curves of position against time were all well-defined parabolas from which the respective acceleration was given by the leading coefficient of the fitted trend line.

Figure 54: Two photographs of the home-made equipment for measuring the moment of inertia of a cylinder.

I made several runs with weights ranging from 58 to 400 grams. It soon became clear that the value of I calculated from the above formula was increasing with the weight on the chord. This was probably because the acceleration was less than theory expected, and increased with the rotational speed. I therefore tried a few refinements. It was necessary to add small (20g) counterpoises to ensure that each object ran freely and evenly in its frame. I followed two approaches to compensating for friction:

1. The first was to determine the smallest weight needed to get the spool to unwind – about 20 g. Hence in some calculations I subtracted 20 g from the actual weights in the pot to obtain the effective weight causing the torque. Comparison with a rectangular block showed that agreement was best with a weight of about 100 to 120 g. Subtracting the 20 g, the values of I at 89 g actual (69 g effective) were $32 \cdot 1 \times 10^{-4}$, and at 122 g (102 effective) $33 \cdot 5 \times 10^{-4}$ kg m^2. These are fairly close to but larger than the theoretical value. However, in a separate run with actual weight 119g (109 effective) I appeared to have increased to $36 \cdot 6 \times 10^{-4}$. If the 20 g allowance for friction were increased to 30 g to allow for greater friction, this reduced to $32 \cdot 9 \times 10^{-4}$.

2. The second approach has been to compare the acceleration of the involute cylinder with that of a rectangular block of wood with about the same weight and size. Since I for this rectangle is known with confidence from a formula, I for the specimen could be determined by comparison. The rectangle was 92 mm by 244 mm and weighed 1058 g, so I is $60 \cdot 0 \times 10^{-4}$. Figure 55 plots the linear acceleration against actual applied weight (no 20 g deduction). The ratio of the two fitted lines is close to $1 \cdot 66$ for weights near 400g. Assuming the friction and all other parameters are unchanged, this implies that I for the involute cylinder is about 36×10^{-4}.

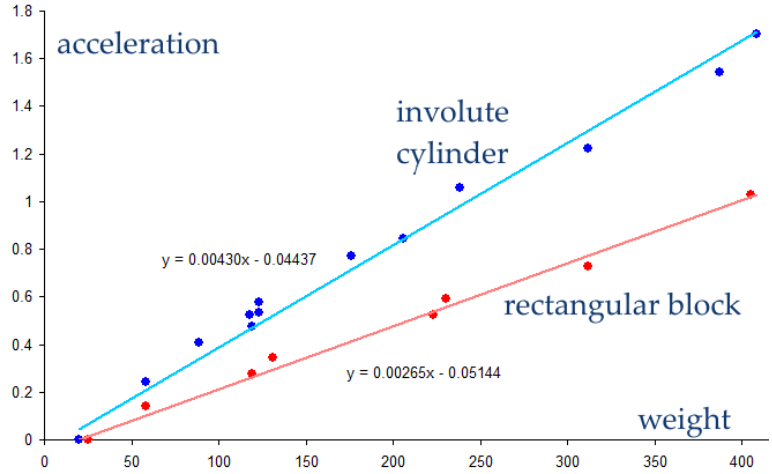

Figure 55: Linear acceleration (m s^{-2}) versus weight on chord for the rectangular block and the involute cylinder.

The results are disappointingly inconsistent. This has been an interesting but rather frustrating side investigation. I find it surprising how complicated finding I can be for any but the simplest shapes. All I can conclude is that the theoretical value of I is $31 \cdot 0 \times 10^{-4}$ kg m^2, while the experiments point to it being in the range 32 to 37. In computing the rocking curves for the involute block shown in Figure 21 of §5 I have tried a few values of I and attenuation to gain a fair fit to the observed trajectory. The value I fixed upon is $32 \cdot 4 \times 10^{-4}$ kg m^2 which corresponds to the normalised value $3 \cdot 3$ units.

John Coffey, April 2021